DOCTORAL THESES IN FOOD SCIENCES AT THE UNIVERSITY OF TURKU

# Structural Analysis of Triacylglycerols and Bioavailability of Docosahexaenoic Acid from Regio- and Enantiopure Triacylglycerols

YUQING ZHANG

Food Sciences
Department of Life Technologies

DOCTORAL THESES IN FOOD SCIENCES AT THE UNIVERSITY OF TURKU
Food Development (tech)

# Structural Analysis of Triacylglycerols and Bioavailability of Docosahexaenoic Acid from Regio- and Enantiopure Triacylglycerols

YUQING ZHANG


**Food Sciences**
**Department of Life Technologies**

**TURKU, FINLAND – 2025**

University of Turku
Department of Life Technologies, Faculty of Technology
Food Sciences
Doctoral Programme in Technology

Supervised by
Professor Baoru Yang, Ph.D.
Department of Life Technologies
University of Turku
Turku, Finland

Marika Kalpio, Ph.D.
Department of Life Technologies
University of Turku
Turku, Finland

Mikael Fabritius, Ph.D.
Department of Life Technologies
University of Turku
Turku, Finland

Reviewed by
Professor Tom Brenna, Ph.D.
Department of Pediatrics, Nutrition, & Chemistry
University of Texas at Austin
Austin, the United States

Professor Stephen Blanksby, Ph.D.
School of Chemistry & Physics
Queensland University of Technology
Queensland, Australia

Opponent
Professor Zheng Ouyang, Ph.D.
Tsinghua Shenzhen International Graduate School
Tsinghua University
Shenzhen, China

Research director
Professor Baoru Yang, Ph.D.
Department of Life Technologies
University of University
Turku, Finland

The originality of this dissertation has been checked in accordance with the University of Turku quality assurance system using the Turnitin Originality Check service

ISBN 978-952-02-0168-5 (print)
ISBN 978-952-02-0169-2 (pdf)
ISSN 2323-9395 (print)
ISSN 2323-9409 (pdf)
Painosalama Oy – Turku, Finland 2025

*I dedicate this thesis to my beloved family. They always stand by my side at every step of my life.*

# TABLE OF CONTENTS

# ABSTRACT

Triacylglycerols (TG) and glycerophospholipids (GPL) are essential lipid molecules found in food and play vital roles in human physiology. The diversity of fatty acids (FAs) and the presence of regioisomers and stereoisomers cause significant challenges to their structural analysis. In natural samples, the distribution of FAs on the glycerol backbone is not random, and the properties of isomers can vary considerably despite structural similarities. These structural variations can affect the physical properties or nutritional significance of fats and oils, such as the melting point and bioavailability of TGs and GPLs.

This thesis focuses on the structural analysis of enantiomeric TGs and the investigation of the bioavailability of FAs from regio- and enantiopure TGs. Using reference compounds, the research begins with a comprehensive study of the chiral chromatographic separation of TG enantiomers. A total of 33 TG enantiomer pairs, each comprising three different fatty acyls, were analyzed using recycling chiral high-performance liquid chromatography (HPLC), of which 26 pairs were successfully separated. The retention time at separation exhibited a negative correlation with the *sn*-3 carbon number of the first eluted enantiomer and a positive correlation with the carbon number difference between the outer positions. TGs with one saturated fatty acid (SFA) and one unsaturated fatty acid (UFA) at the outer positions were easier to separate, whereas TGs with two SFAs or two UFAs at *sn*-1/3 positions were more difficult to separate. Additionally, the results revealed that all three fatty acyls significantly influenced the chromatographic behavior in terms of carbon chain length and the number of double bonds (DBs). These results highlight the importance of steric hindrance and intermolecular interactions in determining the efficiency of the separation mechanism. This systematic study enhanced the understanding of the chiral chromatographic retention behavior and elution order of TG enantiomers.

The second part of this thesis investigated the nutritional and biological implications of fatty acyl positional isomers of TGs through an animal trial by exploring how the positional distribution of docosahexaenoic acid (DHA) in TGs influences the bioavailability and metabolic fate of DHA. Regio- and enantiopure TGs with DHA at the *sn*-1, *sn*-2, or *sn*-3 positions were synthesized and fed to rats for 4 weeks of intervention. During this time, body weight and food intake were monitored to assess physiological responses.

After the intervention, biological samples: plasma, visceral fat, and organs including the heart, liver, brain, lung, testis, spleen, eye, and kidney were collected for analysis. The FA composition of total lipids was analyzed. Additionally, polar and neutral lipids from plasma, liver, and kidney were fractionated, and FA composition was analyzed separately. Using a novel mass

spectrometric methodology recently developed by our group and advanced data processing software, the molecular species and regioisomer composition of phosphatidylcholines (PC) in these tissues were identified, revealing the effects of positional distribution of FAs on lipid composition and metabolism. The results demonstrated significant differences in DHA content in the plasma and visceral fat between groups fed TGs with DHA at the *sn*-1 and *sn*-3 positions. Historically, the effect of positional distribution has been evaluated mainly through FA content and composition in tissues. Therefore, this study provides fresh insights into the impact of the *sn*-position of DHA in dietary TGs on GPL molecular species and regioisomer distribution for the first time. Furthermore, this research is the first to demonstrate that n-3 PUFA deficient diet altered GPL molecular species composition in organs, and DHA supplementation counteract these changes.

In conclusion, this thesis offers valuable contributions to understanding the composition and metabolism of chiral TGs, from analytical methodologies to biological evaluation. The study provides critical insights into the chromatographic behavior of TG enantiomers and highlights the impact of FA positional distribution on lipid chemistry and biology. These findings serve as foundational references for future stereospecific studies of natural lipids.

# SUOMENKIELINEN ABSTRAKTI

Triasyyliglyserolit (TG) ja glyserofosfolipidit (GPL) ovat elintarvikkeiden välttämättömiä lipidimolekyylejä, joilla on elintärkeitä tehtäviä ihmisen fysiologiassa. Rasvahappojen monimuotoisuus sekä regioisomeerien ja stereoisomeerien esiintyminen aiheuttavat merkittäviä haasteita niiden rakenneanalyysille. Luonnon rasvoissa ja öljyissä rasvahapot eivät ole esteröityneet glyserolirunkoon sattumanvaraisesti, ja isomeerien ominaisuudet voivat rakenteellisesta samankaltaisuudestaan huolimatta poiketa huomattavasti toisistaan. Nämä rakenteelliset vaihtelut voivat vaikuttaa rasvojen ja öljyjen fysikaalisiin ominaisuuksiin kuten sulamispisteeseen ja rasvahappojen biosaatavuuteen TG:sta ja GPL:sta.

Tämä väitöskirjatyö keskittyy TG:n enantiomeerien rakenneanalyysiin ja rasvahappojen biosaatavuuteen regio- ja enantiopuhtaista TG:sta. Käytännön osuus alkaa kattavalla tutkimuksella keskittyen TG:n enantiomeerien kiraalikromatografiseen erottamiseen vertailuyhdisteiden avulla. Näytteen kierrätykseen perustuvalla kiraalisella korkean erotuskyvyn nestekromatografilla analysoitiin yhteensä 33 TG-enantiomeeriparia, joista 26 paria erotettiin onnistuneesti. Enantiomeerien erotukseen käytetty retentioaika korreloi negatiivisesti ensimmäisenä eluoituneen enantiomeerin *sn*-3-hiililuvun kanssa ja positiivisesti TG:n uloimpien asemien (*sn*-1 ja *sn*-3) rasvahappojen välisen hiililukueron kanssa. TG:t, joissa oli yksi tyydyttynyt ja yksi tyydyttymätön rasvahappo uloimmissa asemissa, erottuivat helpommin, kun taas TG:t, joissa oli kaksi tyydyttynyttä tai kaksi tyydyttymätöntä rasvahappoa *sn*-1/3-asemissa aiheuttivat suurempia haasteita erottamisessa. Lisäksi tulokset osoittivat, että kaikki kolme TG:n rasvahappoa vaikuttivat merkittävästi kromatografiseen eluutiokäyttäytymiseen hiiliketjun pituuden ja kaksoissidosten lukumäärän suhteen. Nämä tulokset korostavat steerisen esteen ja molekyylien välisten vuorovaikutusten merkitystä kromatografisessa erottumisessa. Tämä systemaattinen tutkimus lisäsi ymmärrystä TG:n enantiomeerien kiraalikromatografisesta retentiokäyttäytymisestä ja eluutiojärjestyksestä.

Työn toisessa osassa selvitettiin eläinkokeen avulla TG:n paikkaisomeerien ravitsemuksellisia ja biologisia vaikutuksia tutkimalla, miten dokosaheksaeenihapon (DHA) sijainti TG:ssa vaikuttaa DHA:n biosaatavuuteen ja metaboliaan. Regio- ja enantiopuhtaita TG:ja, joissa DHA oli *sn*-1-, *sn*-2- tai *sn*-3-asemassa, syntetisoitiin ja syötettiin rotille 4 viikon ajan. Tänä aikana seurattiin ruumiinpainoa ja ruoan saantia fysiologisten vasteiden arvioimiseksi.

Intervention jälkeen biologiset näytteet: plasma, viskeraalinen rasva ja elimet, mukaan lukien sydän, maksa, aivot, keuhkot, kivekset, perna, silmä ja munuaiset kerättiin analysoitavaksi. Näytteistä analysoitiin kokonaislipidien

rasvahappokoostumus. Lisäksi plasman, maksan ja munuaisten polaariset ja neutraalit lipidit fraktioitiin ja rasvahappokoostumus analysoitiin erikseen. Ryhmämme vastikään kehittämän uudenaikaisen massaspektrometrimenetelmän ja kehittyneen tietojenkäsittelyohjelmiston avulla tunnistettiin fosfatidyylikoliiniyhdisteet ja niiden regioisomeerikoostumus näissä kudoksissa, mikä paljasti rasvahappojen paikkajakauman vaikutuksia lipidikoostumukseen ja aineenvaihduntaan. Tulokset osoittivat merkittäviä eroja plasman ja viskeraalisen rasvan DHA-pitoisuudessa niiden ryhmien välillä, joille syötettiin TG:a, joissa DHA oli *sn*-1- ja *sn*-3-asemissa. Perinteisesti paikkajakauman vaikutusta on arvioitu pääasiassa kudosten rasvahappopitoisuuden ja -koostumuksen perusteella. Näin ollen tässä tutkimuksessa saadaan ensimmäistä kertaa uutta tietoa ravinnon sisältämien TG:n DHA:n *sn*-aseman vaikutuksista GPL-molekyyleihin ja regioisomeerikoostumukseen. Lisäksi tämä tutkimus on ensimmäinen, jossa osoitetaan, että n-3 rasvahappojen suhteen puutteellinen ruokavalio muutti GPL:n molekyylikoostumusta ja että DHA-lisäys torjui näitä muutoksia.

Yhteenvetona voidaan todeta, että tämä tutkielma lisää merkittävästi kiraalisten TG-yhdisteiden koostumuksen ja aineenvaihdunnan ymmärtämistä, ulottuen analyyttisistä menetelmistä biologiseen arviointiin. Tutkimus tarjoaa kriittisen näkemyksen TG-enantiomeerien kromatografisesta käyttäytymisestä ja korostaa rasvahappojen paikkajakauman vaikutusta lipidien kemiaan ja biologiaan. Nämä havainnot toimivat perustavanlaatuisina viitteinä luonnollisten lipidien tuleville stereospesifisille tutkimuksille.

# LIST OF ABBREVIATIONS

| | |
|---|---|
| AA | Arachidonic acid [FA 20:4(5,8,11,14)] |
| ACN | Acyl carbon number |
| ALA | α-linolenic acid [FA 18:3(9,12,15)] |
| APCI | Atmospheric-pressure chemical ionization |
| C | Acyl carbon number |
| CID | Collision-induced dissociation |
| DB | Double bond |
| DHA | Docosahexaenoic acid [FA 22:6(4,7,10,13,16,19)] |
| DPA | Docosapentaenoic acid [FA 22:5(3,6,9,12,15)] |
| ECN | Equivalent carbon number |
| EIEIO | Electron impact excitation of ions from organics |
| EPA | Eicosapentaenoic acid [FA 20:5(5,8,11,14,17)] |
| ESI | Electrospray ionization |
| FA | Fatty acid |
| FAME | Fatty acid methyl ester |
| GC-FID | Gas chromatography-Flame ionization detection |
| GPL | Glycerophospholipid |
| HPLC | High-performance liquid chromatography |
| LA | Linoleic acid [FA 18:2(9,12)] |
| LDL | Low-density lipoprotein |
| LPC | Lysophosphatidylcholine |
| LPCAT | Lysophosphatidylcholine acyltransferase |
| LPLAT | Lysophospholipid acyltransferases |
| MALDI | Matrix-assisted laser desorption ionization |
| MDCK | Madin-Darby canine kidney |
| MS | Mass spectrometry |
| MS/MS | Tandem mass spectrometry |
| MSI | Mass spectrometry imaging |
| MUFA | Monounsaturated fatty acid |
| NMR | Nuclear magnetic resonance |
| OzID | Ozone-included dissociation |
| PC | Phosphatidylcholine |
| PL | Phospholipid |
| PUFA | Polyunsaturated fatty acid |
| RP | Reversed-phase |
| SD | Standard deviation |
| SFA | Saturated fatty acid |
| SFC | Supercritical fluid chromatography |
| TG | Triacylglycerol |

| | |
|---|---|
| TOF | Time-of-flight |
| UFA | Unsaturated fatty acid |
| UHPLC | Ultra-high-performance liquid chromatography |
| UVPD | Ultraviolet photodissociation |
| ΔC | Acyl carbon number difference between different positions |

**Definition and nomenclature**

The nomenclature of TGs and GPLs were mainly follows the LIPID MAPS guidelines (Fahy et al., 2005, 2009) and the updates by Liebisch (Liebisch et al., 2020) but with some modifications. The stereospecific numbering system (*sn*) was used to specify the position of FAs on the glycerol backbone. TGs are named A_B_C when the positional distribution of FAs is unknown, but the FA composition is known. When the FA in the middle position is known to be B, A_B(*sn*-2)_C represents the mixture of two enantiomers. Only if the molar ratio of two enantiomers is equal, *rac*-A_B(*sn*-2)_C is introduced to describe the racemic mixture. When the FA composition and positional distribution information are all known, TGs are named A/B/C meaning that FAs A, B, and C are esterified in the positions *sn*-1, 2, and 3, respectively. Similarly, the GPL A_B represents the GPL where FAs are known, but the positions are not assigned. GPL A/B denotes the known positional distribution of the two esterified FAs. In addition, the acyl carbon number: double bond number (ACN: DB) was used as the species name when the FAs composition is unknown, but the total acyl carbon number and the number of the DB are known. For convenience, the letter abbreviation was used in the TG nomenclature to replace the numerical notation. Accurate lipid identification requires that the annotation nomenclature used must always correspond to the identification status of the individual lipids. The annotation nomenclature used in this thesis follows the hierarchy proposed by LipidomicNET and the LIPID MAPS consortium (Holčapek & Ekroos, 2023). **Figure 1** shows the annotation pyramid of a PC as an example.

Abbreviations for individual FAs are denoted as Bu=4:0 (butyric acid), C=10:0 (capric acid), La=12:0 (lauric acid), M=14:0 (myristic acid), P=16:0 (palmitic acid), S=18:0 (stearic acid), O=18:1(9) (oleic acid), L=18:2(9,12) (linoleic acid), Ln=18:3(9,12,15) (α-linolenic acid), A=20:0 (arachidic acid), AA=20:4(5,8,11,14) (arachidonic acid), EPA=20:5(5,8,11,14,17) (eicosapentaenoic acid), and DHA=22:6(4,7,10,13,16,19) (docosahexaenoic acid). The EPA and DHA were further abbreviated as E and D when appear in TGs.

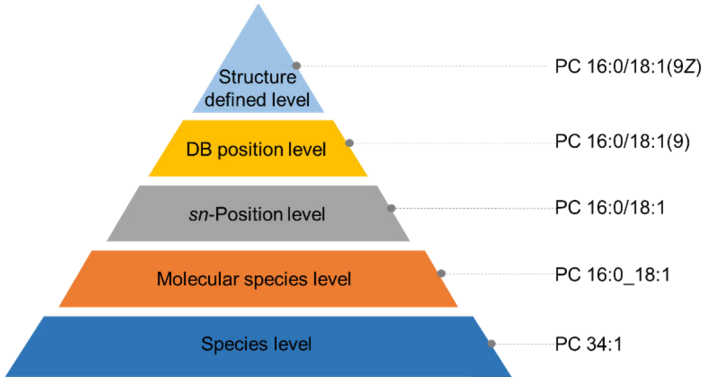


**Fig. 1** The hierarchical annotation pyramid depicted for a PC.

# LIST OF ORIGINAL PUBLICATIONS

I. Zhang, Y., Kalpio, M., Haraldsdóttir, H., Gudmundsson, H. G., Haraldsson, G. G., Sigurjónsson, S., Kristinsson, B., Linderborg, K. M., & Yang, B. (2024). Enantiomeric Separation of Triacylglycerols Consisting of Three Different Fatty Acyls and Their Chiral Chromatographic Elution Behavior. *Analytical Chemistry*, 96, 13936–13943.

II. Zhang, Y., Kalpio, M., Tao, L., Haraldsson, G. G., Guðmundsson, H. G., Fang, X., Linderborg, K. M., Zhang, Y., & Yang., B. (2023). Metabolic Fate of DHA from Regio- and Stereospecific Positions of Triacylglycerols in a Long-term Feeding Trial in Rats. *Food Research International*, *174*, 113626.

III. Zhang, Y., Fabritius, M., Boström, P., Kalpio, M., Gudmundsson, H. G., Haraldsson, G. G., Zhang, Y., Yang, B. Impact of N-3 Deficient Feeding and Supplementation with Docosahexaenoic Acid in Regio- and Enantiopure Triacylglycerols on Phosphatidylcholine Molecular Species and Regioisomers in Rat Organs. *Manuscript.*

# 1 INTRODUCTION

Lipids are essential nutrients that play critical roles in the human body. Beyond their fundamental function in energy storage and transfer, lipids are integral components of biological membranes and precursors of vitamins, and hormones (Lee, 2011). Among lipids, triacylglycerols (TGs) represent the largest lipid reservoir in plants and animals, accounting for over 95% of the lipids found in natural fats and oils. Structurally, TGs are composed of a glycerol backbone to which three fatty acids (FAs) are esterified. The three positions on the glycerol molecule are designated as *sn*-1, *sn*-2, and *sn*-3, where "*sn*" stands for stereospecific numbering. In addition to TGs, polar lipids, primarily glycerophospholipids (GPLs), commonly exist in living organisms, as they form the foundation of biological membranes. GPLs function predominantly within membranes and are associated with numerous health benefits (Schverer et al., 2020). Both TGs and GPLs serve as carriers of FAs, sharing a glycerol backbone esterified with FAs. However, GPLs are distinguished by the presence of a class-specific phosphate head group, typically attached at the third position of the glycerol backbone. The structural diversity of TGs and GPLs arises from variations in FA characteristics, including chain length, degree of saturation, double bond (DB) positions, and DB conformations. Additionally, the FA composition of TGs and GPLs introduces chirality into the molecules, which is closely linked to the stereochemistry of glycerolipids (Sun et al., 2025). These structural differences are illustrated in **Figure 2**.

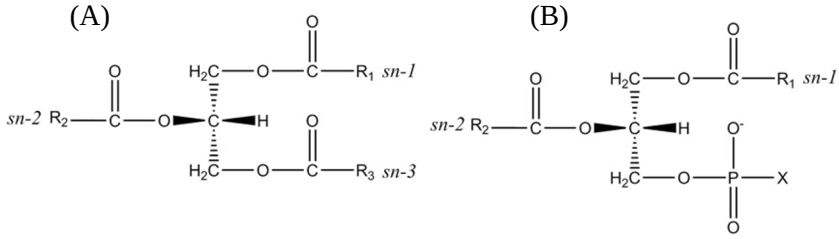


**Fig. 2** General structures of triacylglycerol (A) and glycerolphospholipid (B).

Increasing evidence suggests that the positional isomers of TGs exhibit distinct biological functions (Z. Wang et al., 2023) and physiochemical properties (Foubert et al., 2007), despite their structural similarities. For instance, the presence of palmitic acid at the *sn*-2 position has been shown to enhance the nutritional value of structured TGs in infant formulas, as it better mimics the TG structure of human milk (Ghide & Yan, 2021). However, the analysis of the isomer composition of TGs and GPLs in natural fats and oils remains highly challenging due to their complexity and the presence of a diverse mixture of lipids. Traditional methods for stereospecific analysis typically rely on chemical

or enzymatic hydrolysis. Mattson and Lutton (Mattson & Lutton, 1958) first demonstrated the specificity of FA distribution in natural fats by employing pancreatic lipase digestion. This enzymatic method has major drawbacks such as being labor intensive and lack of structure information of individual isomers. Over time, these conventional approaches have been largely replaced by chromatographic techniques for resolving individual isomers. For examples, Lísa and Holčapek (2013) successfully separated positional isomers of structured TGs using a two-column setup with a stationary phase of 3,5-dimethylphenylcarbamate in normal-phase HPLC. Similarly, Nagai et al. (Nagai et al., 2019) achieved partial separation of all six positional isomers of synthesized S_O_L through chiral chromatography, utilizing a CHIRALPAK IF-3 column (stationary phase: *tris*-3-chloro-4-methylphenylcarbamate) with acetonitrile as the mobile phase. Further developed by our group, chiral chromatography equipped with a sample recycling system was applied in an offline 2D-LC method to resolve the enantiomeric composition of selected TG species from sea buckthorn pulp oil (Kalpio et al., 2021).

N-3 polyunsaturated FAs have gained significant attention from both the public and the scientific community due to their extensive health benefits. Among them, docosahexaenoic acid (DHA) and eicosapentaenoic acid (EPA) have been extensively studied over the past few decades. Their known benefits include promoting brain development (Petrova et al., 2019), improving mental health (Innes & Calder, 2020), and exerting anti-inflammatory effects (Dawczynski et al., 2018). Despite these benefits, the global dietary intake of n-3 PUFAs remains insufficient (Micha et al., 2014), highlighting the need to investigate their bioavailability and optimize their delivery form. Previous research on FAs has predominantly focused on their composition and content in natural fats and oils, with fewer studies examining the bioavailability of FAs in specific lipid forms, such as *sn*-positioning in TGs and GPLs. Recent studies have explored how the different forms of n-3 PUFAs influence their bioavailability. For example, Cuenoud and others (Cuenoud et al., 2020) reported that free FAs exhibit the highest bioavailability, followed by TGs, while ethyl esters have the lowest bioavailability. Additionally, under obesogenic conditions, DHA and EPA esterified in GPLs demonstrated better bioavailability compared to their TG-bound counterparts (Rossmeisl et al., 2012). Positional distribution within TG molecules has also been shown to affect the bioavailability, metabolism (Y. Zhang et al., 2023), and absorption (Linderborg et al., 2019) of FAs. For instance, Yoshinaga et al. (Yoshinaga et al., 2015) found that the EPA located at the outer positions (*sn*-1/*sn*-3) of TGs accumulated more effectively in the liver and adipose tissue than EPA located at the middle position (*sn*-2).

Despite increasing interest in lipid research, limited research exists on how the bioavailability and metabolic fate of DHA vary depending on its *sn*-position within TG molecules. Overall, the stereospecific composition of TGs and the regiospecific composition of GPLs are significantly underexplored. The primary obstacles to advancing this understanding have been the lack of effective analytical methods and the unavailability of isomerically pure reference compounds. These challenges have limited insights into the specific molecular composition and the impact of FA positional distribution in TGs and GPLs. In this thesis, in collaboration with the University of Iceland, regio- and enantiopure structured TGs comprising three distinct fatty acyls (ABC-type TGs) and DHA-containing TGs were synthesized (Halldorsson et al., 2003; Haraldsdottir et al., 2024; Haraldsson et al., 2000), enabling a comprehensive chiral chromatographic study and animal feeding trial. This study represents the first mid- to long-term feeding trial examining DHA bioavailability across various tissues and organs, using regio- and enantiopure TGs as the dietary source. Currently, the regio- or stereospecific structures of TG and GPL are not included in standard untargeted lipidomic pipelines. Taking advantage of the method recently developed by our group, the phosphatidylcholine (PC) regioisomers were analyzed in rat organs. These findings provide novel insights into the effects of dietary position-specific DHA on lipid composition in animal tissues.

The enantiomeric separation results obtained in this thesis provide crucial knowledge on the elution behavior and retention mechanisms. The animal study results provide valuable insights into how the isomeric structure of TG influences DHA's metabolic fate. In addition, this research offers valuable reference data for resolving the regioisomeric composition of PCs in tissues and organs.

# 2 REVIEW OF THE LITERATURE

## 2.1 Stereochemistry of triacylglycerol and phospholipid

Due to the different positional distribution of FAs on the glycerol backbone, the glycerolipids can exist as stereo- and regioisomers. These isomers share the same FA composition but differ in molecular structure. As illustrated in **Figure 3**, a TG molecule containing three different FAs can have up to 6 isomers, including regioisomers and enantiomers. The carbon atom at the middle position acts as a chiral center when the FAs at the outer positions are different; in such cases, the entire TG molecule exhibits chiral properties. Similarly, GPL possesses two regioisomers, given by two different FAs in *sn*-1 and *sn*-2 positions, assuming that the class specific phosphate group is in *sn*-3 position.

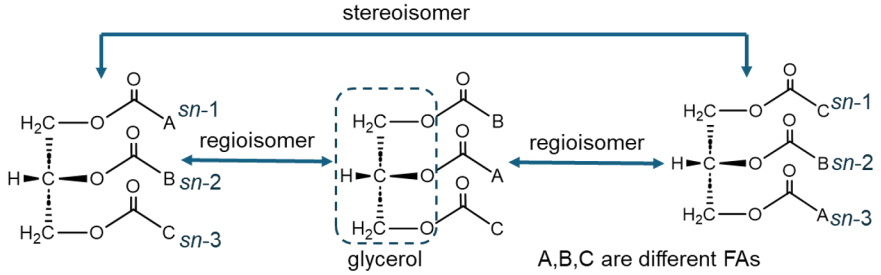


**Fig. 3** The basic structures of triacylglycerols and stereospecific numbering (*sn*).

### 2.1.1 Effect of specific positional distribution of FA on lipid properties

The positional distribution of FAs on TG affects the physical properties of natural fats and oils, which in turn influences their industrial properties in food processing. For instance, hardness and adhesiveness are important factors in food texture. The melting point and crystallization characteristics are essential for achieving the desired properties in food products such as chocolates (Craven & Lencki, 2012; John Craven & Lencki, 2011). Research has shown that melting points are strongly influenced by the FA positional distribution in TG molecules (Smith et al., 1998). Increasing the percentage of stearic acid in the *sn*-1/3 positions of TGs can raise the melting point by as much as 10°C compared to TGs with only stearic acid in the *sn*-2 position. A pig-feeding trial was conducted to study the relationship between the positional distribution of FAs and the physical properties of pig fat (Segura, Ruiz-López, et al., 2015). Pigs were fed with a commercial diet *ad libitum* for 32 days and then slaughtered at 110 kg body weight. The pig thighs were processed into dry-cured ham, and the FA composition and positional distribution of the ham was analyzed. Texture profile

analysis was performed to evaluate the texture characteristics. The results indicate that the higher content of palmitic acid in the *sn*-1/3 positions leads to an increased melting point of pig subcutaneous fat. Similarly, higher levels of oleic acid at the *sn*-2 position lowered the melting point. Additionally, a higher content of stearic acid in the outer positions increases the hardness of pig fat. The study found a positive correlation between the hardness of dry-cured ham and stearic acid on the outer positions, while a negative correlation was observed with linoleic acid (LA) in the *sn*-1 and *sn*-3 positions. Furthermore, more palmitic acid in the middle position improves the adhesiveness of the subcutaneous fat in the ham.

Taking advantage of the impact of positional distribution on the properties of fats and oils, various technologies have been developed to modify the structures of natural fats and oils to achieve the desired properties. For example, hydrogenation is commonly used in the food industry to obtain proper physical and sensory properties of food. By adding hydrogen atoms to UFAs, hydrogenation convert them into more saturated and solid form. However, the hydrogenation process also produces *trans* FAs, which are considered to be unhealthy. Interesterification is a widely used technique to modify the position of FAs on TG molecules without changing the degree of unsaturation or stereochemistry of the DB in the FAs. This method has been applied in the food industry, including in margarine, infant formula, and edible fats, to improve the functional properties of these materials (Sivakanthan & Madhujith, 2020). Interesterification is also employed in clinical applications to create functional foods, such as poorly absorbed fats, which are beneficial for individuals needing to lose weight (Alfieri et al., 2018). Furthermore, TG composition can be used to differentiate between fats and oils and to detect adulteration in natural oils. Araujo and coworkers developed a novel strategy to identify fraudulent practices in marine oils (Araujo et al., 2018). By determining the stereospecific distribution of n-3 PUFAs and analyzing the data using principal component analysis, they successfully discriminated adulteration in several marine oils.

### 2.1.2 Effects of specific positional distribution of FA on metabolism

In addition to affecting physical properties, the positional distribution of FAs in glycerolipids also plays a significant role in their biochemical functions. Gouk et al. determined the impact of the positional distribution of long-chain SFAs in TG using a mouse trial (Gouk et al., 2013). They concluded that it is the positional distribution of SFAs rather than the total amount of SFA, that has exerted a profound effect on fat deposition. Specifically, higher SFA content in the outer positions leads to reduced fat deposition in visceral fat. In a trial with weaned piglets, four groups of pigs were fed pork lard, natural palm olein, chemically inter-esterified palm olein, and enzymatically inter-esterified palm olein. They

found that levels of plasma low-density lipoprotein cholesterol (LDL-C) content and the ratio of LDL-C to high-density lipoprotein cholesterol (HDL-C), were lower in pigs fed palm oil with palmitic acid in the outer positions compared to those fed with palmitic acid in the *sn*-2 position. Additionally, the body weight gain was significantly higher in the *sn*-1/*sn*-3 palmitic acid group compared to other groups (Ponnampalam et al., 2011). Brink et al. (Brink et al., 1995) studied the effect of the positional distribution of stearic acid and oleic acid in a TG on fat absorption in rats. They found that total fat and calcium absorption was significantly lower in rats receiving S_O(*sn*-2)_S compared to those fed with O_S(*sn*-2)_S. However, there was no significant difference in magnesium absorption. Four groups of diets received by pigs had similar nutrition but different fat sources, either palm oil or lard, and the concentrations of glycerol were 0 and 0.5 g/kg (Segura, Cambero, et al., 2015; Segura, Ruiz-López, et al., 2015). The results indicated that dietary intervention during the late fattening phase of pigs had limited effects on the FA composition in the middle position in subcutaneous fat. However, the influences of sex on the outer positions, particularly for stearic acid, arachidonic acid (AA), and α-linoleic acid (ALA) were confirmed. The results suggest a high level of metabolic regulation for FA in the *sn*-2 position.

Research on the lipid structure of human milk is increasing due to its crucial nutritional importance for infants. The FA composition in human milk is influenced by factors such as the maternal diet, age, and body mass index (Tian et al., 2019). However, the preference of FAs for the positions on the TG is not affected by these factors (Linderborg et al., 2014). Numerous studies have shown that palmitic acid located in the *sn*-2 position is crucial for the absorption and digestion of human milk fat. The position of this FA is associated with the development of lung function (Carta et al., 2017), bone strength, and gut microbiota (Bar-Yoseph et al., 2013). Bowel movements and the stool hardness of infants are highly negatively related to the SFAs on the outer positions, which tend to undergo saponification reactions (Lasekan et al., 2017). To better mimic the structure of human milk lipids, it is important to focus not only on FA composition but also on the lipid structure.

The health effects and biochemical functions of lipids are closely associated with their digestion and absorption. Although the exact mechanisms of digestion and absorption are still not fully understood, it has been shown that many lipases involved in lipid digestion, such as lingual lipase, gastric lipase, and pancreatic lipase, are stereospecific. TGs are typically partially hydrolyzed into free FAs and monoacylglycerol, with ester bonds on the outer positions being more susceptible to hydrolysis. Hydrolysis is a complex process that involves multiple enzymes and occurs throughout the digestive tract. It begins with lingual lipase, which plays a crucial role in infant nutrition. This lipase also acts as a catalyst in

the stomach, working in conjunction with gastric lipases (Hamosh & Scow, 1973). Both gastric and lingual lipase has a strong preference for the *sn*-3 position, and when working together, the hydrolysis at the *sn*-3 position occurs about 4 times faster than with gastric lipase alone (Jensen et al., 1982; Mackie et al., 2020). The enzyme activities of these lipases towards the *sn*-3 position is twice as high as the *sn*-1 position (Paltauf et al., 1974). Choi et al. (Choi et al., 2021) studied porcine pancreatic lipase and confirmed that the pancreatic lipase is a *sn*-1,3-regiospecific lipase. This finding aligns with previous studies showing that pancreatic lipase specifically targets the ester bond on the outer positions. However, the lipoprotein lipase hydrolyses TGs from circulating chylomicrons for peripheral tissues and has shown positional specificity towards the *sn*-1 position (Morley & Kuksis, 1972; Paltauf et al., 1974).

On the other hand, the carbon chain length and DBs of the FAs also affect digestion. The stereoselectivity of lipase activity may also be affected by the carbon chain length of the FAs. The activity of the preduodenal lipases towards short-chain, medium-chain, and long-chain FAs was different. The preduodenal lipases, being lingual lipases and gastric lipases, prefer the short and medium chain FA in the *sn*-3 position of the TG (Jensen et al., 1982). Gastric lipase releases medium and long-chain FAs in the stomach, which in turn influence the activity of pancreatic lipases when mixed in the intestinal tract (Bernback et al., 1990). *Candida antarctica* lipase B usually functions specifically at the *sn*-3 position, but as the carbon chain length increases from 8 to 18, the selectivity of the lipase switches to the *sn*-1 position (Rogalska et al., 1993). When there are PUFAs with DBs close to a carboxyl group, especially in outer positions, pancreatic lipase may be partially suppressed because of the steric hindrance (Bottino et al., 1967). However, recent research on pancreatic lipase reported a different conclusion: it is not only the regioselectivity and stereoselectivity that affects PUFA hydrolysis, but the location of the DBs also determines how PUFAs are broken down (Akanbi et al., 2014). Overall, the digestion and absorption of lipids are complex, and further research is needed to reveal the comprehensive effects of these multiple factors.

## 2.2 Identification and composition of TG molecular species

For a long time, lipid compositional analysis has focused on the FA composition, the overall FA composition at different *sn*-positions, and the positional distribution of different FAs. TG represents the major lipid fraction in natural fats and oils, and therefore insights into the molecular species profiles are essential for understanding lipids in nutrition and metabolism. Many studies have

examined TG compositions at the species level, often identifying the most abundant molecular species.

Han and Gross utilized a positive-ion ESI-MS/MS method to quantify TG molecular species from chloroform extracts of biological samples (Han & Gross, 2001). Using this technique, they analyzed the TG molecular species fingerprint of rat hearts by two-dimensional scanning, where one dimension represented FA composition, and the other dimension showed precursor ions. By calculating the carbon chain length and number of double bonds in each fatty acyl, the researchers were able to interpret the cross-peak ion abundance in the 2D spectrum. Similarly, Lin and Chen (Lin & Chen, 2014) quantified TG molecular species in Lesquerella (*Physaria fendleri*) oil using HPLC equipped with a light scattering detector and MS detector. Around 98% of TG molecular species were identified. Lesquerolic acid (20-hydroxy-*cis*-11-eicosenoic acid) (Ls) is the most abundant FA in Lesquerella oil. The most abundant TGs were Ls_Ls_O, Ls_Ls_Ln, Ls_Ls_L. Yeo and Parrish (Yeo & Parrish, 2020) examined TG profiles in salmon muscle tissue using ESI tandem MS. A total of 98 molecular species were identified, with S_O_D being the most abundant, accounting for 16.4% of the TGs in salmon muscle. Youzbachi et al. explored the TG composition of Tunisian Acacia species seed oil using positive-ion ESI-quadrupole time-of-flight-MS (ESI-QTOF-MS), identifying it as a promising food resource because of the high content of PUFA (Youzbachi et al., 2019). The results showed that Acacia seed oil is rich in UFAs, with significant differences in TG composition between different species. The most abundant molecular species were P_L_L, P_L_O, Ln_L_O, and O_O_L.

These studies illustrate how TG molecular species analysis provides valuable insights into the structural and functional diversity of lipids. Furthermore, understanding variations in TG molecular species is critical for applications in nutrition, food science, and even detecting adulterations in oils. With the continuous deepening of the research on TG molecular species, another important research direction is TG regioisomers, that is, the positional distribution of FAs on the glycerol backbone.

### 2.2.1 Identification and quantification of TG regioisomers

The detailed analysis of TG molecules, including the positional distribution of FAs, such as regioisomers and stereoisomers, and the carbon-carbon DBs location, is crucial for advancing our understanding of the structure and functionality of natural fats and oils. Despite its importance, this area of study is very challenging due to the diversity of FAs and the complexity of TG isomerism. A significant obstacle lies in the scarcity of pure regioisomer or enantiomer standards and the lack of sufficiently advanced analytical techniques.

Consequently, only a limited number of studies have successfully delved into the deeper structural levels of TG molecules.

In recent decades, considerable progress has been made in the development of analytical methodologies for TG regioisomer analysis. Modern advancements, particularly in mass spectrometers, have significantly enhanced our ability to analyze TG structures. MS-based approaches exploit various fragmentation mechanisms, for example, the preferential neutral loss of FAs from the outer positions, to identify TG regioisomers (Harvey, 2005). Separation techniques, supercritical fluid chromatography (SFC) (Xinghe Zhang et al., 2019), chiral chromatography (Řezanka et al., 2013), silver-ion chromatography (Holčapek et al., 2010), normal phase (Kalo et al., 2003) and reversed-phase (RP) chromatography (Lévêque et al., 2010), have been widely employed in TG analysis, serving not only as separation tools but also as integral components for structural elucidation, isomer discrimination, and quantification when coupled with mass spectrometry.

Studies on natural samples such as human and bovine milk have highlighted the importance of TG regioisomeric composition, especially in applications like infant formula development. Human milk triglycerides feature palmitic acid primarily at the *sn*-2 position, with UFAs occupying the outer positions (Kallio et al., 2017; Linderborg et al., 2014). However, the oil source used in the infant formula usually contains palmitic acid predominantly in the *sn*-1 and *sn*-3 positions (Fabritius et al., 2020). Recent profiling of human milk TG molecular species across lactation stages showed that compositional changes are most pronounced early in lactation and stabilize after 200 days (Lan et al., 2022).

Innovative analytical methods continue to push the boundaries of TG regioisomer research. For instance, Herrera et al. (Cubero Herrera et al., 2013) used RP-LC coupled with $MS^3$ to quantify PUFA regioisomers in fish oils, providing calibration curves for accurate quantification. Similarly, Leveque et al. (Lévêque et al., 2010) employed an RP-HPLC-ESI-MS method to analyze a series of pure regioisomer pairs of TG. To improve regioisomer sensitivity, silver nitrate was used as a post-column reagent to rationalize the TGs after the chromatographic separation. The regioisomer pairs P_O(*sn*-2)_O and O_P(*sn*-2)_O, P_P(*sn*-2)_O and P_O(*sn*-2)_P, and S_O(*sn*-2)_O and O_S(*sn*-2)_O in soya oil and rapeseed oil were identified and quantified by this method. Leveque and coworkers (Leveque et al., 2012) proposed a kinetic methodology to differentiate and quantify TG regioisomers. This was achieved by generating an alkali metal ion-bound dimeric cluster with a TG reference compound. The dimeric clusters were mass-selected and subjected to competitive dissociations in a quadrupole ion trap MS. The method was validated by soybean oil and the regioisomer pairs L_L(*sn*-2)_O and L_O(*sn*-2)_L, O_O(*sn*-2)_P and O_P(*sn*-2)_O and S_S(*sn*-2)_P and S_P(*sn*-2)_S were detected and quantified. However,

challenges persist, such as the dependency on dimer formation for certain methods.

Algorithmic approaches are gaining ground for addressing the complexity of TG compositions in natural samples. For example, Zhang et al. (Xinghe Zhang et al., 2022) developed an UPSFC-Q-TOF-MS method for identifying palmitic acid-containing TGs in various oils. They applied a calculation equation to quantify the TG regioisomers. The method was validated by analyzing human milk, mammalian milk, lard, and fish oil. The results showed that the lard had the most similar regioisomer composition with human milk, while the fish oil showed the highest palmitic acid content at the *sn*-2 position. Aiming to quantify the regioisomer compositions of those without standard reference, Balgoma and others (Balgoma et al., 2019) developed a fragmentation model. The results of sunflower oil and olive oil were in agreement with previous studies. For example, the S_O_L in sunflower oil showed the composition of 42% S_O(*sn*-2)_L, 58% S/L/O. Fabritius and others (Fabritius et al., 2020) revealed the TG regioisomer composition in human milk and infant formulas using a direct inlet MS/MS method. The MSPECTRA 1.4 software was used to calculate the regioisomer abundance. In total, 241 regioisomers were identified and quantified in human milk. The amount is more than 60 mol% of the total TGs. The human milk samples from China and Finland were compared. Eleven commercial infant formulas were also analyzed, and the results deviated largely from the human milk samples. Tarvainen et al. (Tarvainen et al., 2019) developed an ammonium adduct ESI-MS/MS method to analyze the regioisomers of TGs processing two kinds of FAs or three different FAs, so-called AAB and ABC-type TGs. The method was applied to two commercial olive oils. The regioisomer composition of nine major ACN: DB species was identified and quantified. Recently, Sazzad and coworkers (Sazzad et al., 2022) analyzed olive oil and human milk with a UHPLC-ESI-MS/MS method. To improve the efficiency and accuracy of data processing, an automatic calculation software with a fragmentation model created with reference compounds was introduced. Compared to the manual calculation, the results given by the software were similar, with a few exceptions. The fragmentation model is necessary to resolve the complex regioisomer profiles of natural fats and oils, where isobaric interference presents a commonly seen challenge.

Despite these advances, complete resolution of the regioisomeric composition of all TG molecular species remains a challenge, particularly for complex natural samples. Future research must address these gaps by developing more robust analytical methodologies, paving the way for a comprehensive understanding of TG structures and their implications for health and nutrition.

### 2.2.2 Identification and quantification of TG enantiomers

Detailed analysis of TG structures must also account for stereoisomers. When different FAs occupy the outer positions of a TG molecule, chirality arises, leading to enantiomeric pairs. These molecules exhibit distinct chiral properties; however, commonly used detectors like MS and nuclear magnetic resonance (NMR), despite their utility in lipid structural analysis, cannot differentiate enantiomers. This highlights the critical need for enantiopure standards to support their identification. Chromatographic methods, particularly chiral LC and SFC, have been the primary approaches for analyzing TG enantiomers (Han & Ye, 2021). Among these, chiral columns are indispensable, though their selection remains limited. The literature on TG enantiomer separation is sparse, reflecting the challenges in this field.

Lísa and Holčapek (Lísa & Holčapek, 2013) analyzed synthesized enantiopure TG standards and natural samples with chiral HPLC/APCI-MS. Two Lux Cellulose-1 columns coated with cellulose-tris- (3,5-dimethylphenylcarbamate) silica gel were connected in series. Using hexane and hexane: isopropanol (99:1) as mobile phases, they separated several enantiomeric pairs, including TGs with three distinct FAs, such as O_Ln(*sn*-2)_A, Ln_A(*sn*-2)_O, and Ln_O(*sn*-2)_A. They concluded that the number of DBs in the outer positions primarily dictated enantiomeric separation. However, our latest study demonstrated that enantiomeric separation depends on all three FA positions, including the carbon chain length and degree of unsaturation of the FA esterified at each position (Y. Zhang et al., 2024).

Řezanka and coworkers have extensively studied TG positional isomers and enantiomers. For instance, the TG composition of diatom *Phaeodactylum tricornutum* was compared between the normal and starvation status (Řezanka et al., 2012). Using a chiral column Astec cyclobond™ I 2000 DMP (3,5-dimethyl-phenyl-carba-mate modified β-cyclodextrin) with methanol: 10 mM ammonium acetate (99:1) as mobile phase, and coupled with APCI-MS, they identified shifts in regioisomer ratios, such as P/P/E and P/E/P, under starvation. Besides, they investigated biosynthesized TGs with odd number FAs confirming stereospecific endosynthesis (Řezanka, Vítová, et al., 2015). In other work, they explored TGs in algae such as *Sitchococcus* for its high levels of 7, 10, 13-hexadecatrienoic acid (Pn) and 7, 10-hexadecadienoic acid (Pl) as a potential resource of C16 PUFAs, separating regioisomers and enantiomers with similar chiral LC-MS methods (Řezanka, Nedbalová, et al., 2015). The regioisomers and enantiomers (Pn/Pn/Pl, Pl/Pn/Pn, Pn/Pl/Pn and Pl/Pl/Pn, Pn/Pl/Pl, Pl/Pn/Pl) were separated simultaneously. The results showed that the temperature influences the ratio of regio- and enantiomers: achiral TGs increase at lower temperatures. Moreover, dienoic FAs tend to esterify at the *sn*-3 position, whereas trienoic FAs preferentially esterify at the *sn*-1 position of the glycerol backbone. This

conclusion was again confirmed with the *Trachydiscus Minutus* (Řezanka, Lukavský, et al., 2015). The results indicate that both regioisomer and enantiomer distributions of C20 containing TGs (such as EPA and AA) are temperature-dependent. Specifically, lower cultivation temperatures lead to an increase in achiral TGs and a shift in enantiomeric ratios away from 1:1. Two Astec cyclobond™ I 2000 DMP columns were connected in series using hexane and isopropanol as the mobile phases. Different TG enantiomers and regioisomers containing EPA and AA were successfully separated. The results showed the enantiomer with more DBs on the *sn*-1 position eluted earlier than the other enantiomer. The TG species containing very long chain FAs were analyzed with a similar method (Řezanka et al., 2018). The enantiomer pairs from natural lipids, such as green alga (*Botryococcus braunii*), brewer's yeast (*Saccharomyces pastorianus*), and dinoflagellate (*Amphi-dinium carterae*), were separated.

Nagai et al. (Nagai et al., 2011) developed innovative recycling HPLC systems to improve separation efficiency. A polysaccharide-based chiral column (CHIRALCEL OD-RH) was used to separate TGs with methanol as a mobile phase. The method was able to separate the *rac*-P_P(*sn*-2)_O, *rac*-O_O(*sn*-2)_P, and *rac*-P_P(*sn*-2)_L but not *rac*-O_O(*sn*-2)_L and *rac*-P_P(*sn*-2)_S. The method was designed to resolve TGs containing both SFA and UFA at the outer (*sn*-1 and *sn*-3) positions. It was applied to the palm oil and determined the O/O/P to P/O/O ratio for the first time. The same method was also validated for the analysis of egg yolk (Nagai et al., 2017). The ratio of P/O/O to O/O/P was analyzed in egg yolk, immature egg yolk, and chicken meat. They further identified the major enantiomer pairs through LC separation and quantified their ratios using tandem MS detection (Nagai et al., 2013). The P_P(*sn*-2)_D, P_D(*sn*-2)_D, and P_P(*sn*-2)_E pairs were separated with the CHIRALCEL OD-RH column. The P_E(*sn*-2)_E was separated with a similar column CHIRALCEL OZ-3R. Methanol was used as mobile phase. The method was further developed to resolve TG enantiomers containing two palmitic acids (Nagai et al., 2015). The standards with two palmitic acids on the backbone and another SFA with a carbon chain length from 4 to 12 were synthesized. Even though these TGs possess only SFAs, they were separated with the chiral column CHIRALCEL OD-3R and methanol as mobile phase. This method was applied to bovine milk TGs and the enantiomeric ratios were determined. Recently, Nagai et al. combined chiral LC with MS to simultaneously analyze TG regioisomers and enantiomers. This approach separated TGs containing palmitic and oleic acids, providing insights into the TG composition of palm oil and lard (Nagai et al., 2019). The column used in this method was the CHIRALCEL IF-3, and acetonitrile was the mobile phase (Nagai et al., 2020). All TGs containing palmitic acid and oleic acid were separated and quantified.

Kalpio and others (Kalpio et al., 2015) also explored recycling LC for TG enantiomer separation, employing two CHIRALCEL OD-RH columns and methanol as the mobile phase. The method was able to separate 11 racemic TGs with FAs that consist of 12–22 carbons and 0–2 DBs. The TGs containing both SFA and UFA on the outer positions were more easily separated. However, the TGs containing three UFAs could not be separated by the current method. The elution order and chromatographic elution behaviors were discussed, which provided a valuable reference for investigating the lipid composition. Compounds were eluted according to their equivalent carbon number (ECN), defined as the number of carbon atoms in the FA residues minus twice the number of double bonds. Both FA chain length and degree of unsaturation significantly affected elution; shorter chain lengths and higher unsaturation levels led to faster elution and reduced retention times.

In summary, the selection of chiral columns is limited. Most of the current columns commonly used for the separation of TG enantiomers contain the 3,5-dimethylphenyl carbamate. Further research is essential to develop new chiral columns and optimize solvent combinations, aiming for faster and more precise TG enantiomer separation.

## 2.3 Identification and composition of GPL molecular species and regioisomers

GPLs represent a major lipid class in the human body alongside TGs. The primary role of GPLs lies in their function as essential components of biological membranes (Ramos-Martín & D'Amelio, 2022). Together with proteins, cholesterol, and other molecules, GPLs play critical roles in cell-to-cell communication, maintaining basal metabolism and balancing hormone secretion. Beyond these functions, GPLs have been shown to lower serum cholesterol levels and reduce the risk of cardiovascular diseases (Lagace & Ridgway, 2013). Understanding the structure of GPLs is therefore crucial for elucidating their metabolic mechanisms. Despite their importance and the similarity with TGs (**Figure 4**), the structural analysis of GPLs remains less explored compared to TGs. The diversity of FA compositions and the limited availability of regioisomeric standards for GPLs have significantly hindered the development of analytical methods. Consequently, research in this area has been relatively sparse, with much of the existing literature focusing on PCs, largely due to the relative ease of access to PC standards.

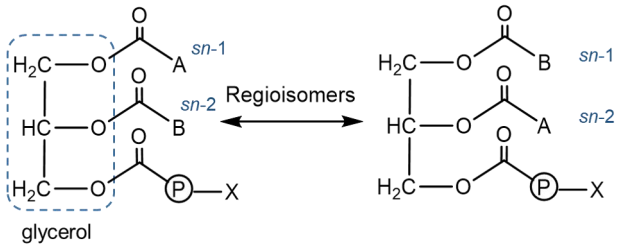


**Fig. 4** The basic structures of GPL and stereospecific numbering (*sn*). A and B are different fatty acids. X represents different substitutes.

The molecular composition of PCs in natural fats and oils has been a research focus, given its implications for understanding GPL functions and metabolism. In early studies, Ekroos and others (Ekroos et al., 2003) utilized FA scanning and $MS^3$ ion trap fragmentation to analyze PCs in negative ion mode. Upon collision-induced dissociation (CID), they observed that the abundance of fatty acid product ions correlated with the *sn*-position. Notably, the neutral loss product ions were found to be exclusively dependent on the *sn*-position. The acyl anion fragment derived from the *sn*-2 FA was consistently more abundant than that from the *sn*-1 position, which enabled structural assignment of *sn*-positional isomers. This method was validated in analysis of human red blood cells and Madin-Darby canine kidney (MDCK) II cells. They identified 18 PC species in red blood cells and 25 in MDCK II cells, but regioisomer quantification was limited by the availability of synthetic references. Twenty-two molecular species were detected in human red blood cells, and seven regioisomer pairs were identified based on the synthesized reference compounds. The results of the MDCK II cell reported 44 molecular species, however, only five regioisomer pairs were quantified by this method. Campbell & Baba (Campbell & Baba, 2015) used electron impact excitation of ions from organics (EIEIO) with MS to detect 14 PC species in egg yolk lipids, determining DB positions but encountering challenges in regioisomer identification due to limited standards. A combination of the FA fragment $[RCOO]^-$ ion ratio and partial chromatographic separation was employed to calculate regioisomer ratios (Wozny et al., 2019). This method quantified the regioisomers of PC 16:0_18:1 and PC 18:0_18:1 in both bovine liver and *E. coli* lipid extracts. Validation was performed using an enzyme-catalyzed approach, wherein phospholipase $A_2$, which specifically liberates the FA at the *sn*-2 position, was applied to PC standards. The results demonstrated that biological samples exhibited higher regioisomeric purity compared to synthetic lipid standards. However, the reliance of the method on standard compounds restricts its broader applicability. Young et al. (Young et al., 2022) combined triple-stage fragmentation with matrix-assisted laser desorption ionization-mass spectrometry imaging (MALDI-MSI) to examine PC regioisomers in prostate cancer tissues. Their approach allowed comprehensive

structural characterization, including *sn*-positions and DB locations, revealing metabolic differences between dietary and endogenously synthesized FAs. The DBs of glycerophospholipids were determined by combining sequential CID and ozone-included dissociation (OzID). The cancer cells were labeled with isotope-labelled FAs. The results showed that the labeled FA uptake was strongly associated with the *sn*-positions. These labeled FAs influence the repartitioning of PUFAs on the glycerophospholipid classes as well. This confirmed the differences in the metabolic fate of dietary and endogenous FAs.

Advancements in analytical methods have enhanced our ability to characterize GPL structures. Liu and Rochfort (Liu & Rochfort, 2022) employed Paterno-Buchi photochemical tagging combined with LC-MS/MS to identify the *sn*-positions and DB locations of FAs in PC and PE species from bovine milk. The study analyzed six PC species (PC 32:1, PC 34:1, PC 34:2, PC 36:1, PC 36:2, and PC 36:3) along with six PE species (PE 32:1, PE 34:1, PE 34:2, PE 36:1, PE 36:2, and PE 36:3). Their results highlighted the prevalence of DB positional isomers in major FA species, underscoring the complexity of GPL metabolism. Pham et al. (Pham et al., 2014) described a targeted lipidomic approach that combines CID with OzID to analyze PC 16:0_18:1 in bovine brain and kidney tissues. Their findings demonstrated that the relative abundance of regioisomer pairs, such as PC 16:0/18:1 and PC 18:1/16:0, varies between organs. Tang and coworkers (Tang et al., 2022) further advanced tandem MS methodologies by combining CID with a hybrid ion trap-Orbitrap MS, enabling simultaneous analysis of GPL head groups, FA chains, DB locations, and *sn*-positions in mouse prostate cancer tissue. Their comprehensive analysis identified 13 major PC species, 25 FA chain length isomers, 37 DB location isomers, and 47 *sn*-positional isomers, revealing significant differences between cancerous and healthy tissues. In addition, ultraviolet photodissociation (UVPD) was applied to analyze glycerophospholipids. Williams and others (Williams et al., 2017) used the ESI-UVPD-$MS^3$ to analyze the lipid extracts of biological samples. Via a direct infusion approach, the bovine liver and porcine brain extracts were analyzed. The molecular species PC 16:0_18:1 was composed of four isomers, PC 16:0/18:1(9), PC 18:1(9)/16:0, PC 16:0/18:1(11), PC 18:1(11)/16:0, including the FA positional and DB positional isomers. Besides the PC, 21 PE isomers were identified by this method in *Escherichia coli* lipid extract.

Mass spectrometry imaging (MSI) has become a powerful technique for visualizing GPL structures and their spatial distribution in tissues. Although MSI offers a high level of molecular specificity, the chemical complexity of tissue samples presents unique challenges for the resolution and identification of compounds. Paine et al. (Paine et al., 2018) used MSI to analyze PC regioisomers in the mouse brain, discovering distinct differences between tumorous and normal brain regions. Lillja and Lanekoff (Lillja & Lanekoff, 2022) combined

silver ion cationization with tandem MS to localize PC molecular species in the mouse brain, demonstrating that certain regioisomers, such as PC 18:1/16:0, accumulate in sub-hippocampal regions. Consistent with those findings, Claes and others (Claes et al., 2021) revealed a distinct distribution of regioisomers in rat brains. With the OzID and sequential CID-OzID combined with MALDI-MSI, they were able to image both DB and positional isomers in biological samples. These findings provide references for studying the structurally defined lipids in animal tissues.

Alterations in GPL metabolism are increasingly associated with disease states. Some researchers developed GPL regioisomer analytical methods to detect disease-driven chemical alterations in the lipid profile. For example, Zhao et al. (Zhao et al., 2019) developed a workflow to determine the positional distribution of FAs and the DB location of PC molecules. There were 82 distinct PC molecular species were detected in the polar extract of bovine liver. Among them, 19 pairs of regioisomers were quantified. Application of this method to human breast cancer cells revealed significant alterations in PC regioisomer composition. Klein and coworkers (Klein et al., 2018) explored GPL profiles across a range of human tissues, including endometrial, kidney, lymph node, ovarian, pancreas, and brain tissues. Their findings align with those of Paine et al. (Paine et al., 2018), detecting differences in the relative abundances of GPL regioisomers between normal and cancerous tissue, for example, medulloblastoma tumors in the brain. Cao et al. (Cao et al., 2020) used Paternò-Bǜchi (PB) reaction with MS/MS to elucidate lipid structures on a large scale. Their analysis showed that lipid regioisomer quantification alone could distinguish human breast cancer cells, but identifying lung cancer tissues required both DB location and regioisomer quantification. Recently, Yan et al. (Yan et al., 2025) developed a methodology for mapping PC *sn*-positional isomers using the CID of divalent metal complexes in MSI. By forming PC-metal complexes, this approach enables the differentiation of PC regioisomers. The methodology was applied to rat brain and glioblastoma tissues, revealing significant differences in the spatial distribution of regioisomers across regions such as white matter, molecular layers, and granular layers. Notably, PC 16:0/18:1 was more abundant in non-tumor regions compared to its regioisomer PC 18:1/16:0, highlighting its potential for clinical diagnosis.

In neurological disorders, lipidomics has revealed a strong connection between GPL profiles and Alzheimer's disease (AD). Khan et al. (M. J. Khan et al., 2022) conducted a targeted lipidomic analysis of human plasma samples and identified five GPL molecular species that were significantly decreased in AD patients: PS 18:0_18:0, PC 16:0_22:6, PC 18:0_22:6, PS 18:0_20:0, and PC 18:1_22:6. Interestingly, the study observed racial differences in GPL composition, with PS 20:0_20:1 levels differing between African American and

non-Hispanic white adults, highlighting its potential as a key biomarker for early diagnosis. A recent study provided further insights into the relationship between GPL metabolism and AD using a mouse brain model (Xu et al., 2024). The researchers developed a four-dimensional lipidomic strategy based on high-resolution demultiplexing ion mobility spectrometry (IMS), complemented by an in-house database and machine learning predictions. This technology simultaneously obtained information from *m*/*z*, retention time, collision cross section, and MS/MS spectra these four dimensions. Analyzing the hippocampus, cerebellum, and cortex separately, the study identified 592 GPLs, including 130 regioisomer pairs. The distribution of GPLs varied across brain regions, with PC and PE species being dominant in all areas. Notably, the AD group exhibited a marked reduction in glycerophospholipid content compared to wild-type controls. Specifically, the abundances of PE 16:0/22:6 and PE 18:0/22:6 were significantly lower in AD mice. These findings underscore the potential of lipid biomarkers, such as molecular species and regioisomers, to facilitate early clinical diagnosis of AD and other diseases. Further advancements in analytical methods and biomarker discovery will enhance our understanding of the role of GPL metabolism in disease progression.

## 2.4 N-3 polyunsaturated fatty acids

N-3 PUFAs, also known as omega-3 FAs, are a group of PUFA characterized by carbon DBs at the third carbon atom from the terminal methyl group. The most well-known n-3 PUFAs are ALA, DHA, and EPA. The molecular structures of them are shown in **Figure 5**. Among them, DHA and EPA are particularly crucial due to their limited endogenous synthesis and numerous health benefits throughout life. This thesis focuses on the positional distribution of n-3 PUFAs to better understand their functional properties and optimize their utilization as a valuable resource, exploring their potential to improve health outcomes and support biological functions.

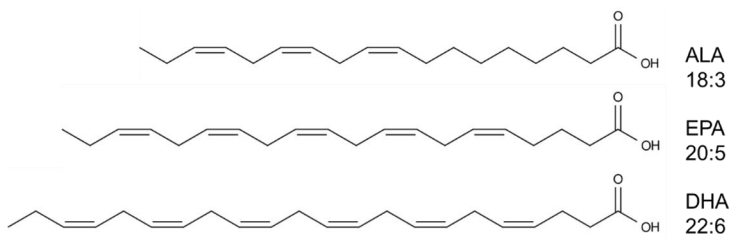


**Fig. 5** The molecular structure of ALA, EPA, and DHA.

### 2.4.1 Health effects

The study of n-3 PUFAs has attracted enduring interest, as their numerous health benefits are widely recognized and well-established. As illustrated in **Figure 6**, extensive literature has linked n-3 PUFAs to various health outcomes, including the prevention and management of cardiovascular diseases (Laguzzi et al., 2024), diabetes (Georgiou & Prokopiou, 2023), arthritis (Léger et al., 2023), obesity (Smorenburg et al., 2025), Alzheimer's disease (Oye Mintsa Mi-Mba et al., 2024), maternal and child health (Y. Wang et al., 2023), and retina health (Swinkels & Baes, 2023). Extensive research has been conducted on the health effects of n-3 PUFAs, and previous reviews have thoroughly and systematically covered various aspects of this field (Innes & Calder, 2020; I. Khan et al., 2023; Saini et al., 2021). Instead of revisiting these established findings, this review highlights recent advances in n-3 PUFA research and provides insights into the latest developments and current progress.

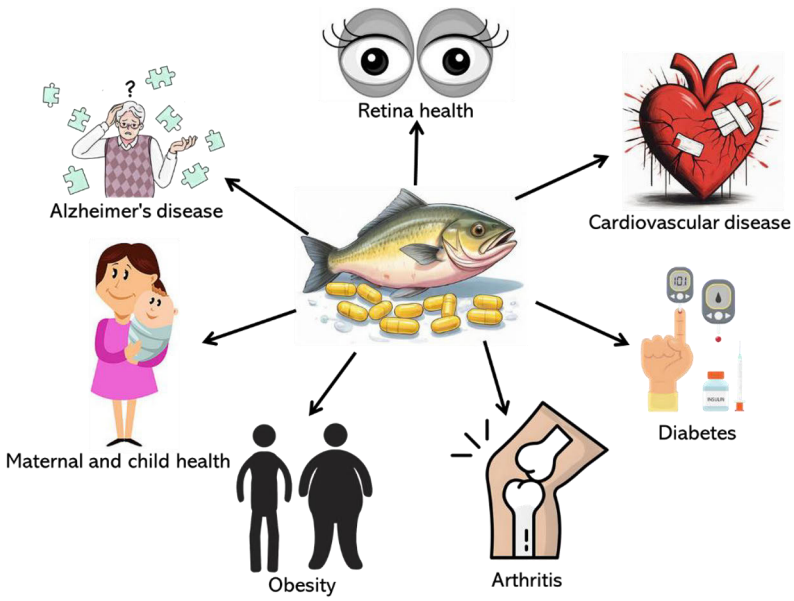


**Fig. 6** Health benefits of n-3 PUFAs.

DHA is particularly and widely promoted for pregnant women and young children due to its remarkable benefits. For example, Toro et al. (De Toro et al., 2024) investigated the effects of an 800 mg/day DHA supplementation during pregnancy, compared to 200 mg/day, on the growth patterns of infants born to mothers with pre-pregnancy obesity, which is one of the most relevant perinatal factors leading to high birth wight and childhood obesity. Volunteer mothers who were overweight or obese before 15 weeks of pregnancy were recruited and received the supplements until delivery. Their findings revealed that the higher

dose of DHA limited postnatal weight gain during the first four months of life. However, Gould et al. reported no significant benefits of prenatal DHA supplementation on child behavior, highlighting the need for further research (Gould et al., 2021).

The impact of n-3 PUFAs on gut microbiota has previously been investigated in healthy adults (Miao et al., 2022). Recently, Kawamura et al. (Kawamura et al., 2023) conducted a randomized trial on female athletes, a group requiring high levels of adaptation in muscle and other organ functions, to evaluate the effects of an 8-week intervention with perilla oil, which is abundant in ALA. The results showed that a daily intake of 3 g/day and 9 g/day of perilla oil improved gut function. Notably, the higher dosage group exhibited more pronounced benefits, including increased abundance of butyrate-producing bacteria (*Lachnospiraceae*), reduced levels of *Proteobacteria*, and decreased urinary indoxyl sulfate levels. These findings suggest that daily supplementation with perilla oil is beneficial for female athletes. In contrast, Schoeler et al. (Schoeler et al., 2023) investigated the effects of diets with different FA compositions in mice. Their findings revealed that diets enriched with n-3 PUFAs or medium-chain SFAs significantly reduced steatosis compared to a milk-fat diet. However, these dietary changes had no measurable effect on the gut microbiota. This suggests that the ability of moderate levels of dietary n-3 PUFAs to reduce steatosis and influence hepatic metabolism occurs primarily through microbiota-independent mechanisms, rather than *via* modulation of the gut microbiota.

Many of the health benefits of n-3 PUFAs are attributed to their anti-inflammatory properties. For example, Costenbader et al. (Costenbader et al., 2024) reported the outcomes of a double-blind, placebo-controlled trial conducted on more than 20,000 men and women over 50 years old across the United States. Participants received marine n-3 PUFA capsules containing 460 mg of EPA and 380 mg of DHA for over five years, while the placebo group received olive oil. Two years after the intervention, results indicated a 15% reduction in autoimmune disease incidence in the n-3 PUFA supplementation group, demonstrating a sustained protective effect. A placebo-controlled crossover clinical trial by Peña-de-la-Sancha et al. (Peña-de-la-Sancha et al., 2023) evaluated the efficacy of n-3 PUFAs in 18 hypertriglyceridemic patients. Participants received 460 mg of EPA and 380 mg of DHA twice daily for five weeks. The supplementation significantly decreased body mass index, waist circumference, and plasma TGs, while plasma HDL-TG, HDL-cholesterol, and HDL-phospholipids significantly increased. Additionally, the EPA-to-AA ratio within HDLs more than doubled, indicating enhanced anti-inflammatory properties of these lipoproteins.

The immunomodulatory properties of n-3 PUFAs were reported to reduce bone loss as well (Dou et al., 2022). Feehan et al. (Feehan et al., 2023)

investigated the relationship between n-3 PUFAs and bone mineral density and turnover in postmenopausal women, a group at high risk of osteoporosis. A favorable n-6: n-3 ratio was also linked to increased femoral bone mineral density, highlighting their role in bone health preservation.

In addition to bone health, the n-3 PUFAs show health benefits for skeletal muscle as well. An 8-week trial on elderly people studied the effects of a whey-enriched diet with n-3 PUFA supplementation on muscle strength. The participants did exercises daily within the intervention period (Cornish et al., 2022). The results indicated that the exercise together with the high-protein diet with n-3 PUFA supplementation increased muscle strength and reduced inflammation in elderly men but not in old women. Another randomized clinical trial examined the effects of daily n-3 PUFA supplementation on daily protein homeostasis in patients with chronic obstructive pulmonary disease. After 4 weeks of intervention, the protein breakdown was lower. The results suggested daily supplementation with DHA+EPA is beneficial for patients with chronic obstructive pulmonary disease (Engelen et al., 2022).

Recent findings reveal that n-3 PUFAs also play a pivotal role in actively resolving inflammation by promoting the biosynthesis of specialized pro-resolving mediators (SPMs), a distinct class of bioactive lipid mediators critical for orchestrating the resolution phase of inflammation. SPMs derived from n-3 PUFAs include protectins, resolvins (13-, E-, and D-series), and maresins. Research has shown that these mediators reduce inflammation-related symptoms such as pain, swelling, and redness (Dyall et al., 2022). The effects of oral treatment with maresin 1 on behavioral pain responses and spinal neuroinflammation were investigated in a mouse model. The results demonstrated that oral administration of maresin 1 produced significant antinociceptive effects in a spared nerve injury-induced model of neuropathic pain. Notably, these effects persisted for several days beyond the intervention period. These findings highlight the potential of SPMs as promising therapeutic strategies for the management of neuropathic pain (Teixeira-Santos et al., 2023). Aguirre et al. (Aguirre et al., 2023) investigated the role of SPMs in pancreatic stellate cell activation to evaluate their role in limiting disease progression. The study identified n-3 DPA-derived resolvin R5 ($RvD5_{n\text{-}3\ DPA}$) as a critical SPM involved in regulating cancer-stroma interactions and reducing cancer cell invasion in pancreatic ductal adenocarcinoma. The study revealed that $RvD5_{n\text{-}3\ DPA}$ suppressed pancreatic stellate cell-mediated cancer cell invasion, while its inhibition exacerbated invasion. Furthermore, circulating levels of $RvD5_{n\text{-}3\ DPA}$ were lower in metastatic patients compared to non-metastatic patients, underscoring its potential role in limiting disease progression and chemoresistance.

These findings collectively highlight the diverse mechanisms through which n-3 PUFAs exert their health benefits. By promoting the biosynthesis of SPMs, n-3 PUFAs offer promising therapeutic potential, paving the way for novel drug design and innovative treatments for chronic inflammation and associated diseases. Expanding our understanding of these mechanisms provides new opportunities for harnessing n-3 PUFAs to improve human health.

### 2.4.2 Bioavailability

While most research on n-3 PUFAs focuses on their health benefits, studies on their bioavailability remain relatively scarce. Bioavailability, defined as the degree to which a nutrient or chemical is freely available for absorption, is a critical factor in maximizing the efficacy of these valuable FAs. A systematic investigation of their bioavailability would provide insights to support the food and feed industries in developing efficient n-3 PUFA supplement products, as well as benefiting manufacturers of nutraceuticals and functional foods.

The bioavailability of FA is influenced by multiple factors, including the chemical binding form, food composition, and hormone levels. For example, a crossover study involving 13 healthy women evaluated the impact of food structure on n-3 PUFA absorption. Participants consumed intact salmon (preserved structure), minced salmon (partially preserved structure), and defatted salmon flour supplemented with salmon oil (no structure) (Ahmed Nasef et al., 2021). Plasma concentrations of DHA and EPA were significantly higher after consuming intact salmon, indicating that the natural food matrix structure enhances n-3 PUFA bioavailability. Similarly, Ghasemifard et al. (Ghasemifard et al., 2015) demonstrated that bioavailability is also influenced by gender, with female rats exhibiting significantly higher absorption of n-3 PUFAs compared to males in an animal study.

The chemical form of n-3 PUFAs plays a key role as well. For example, DHA and EPA extracted from anchovy oil showed significantly lower bioavailability in their ethyl ester form compared to the TG form after 24 hours of incubation with Caco-2 cell (R. Song et al., 2023). This result is consistent with the findings of some previous studies. Cui et al. (Cui et al., 2022) compared EPA-lysophosphatidylcholine (LPC), DHA-LPC, and EPA-PC in a mouse study. Brain DHA levels in the LPC groups were significantly higher than in the PC group after two weeks of intervention. Moreover, Calanus oil, which contains DHA primarily as a wax ester, demonstrated comparable efficacy to fish oil and krill oil in increasing DHA levels in humans, confirming its bioavailability close to that of DHA in TG form (Vosskötter et al., 2023).

The positional distribution of FAs on the glycerol backbone of TG is increasingly recognized as another critical factor. Christensen et al. (M.

Christensen et al., 1995) found that EPA and DHA at the *sn*-2 position were more readily absorbed than TGs with random FA distribution. In a 12-week hamster trial, Bandarra et al. (Bandarra et al., 2016) showed that the presence of DHA at the *sn*-2 position in TGs was associated with enhanced accumulation of EPA and DHA in the liver, erythrocytes, and brain. Despite these findings, some researchers suggest that the advantages of the *sn*-2 position may be minimal or short-termed advantages (Mensink et al., 2016; Sala-Vila et al., 2008). In contrast, research comparing the *sn*-1 and *sn*-3 positions remains limited. Linderborg et al. (Linderborg et al., 2019) conducted a 5-day feeding trial to examine the differences between DHA in three positions of dietary TG in DHA bioavailability in mildly n-3 deficient rats. The results suggested that the *sn*-2 position provided better bioavailability for DHA than the outer positions, with the *sn*-1 group showing slightly higher plasma DHA levels than the *sn*-3 group, although the difference was not statistically significant. A longer 4-week feeding trial revealed that DHA at the *sn*-3 position in TG, supplemented on top of n-3 deficient diet, resulted in high DHA accumulation in visceral fat, while DHA from the *sn*-1 position led to the highest plasma levels in rats (Y. Zhang et al., 2023). These findings underscore the complexity of n-3 PUFA bioavailability and highlight the need for further research to optimize their utilization in dietary and therapeutic applications.

### 2.4.3 Deficiency status

Research on the n-3 FAs deficiency provides critical insights into their health effects and the underlying mechanisms of various diseases. Beyond the well-established importance of preventing n-3 PUFA deficiency in early life, numerous diseases have been linked to inadequate n-3 PUFA intake, including AD (Xin Zhang et al., 2024), cardiovascular disease (Michaeloudes et al., 2023), and diabetes (Ding et al., 2023). DHA has been shown to promote cell cycle exit and suppressing cell death (Kawakita et al., 2006). In this way, it enables hippocampal neurogenesis *in vivo*, which is related to memory and spatial orientation and AD (Pomponi & Pomponi, 2008). Additionally, n-3 PUFAs also reduce the risk of cardiovascular disease by inhibiting the development of endothelial cell inflammation and affecting the function and regulation of vascular biomarkers (Yamagata, 2017).

Despite these benefits, global n-3 PUFA intake remains insufficient, with approximately 70% of the population consuming inadequate amounts (Dempsey et al., 2023). Early clinical trials, such as the one by Uauy and others (Uauy et al., 1990) revealed the consequences of n-3 PUFA deficiency in infants. Their study demonstrated significantly reduced rod electroretinogram amplitudes in infants fed n-3 deficient formula compared to those receiving breast milk or n-3-rich formula. However, due to ethical constraints, human clinical trials on n-3

PUFA deficiency are limited, necessitating reliance on animal studies for further understanding. Animal studies have provided valuable insights. For instance, Weisinger and colleagues conducted multiple trials on guinea pigs to evaluate the effects of n-3 PUFA deficiency (Weisinger et al., 1996, 1998, 1999). Analysis of retinal samples revealed that approximately 90% of DHA loss occurred during the first 12 weeks of deficiency, with minimal change thereafter. These findings suggest that retinal DHA levels are highly responsive in early life but are strongly influenced by age. Notably, functional deficits induced by deficiency were reversed after 10 weeks of ALA supplementation. The study revealed that a small amount of PUFAs in the maternal diet resulted in an increase of approximately 60% in retinal DHA levels in the retina of weaning pigs. This finding underscores the significance of maternal n-3 PUFA intake, demonstrating that adequately nourished mothers could provide infants with sufficient reserves to withstand prolonged periods of post-weaning deficiency. Zou et al. (Zou et al., 2023) investigated the effects of n-3 PUFA level on pancreatic injury in mice. The 30-day deficiency diet results in aggravated streptozotocin-induced pancreas injury by reducing the insulin level and pancreatic β-cell function.

On the other hand, the dietary recommendations for DHA and EPA intake vary worldwide. The Global Organization for EPA and DHA (GOED) compiles statistics on current dietary recommendations for n-3 PUFA all over the world. There were 165 recommendations, issued by 58 organizations in 25 countries on the list published in 2014. The GOED recommended the following intake based on the current body of scientific evidence: For generally healthy adults, the recommended daily intake is 500 mg EPA+DHA; for pregnant and lactating women, the optimal intake is 700 mg per day and 1000 mg for secondary prevention of coronary heart diseases. For a range of additional health conditions, such as blood pressure, TGs, and so on, a higher intake of 1 g per day is supported. However, the World Health Organization, the Food and Agriculture Organization of the United Nations, the International Society for the Study of Fatty Acids and Lipids, and other global organizations suggested similar or different recommendations. This highlights the need for systematic studies to harmonize global guidelines and policies regarding n-3 PUFA recommendations.

## 2.5 Summary

TG molecular structure is not complex itself, but when analyzing natural fats and oils, the mixture of many different TGs and their structural isomers makes the task very challenging. The composition of TGs is the result of complex biosynthetic processes driven by stereospecific enzymes, producing unique species-specific patterns of FA content and their spatial organization within the

molecules. Although the study of chirality in various food components is gaining attention, the relevance and role of chirality in TGs are not yet fully understood. Nevertheless, the arrangement of FAs in TGs plays a significant role in several areas, including metabolomics, biochemistry, and physical properties of fats and oils, as well as in food products.

The positional distribution of FAs within lipid molecules plays a critical role in their digestion, absorption, and subsequent metabolism. For instance, n-3 PUFAs exhibit distinct accumulation preferences depending on their *sn*-positions, which directly influence their bioavailability and health benefits, including their potent anti-inflammatory effects. Additionally, the n-3 PUFA-derived SPMs further highlight their therapeutic potential in resolving inflammation and promoting tissue homeostasis. Advanced analytical techniques, including MS, and HPLC, have been extensively applied to uncover the lipid structural profiles, providing valuable insights into the structure-function relationships of lipid molecules. However, the role of TG chirality, particularly concerning n-3 PUFAs, remains an area requiring deeper investigation. Furthermore, analytical methodologies for studying natural fats and oils require continued innovation to improve accuracy and efficiency.

By bridging the gap in understanding TG structural dynamics and the unique properties of n-3 PUFAs, future research can drive advancements in functional foods, nutraceuticals, and novel therapeutics. Continued progress in this field holds the potential to unlock new opportunities for optimizing lipid utilization and enhancing human health.

# 3 AIMS OF THE STUDY

The general aim of this thesis was to optimize the novel chiral chromatographic method (Study I) and enhance the current understanding of the effect of stereo- and regiospecific position of DHA on the bioavailability of n-3 PUFAs (Study II) and the GPL regioisomers in rat organs (Study III). There were three studies included in this thesis. The first one focused on the chiral chromatographic separation of enantiomers; the second and the third ones were related to an animal trial.

The objectives of individual studies were:

1) To provide new insights into the chromatographic elution behavior and retention mechanism of chiral ABC-type TGs, thereby facilitating the analysis of complex natural lipids (Study I). Hypothesis: The elution order and the time needed for separation are dependent on the FA structure at different *sn*-positions of TG, affected by both the acyl carbon chain length and the number of DBs.

2) To investigate the impact of the n-3 deficiency on the FA composition of tissues and organs in rats (Study II). Hypothesis: Four-week n-3 deficient feeding results in tissue-/organ-specific alteration in FA composition, with decreased levels of n-3 PUFAs and increased levels of n-6 PUFAs.

3) To study the impact of stereospecific positioning of DHA in dietary TG molecules on the bioavailability and tissue accumulation of these important n-3 PUFAs in a four-week feeding trial (Study II). Hypothesis: DHA supplementation reverts the impact of an n-3 deficient diet, and the bioavailability of DHA depends on its stereospecific positioning in the TG molecules.

4) To reveal the PC species and regioisomer profile in various rat organs (Study III). Hypothesis: Using the newly developed methods and software, the molecular species and regioisomer profiles of PC of rat tissues and organs can be revealed for the first time.

5) To study the impact of n-3 deficient diet and supplementation with structured TGs containing DHA at *sn*-1, 2, or 3 positions on PC species and regioisomer profiles in tissues and organs (Study III). Hypothesis: Feeding with an n-3 deficient diet may alter the molecular species profile and regioisomeric

composition of PC in tissues and organs of rats, and positioning of DHA in dietary TGs may influence the regioisomeric composition of PC.

# 4 MATERIALS AND METHODS

## 4.1 Materials

The commercial standards included 16 racemic TG samples with ECN within 42-52 (**Table 1**), and two internal standards triheptadecanoin (17:0/17:0/17:0) and dinonadecanoyl-phosphatidylcholine (PC 19:0/19:0) for FA analysis. The GPL standards were 1,2-diheptadecanoyl-phosphatidylcholine (PC 17:0/17:0), 1,2-diheptadecanoyl-phosphotidylserine (sodium salt) (PS 17:0/17:0) and 1,2-diheptadecanoyl-phosphoethanolamine (PE 17:0/17:0). All of them were purchased from Larodan (Solna, Sweden). **Table 2** lists the synthesized enantiopure TGs analyzed in this thesis. The TGs were categorized into several types for ease of description. TGs having two SFAs but not on the outer positions were categorized as USS-type. Those with two SFAs on the outer positions were called SUS-type. Similarly, TGs containing two UFAs were divided into UUS and USU-type. The USS' indicates the SFA is not identical with the other (S is not identical with S').

The chemical synthesis of the structured TGs in this thesis refers to several different chemical synthesis methods based on the features of the TG molecule and FA composition. First, the TGs with only one UFA, the USS'-type TGs were synthesized by a six-step chemo enzymatic route described by Gudmundsson et al. (Gudmundsson et al., 2020). Additionally, when synthesizing the enantiostructured TGs containing DHA, the method used was published by Kalpio et al. (Kalpio et al., 2020). The SUS'-type, which contains two SFA at the *sn*-1 and *sn*-3 positions were mostly prepared by a similar six-step chemo enzymatic approach described by Gudmundsson et al. (Gudmundsson et al., 2020) and Kristinsson and Haraldsson (Kristinsson & Haraldsson, 2008). Some of the SUS'-type TGs were synthesized in the same way as UU'S and USU' by a modified method developed by Haraldsdottir (Haraldsdottir et al., 2024). A different *p*-methoxybenzyl protecting group was introduced in a similar six-step chemo enzymatic method. Finally, the tripalmitin was synthesized with the aid of the immobilized *Candida antarctica* lipase (Haraldsson et al., 2000). All intermediate and final TG products were achieved with high chemical and enantiomeric purity. The molecular structures were fully characterized using $^{1}H$ and $^{13}C$ NMR, IR spectroscopy, and MS analyses. Additionally, enantiomeric purity was determined through specific optical rotation measurements and chiral recycling HPLC.

The standard mixtures of fatty acid methyl esters (FAME) used for the FA analysis were Supelco 37 Component FAME Mix (Sigma-Aldrich, St. Louis, MO, USA) and GLC-566c (Nu-Chek-Prep, Elysian, MN, USA). The reference compounds were at least 98% purity or higher. All organic solvents used in lipid

extraction, fractionation, and chromatographic analysis such as methanol, chloroform, and hexane were HPLC grade. The mobile phase, including the water used for the MS analysis, was MS-grade.

**Table 1** List of commercial TG reference compounds from Larodan

| TG | Trivial name | Abbreviation | ECN | Type |
|---|---|---|---|---|
| *rac*-18:2_18:1(*sn*-2)_12:0 | 1(3)-linoleoyl-2-oleoyl-3(1)-lauroyl-*rac*-glycerol | *rac*-L_O(*sn*-2)_La | 42 | USS' |
| *rac*-18:1_12:0(*sn*-2)_18:2 | 1(3)-oleoyl-2-lauroyl-3(1)-linoleoyl-*rac*-glycerol | *rac*-O_La(*sn*-2)_L | 42 | USU' |
| *rac*-18:1_18:2(*sn*-2)_12:0 | 1(3)-oleoyl-2-linoleoyl-3(1)-lauroyl-*rac*-glycerol | *rac*-O_L(*sn*-2)_La | 42 | UU'S |
| *rac*-16:0_18:1(*sn*-2)_12:0 | 1(3)-palmitoyl-2-oleoyl-3(1)-lauroyl-*rac*-glycerol | *rac*-P_O(*sn*-2)_La | 44 | SUS' |
| *rac*-18:1_12:0(*sn*-2)_16:0 | 1(3)-oleoyl-2-lauroyl-3(1)-palmitoyl-*rac*-glycerol | *rac*-O_La(*sn*-2)_P | 44 | USS' |
| *rac*-18:1_16:0(*sn*-2)_12:0 | 1(3)-oleoyl-2-palmitoyl-3(1)-lauroyl-*rac*-glycerol | *rac*-La_P(*sn*-2)_O | 44 | USS' |
| *rac*-16:0_18:1(*sn*-2)_18:2 | 1(3)-palmitoyl-2-oleoyl-3(1)-linoleoyl-*rac*-glycerol | *rac*-P_O(*sn*-2)_L | 46 | SUU' |
| *rac*-18:1_18:2(*sn*-2)_16:0 | 1(3)-oleoyl-2-linoleoyl-3(1)-palmitoyl-*rac*-glycerol | *rac*-O_L(*sn*-2)_P | 46 | UU'S |
| *rac*-18:1_16:0(*sn*-2)_18:2 | 1(3)-oleoyl-2-palmitoyl-3(1)-linoleoyl-*rac*-glycerol | *rac*-O_P(*sn*-2)_L | 46 | USU' |
| *rac*-18:1_16:0(*sn*-2)_18:0 | 1(3)-oleoyl-2-palmitoyl-3(1)-stearoyl-*rac*-glycerol | *rac*-O_P(*sn*-2)_S | 50 | USS' |
| *rac*-16:0_18:0(*sn*-2)_18:1 | 1(3)-palmitoyl-2-stearoyl-3(1)-oleoyl-*rac*-glycerol | *rac*-P_S(*sn*-2)_O | 50 | SS'U |
| *rac*-16:0_18:1(*sn*-2)_18:0 | 1(3)-palmitoyl-2-oleoyl-3(1)-stearoyl-*rac*-glycerol | *rac*-P_O(*sn*-2)_S | 50 | SUS' |

**Table 1** List of commercial TG reference compounds from Larodan (continue)

| TG | Trivial name | Abbreviation | ECN | Type |
|---|---|---|---|---|
| *rac*-16:0_18:1(*sn*-2)_20:0 | 1(3)-palmitoyl-2-oleoyl-3(1)-arachidoyl-*rac*-glycerol | *rac*-P_O(*sn*-2)_A | 52 | SUS' |
| *rac*-18:1_20:0(*sn*-2)_16:0 | 1(3)-oleoyl-2-arachidoyl-3(1)-palmitoyl-*rac*-glycerol | *rac*-O_A(*sn*-2)_P | 52 | USS' |
| *rac*-18:1_16:0(*sn*-2)_20:0 | 1(3)-oleoyl-2-palmitoyl-3(1)-arachidoyl-*rac*-glycerol | *rac*-O_P(*sn*-2)_A | 52 | USS' |
| *rac*-14:0_18:1(*sn*-2)_16:0 | 1(3)-myristoyl-2-oleoyl-3(1)-palmitoyl-*rac*-glycerol | *rac*-M_O(*sn*-2)_P | 46 | SUS' |
| 17:0-17:0-17:0 | 1,2,3-heptadecanoic-glycerol | | 51 | SSS |

**Table 2** List of the synthesized enantiopure TG reference compounds

| TG | Trivial name | Abbreviation | ECN |
|---|---|---|---|
| 10:0/16:0/18:1 | 1-decanoyl-2-palmitoyl-3-oleoyl-glycerol | C/P/O | 42 |
| 10:0/18:1/16:0 | 1-decanoyl-2-oleoyl-3-palmitoyl-glycerol | C/O/P | 42 |
| 12:0/14:0/18:1 | 1-lauroyl-2-myristoyl-3-oleoyl-glycerol | La/M/O | 42 |
| 12:0/16:0/18:2 | 1-lauroyl-2-palmitoyl-3-linoleoyl-glycerol | La/P/L | 42 |
| 12:0/18:1/14:0 | 1-lauroyl-2-oleoyl-3-myristoyl-glycerol | La/O/M | 42 |
| 12:0/18:1/16:0 | 1-lauroyl-2-oleoyl-3-palmitoyl-glycerol | La/O/P | 44 |
| 12:0/18:2/16:0 | 1-lauroyl-2-linoleoyl-3-palmitoyl-glycerol | La/L/P | 42 |
| 12:0/20:5/18:0 | 1-lauroyl-2-5,8,11,14,17-eicosapentaenoyl-3-stearoyl-glycerol | La/E/S | 40 |
| 12:0/22:6/18:0 | 1-lauroyl-2-4,7,10,13,16,19-docosahexaenoyl-3-stearoyl-glycerol | La/D/S | 40 |
| 14:0/12:0/18:1 | 1-myristoyl-2-lauroyl-3-oleoyl-glycerol | M/La/O | 42 |
| 14:0/16:0/18:1 | 1-myristoyl-2-palmitoyl-3-oleoyl-glycerol | M/P/O | 46 |
| 14:0/18:1/12:0 | 1-myristoyl-2-oleoyl-3-lauroyl-glycerol | M/O/La | 42 |

**Table 2** List of the synthesized enantiopure TG reference compounds (continue)

| TG | Trivial name | Abbreviation | ECN |
|---|---|---|---|
| 14:0/18:1/16:0 | 1-myristoyl-2-oleoyl-3-palmitoyl-glycerol | M/O/P | 46 |
| 16:0/10:0/18:1 | 1-palmitoyl-2-decanoyl-3-oleoyl-glycerol | P/C/O | 42 |
| 16:0/12:0/18:2 | 1-palmitoyl-2-lauroyl-3-linoleoyl-glycerol | P/La/L | 42 |
| 16:0/14:0/18:1 | 1-palmitoyl-2-myristoyl-3-oleoyl-glycerol | P/M/O | 46 |
| 16:0/18:1/10:0 | 1-palmitoyl-2-oleoyl-3-decanoyl-glycerol | P/O/C | 42 |
| 16:0/18:1/14:0 | 1-palmitoyl-2-oleoyl-3-myristoyl-glycerol | P/O/M | 46 |
| 16:0/18:2/12:0 | 1-palmitoyl-2-linoleoyl-3-lauroyl-glycerol | P/L/La | 42 |
| 18:0/14:0/18:1 | 1-stearoyl-2-myristoyl-3-oleoyl-glycerol | S/M/O | 48 |
| 18:0/18:1/18:2 | 1-stearoyl-2-oleoyl-3-linoleoyl-glecreol | S/O/L | 48 |
| 18:0/20:5/12:0 | 1-stearoyl-2-5,8,11,14,17-eicosapentaenoyl-3-lauroyl-glycerol | S/E/La | 40 |
| 18:0/20:5/4:0 | 1-stearoyl-2-5,8,11,14,17-eicosapentaenoyl-3-butyryl-glycerol | S/E/Bu | 32 |
| 18:0/22:6/12:0 | 1-stearoyl-2-4,7,10,13,16,19-docosahexaenoyl-3-lauroyl-glycerol | S/D/La | 40 |

**Table 2** List of the synthesized enantiopure TG reference compounds (continue)

| TG | Trivial name | Abbreviation | ECN |
|---|---|---|---|
| 18:1/12:0/14:0 | 1-oleoyl-2-lauroyl-3-myristoyl-glycerol | O/La/M | 42 |
| 18:1/12:0/16:0 | 1-oleoyl-2-lauroyl-3-palmitoyl-glycerol | O/La/P | 44 |
| 18:1/14:0/12:0 | 1-oleoyl-2-myristoyl-3-lauroyl-glycerol | O/M/La | 42 |
| 18:1/14:0/16:0 | 1-oleoyl-2-myristoyl-3-palmitoyl-glycerol | O/M/P | 46 |
| 18:1/14:0/18:0 | 1-oleoyl-2-myristoyl-3-stearoyl-glycerol | O/M/S | 48 |
| 18:1/14:0/18:2 | 1-oleoyl-2-myristoyl-3-linoleoyl-glycerol | O/M/L | 44 |
| 18:1/16:0/10:0 | 1-oleoyl-2-palmitoyl-3-decanoyl-glycerol | O/P/C | 42 |
| 18:1/16:0/12:0 | 1-oleoyl-2-palmitoyl-3-lauroyl-glycerol | O/P/La | 44 |
| 18:1/16:0/14:0 | 1-oleoyl-2-palmitoyl-3-myristoyl-glycerol | O/P/M | 46 |
| 18:1/16:0/18:0 | 1-oleoyl-2-palmitoyl-3-stearoyl-glycerol | O/P/S | 50 |
| 18:1/16:0/20:0 | 1-oleoyl-2-palmitoyl-3-arachidoyl-glycerol | O/P/A | 52 |
| 18:1/18:0/16:0 | 1-oleoyl-2-stearoyl-3-palmitoyl-glycerol | O/S/P | 50 |
| 18:1/18:2/12:0 | 1-oleoyl-2-linoleum-3-lauroyl-glycerol | O/L/La | 42 |

**Table 2** List of the synthesized enantiopure TG reference compounds (continue)

| TG | Trivial name | Abbreviation | ECN |
|---|---|---|---|
| 18:1/18:2/16:0 | 1-oleoyl-2-linoleum-3-palmitoyl-glycerol | O/L/P | 46 |
| 18:1/20:0/16:0 | 1-oleoyl-2-arachidoyl-3-palmitoyl-glycerol | O/A/P | 52 |
| 18:2/12:0/16:0 | 1-linoleoyl-2-lauroyl-3-palmitoyl-glycerol | L/La/P | 42 |
| 18:2/14:0/18:1 | 1-linoleoyl-2-myristoyl-3-oleoyl-glycerol | L/M/O | 44 |
| 18:2/16:0/12:0 | 1-linoleoyl-2-palmitoyl-3-lauroyl-glycerol | L/P/La | 42 |
| 18:2/16:0/18:1 | 1-linoleoyl-2-palmitoyl-3-oleoyl-glycerol | L/P/O | 46 |
| 18:2/18:1/12:0 | 1-linoleoyl-2-oleoyl-3-lauroyl-glycerol | L/O/La | 42 |
| 18:2/18:1/16:0 | 1-linoleoyl-2-oleoyl-3-palmitoyl-glycerol | L/O/P | 46 |
| 18:2/18:1/18:0 | 1-linoleoyl-2-oleoyl-3-stearoyl-glycerol | L/O/S | 48 |
| 20:0/18:1/16:0 | 1-arachidoyl-2-oleoyl-3-palmitoyl-glycerol | A/O/P | 52 |
| 4:0/20:5/18:0 | 1-butyryl-2-5,8,11,14,17-eicosapentaenoyl-3-stearoyl-glycerol | Bu/E/S | 32 |

## 4.2 Design of the animal trial (Study II, III)

All animal experiments were conducted in compliance with national and international guidelines for the care and use of laboratory animals and were approved by the Institutional Animal Ethics Committee of Peking University (LA2021291). Seventy-two male Sprague-Dawley rats (21 ± 2 days old) were obtained from Beijing Vital River Laboratory Animal Technology Co., Ltd and maintained in a specific pathogen-free environment. The animals were housed in isolation for 7 days under controlled conditions: a temperature of 20°C–23°C, humidity of 50%–55%, and a 12-hour light/dark cycle. During this period, the rats were acclimated to a standard AIN-93G diet (Beijing BioPike Biotechnology Co., Ltd.), which included soybean oil as the n-3 FA source (**Table 3**). Each rat was housed individually in stainless steel metabolic cages with *ad libitum* access to food and water.

After the 7-day acclimation period, the rats were randomly assigned to six experimental groups (n = 12 per group; **Table 4**). The Control Group received the standard AIN-93G diet with soybean oil as the n-3 FA source. The second group, the n-3 deficiency group, was fed a modified AIN-93G diet in which soybean oil was replaced with peanut oil, which is naturally low in n-3 FA (**Table 3**). The remaining four groups were fed the modified (n-3 deficient) AIN-93G diet supplemented with one of the following experimental fats: P/P/P (Tripalmitin), D/P/P (*sn*-1 DHA), P/D/P (*sn*-2 DHA), or P/P/D (*sn*-3 DHA). These latter three groups are collectively referred to as the DHA groups.

**Table 3** Fatty acid composition (% of total fatty acid) of peanut and soybean oils used in the feed. Reprinted from the original publication (Y. Zhang et al., 2023) with the permission of Elsevier.

| Fatty acid | Soybean oil | Peanut oil |
|---|---|---|
| 16:0 | 10.40 | 9.61 |
| 18:0 | 4.46 | 3.54 |
| 18:1(9) | 22.95 | 49.75 |
| 18:2(9,12) | 53.30 | 31.29 |
| 18:3(9,12,15) | 7.50 | 0.11 |
| 20:0 | 0.40 | 1.24 |
| 22:0 | 0.40 | 2.39 |
| 24:0 | 0.12 | 1.04 |
| Others[1] | 0.47 | 1.03 |

The values are expressed as mean mass percentages of the two replicates. [1]This category includes 14:0, 16:1(9), 20:1(11), and 24:1(15).

**Table 4** Experiment groups and feeding treatments. Reprinted from the original publication (Y. Zhang et al., 2023) with the permission of Elsevier.

| Group | Group name | Treatment feed |
|---|---|---|
| 1 | Normal feed group | AIN-93G[1] |
| 2 | n-3 FA deficiency group | AIN-93G contained peanut oil[2] |
| 3 | Tripalmitin group | Tripalmitin + AIN-93G contained peanut oil |
| 4 | *sn*-1 DHA group | *sn*-1- DHA+ AIN-93G contained peanut oil |
| 5 | *sn*-2 DHA group | *sn*-2- DHA+ AIN-93G contained peanut oil |
| 6 | *sn*-3 DHA group | *sn*-3- DHA+ AIN-93G contained peanut oil |

[1] The standard AIN-93G diet contains soybean oil as a fat resource.
[2] Peanut oil which is naturally deficient in n-3 FA was used to make an n-3 FA deficiency group.

In Groups 3–6 (**Table 4**), each rat was administered experimental fat at a daily dosage of 500 mg/kg body weight in the form of structured TGs. The intervention feeding period lasted four weeks. The rats were weighed weekly, and the precise daily dosage was adjusted based on their body weight.

The experimental fats were prepared by adding α-tocopherol (100 mg/100 g) and dividing them into individual weekly doses, which were then stored under nitrogen at -80°C. Prior to feeding, the fats were melted in a 40°C water bath and embedded into two halves of a feed pellet. Fresh pellets were prepared nightly and stored in the dark at 4°C. These pellets were provided to the rats as their first meal each day and were consumed entirely before access to the remaining food. After consuming the test fat, the rats had *ad libitum* access to food and water.

At the end of the 4-week intervention, the rats were fasted, sedated via isoflurane inhalation, and sacrificed by exsanguination. Body weights were recorded at baseline (end of adaptive feeding) and weekly throughout the intervention. Heart blood was collected and centrifuged (Zonkia, Hefei, China) at 1000 *g* for 10 minutes to obtain plasma samples. Organs, including the kidney, lung, spleen, heart, testis, eye, liver, brain, and visceral fat, were excised, weighed, and stored at -80°C for subsequent analysis.

## 4.3 Sample preparation

### 4.3.1 Lipid extraction (Study II, III)

Total lipids in rat plasma and organs, including the liver, heart, kidney, spleen, lung, eye, testicle, and brain were extracted using the Folch method. Tissues were weighed into 2 mL Eppendorf tubes and homogenized at 30 Hz for 2 to 4 mins. Organs were homogenized in chloroform with a bead mill (TissueLyzer, Qiagen,

Germany). The internal standards 17:0/17:0/17:0 and PC 19:0/19:0 were added. After homogenization, 1.5 mL methanol, 2 mL chloroform, and 0.8 mL 0.88% potassium chloride were added to the sample. After each addition, the matrix was thoroughly mixed for 30 s. The sample was then centrifuged (Eppendorf, Hamburg, Germany) at 1000 *g* for 5 min. The lower phase was collected with a pasture pipette into a weight glass tube. Another 4 mL chloroform: methanol (84:16) was added to the upper phase and vortexed for 30 s. After centrifugation, the lower phase was collected and combined with the first extraction. The extract was evaporated under a nitrogen flow at 40°C and redissolved in chloroform for storage.

### 4.3.2 Lipid fractionation (Study II, III)

The total lipids extracted from plasma and organ tissues, including kidney and liver were isolated into neutral and polar lipids with a solid phase extraction method. The Sep-Pak Vac silica 1cc (100 mg) columns or 3cc (200 mg) columns (Waters, Dublin, Ireland) were conditioned by eluting with 3 mL hexane: diethyl ether (1:1). The neutral fraction was eluted with hexane: diethyl ether (1:1), and the polar fraction was eluted with methanol: chloroform: water (5:3:2). Both fractions were evaporated to dryness under a nitrogen flow at 40°C. The neutral lipid fraction was dissolved in 1 mL hexane and the polar lipid fraction was dissolved in 1 mL chloroform: methanol (2:1). Samples were stored at -80°C before analysis.

### 4.3.3 Fatty acids methyl ester preparation (Study II)

The FAMEs were prepared by using the acid-catalyzed method from plasma, liver, visceral fats, and brain lipids. The lipid samples were evaporated under nitrogen flow. Then, 2 mL of acetyl chloride: methanol (1:10) was added to the lipid sample. After vigorous shaking, the sample was kept at 50°C overnight to complete the reaction. After cooling down, 2 mL of 1 mol/L potassium carbonate and 1 mL of hexane were added, and the sample was shaken briefly and centrifuged at 1000 *g* for 5 min. The top layer was collected. The samples were stored in a freezer until analysis with gas chromatography.

## 4.4 Analysis methods

### 4.4.1 Chiral liquid chromatography (Study I)

The synthesized and commercial racemic ABC-TG samples and mixture TG samples were analyzed according to the method published previously by our group (Kalpio et al., 2015). Using two chiral columns CHIRALCEL OD-RH (150 x 4.6 mm, 5µm, Chiral Technologies Europe, Illkirch, France) and a sample

recycling system was used. A Shimadzu Prominence HPLC instrument (Tokyo, Japan) equipped with a SIL-20A autosampler, an LC-20AB pump, and a CTO/10AC column oven was used. Methanol was used as a mobile phase in isocratic mode, and the flow rate was 0.5 mL/min. The samples were detected by an SPD-20A UV detector at 205 nm at 25°C. The recycling system consisted of a CS3080 Sample Peak Recycler (Chiralizer Services, Newtown, PA, USA), a controlling device, and a high-pressure valve. Both automatic valve-switching (by the LCsolution program) and manual switching methods were used in this study.

### 4.4.2 Gas chromatography (Study II)

The FAMEs were analyzed using a Shimadzu GC-2030 gas chromatograph (Shimadzu Corporation, Kyoto, Japan) equipped with an AOC-20i auto-injector and a flame ionization detector. Separation was performed on a DB-23 capillary column (60 m × 0.25 mm i.d., 0.25 μm liquid film, Agilent Technologies, J.W. Scientific, Santa Clara, CA, USA), composed of 50% cyanopropyl and 50% methylpolysiloxane. The injection mode was splitless, with the split opened 1 minute after injection. The injection volume was 0.5 μL, with the injector and detector temperatures set at 270°C and 280°C, respectively.

The column oven temperature program was as follows: initial hold at 130°C for 1 min, followed by an increase of 6.5°C/min to 170°C, then a rise of 2.75°C/min to 205°C, which was maintained for 18 min. Finally, the temperature was decreased at 30°C/min to 230°C and held for 2 min.

FA identification was achieved by comparing retention times with those of FAME 37 and GLC-566c standard mixtures, analyzed under the same GC-FID conditions as the samples. Quantification of FAs was performed using the internal standard method, with correction factors derived from the analysis of FA standard mixtures (FAME 37 and GLC-566c).

### 4.4.3 UHPLC-ESI-MS analysis of phosphatidylcholine in organ tissues (Study III)

A RP-UHPLC system consisting of a Bruker Elute HPG 1300 pump unit (Bruker Corp., Billerica, MA, USA) was employed to analyze the GPL fraction of the organ tissues. The separation was carried out using an Acquity Premier BEH C18 column (2.1 × 150 mm, 1.7 μm particle size; Waters Corp., Milford, MA, USA) equipped with a Vanguard FIT column. Mobile phase A comprised water, while mobile phase B consisted of isopropanol: acetonitrile: water (50:45:5, v/v) with 10 mM ammonium formate and 0.1% formic acid added to both solvents. The gradient program initiated with 35% mobile phase B, ramped up to 85% over 2 min, then further increased to 99% by 15 min, which was held for 5 min.

Subsequently, the gradient returned to 35% B over 1 min and was maintained at 35% for 7 min. The flow rate was set at 0.4 mL/min, and the column oven temperature was maintained at 60°C. The injection volume for each sample was 2 µL (Fabritius, 2023).

An Impact II quadrupole time-of-flight (QTOF) tandem mass spectrometer (Bruker Corp.) was utilized for $MS^2$ analysis of GPL regioisomers. The electrospray ionization (ESI) source was operated in negative mode with a capillary voltage of 3500 V and an end-plate offset of 500 V. Nebulizer gas pressure was maintained at 2 bars, while the drying gas flow rate was set to 8 L/min at 300°C. Collision energy was adjusted to 40 eV. A non-targeted data-dependent Auto MS/MS method was applied, with precursor ion fragmentation triggered when intensity exceeded 600 counts.

The calculation of GPL regioisomers was demonstrated in previous work (Fabritius and Yang, 2021). Briefly, the determination of PC regioisomer ratios is based on the preferential dissociation of *sn*-2 FA. Utilizing regiopure standards, calibration curves were prepared, showing the change in the relative abundances of structurally informative $[RCOO]^-$ fragment ions with five mixtures of two different regioisomers (100:0, 75:25, 50:50, 25:75, 0:100). In that study, the GPL regioisomerswere analyzed with two different methods. First, the individual PL regioisomer standards were analyzed with direct infusion. The calculated results of test mixtures for individual GPL regioisomer pairs were accurate in absence of other, potentially interfering compounds. More complex test mixtures containing all GPL regioisomer standard pairs were also analyzed using hydrophilic interaction liquid chromatography (HILIC), which separates GPLs primarily based on the polar head group of the class. However, in this case there were issues with partially overlapping GPL species that differ only by one double bond. There are two important reasons why this kind of overlap interferes with the GPL regioisomer calculations. First, the precursor ion isolation window of the quadrupole for the MS/MS analysis needs to be narrow enough not to select the chromatographically overlapping GPL species that only differ by one double bond, which results in a mass difference of *m/z* 2, for example PC 34:2 and PC 34:1. Secondly, if there is chromatographic overlap, the M+2 isotope of PC 34:2 will inevitably also be fragmented when the instrument is trying to isolate the PC 34:1 precursor ion, resulting in distorted structurally informative fragment ion ratios, as PC 34:2 and PC 34:1 possibly share one $[RCOO]^-$ fragment, for example FA 16:0 in the case of PC 16:0_18:2 and PC 16:0_18:1. This would lead to incorrect regioisomer calculations. This is the main reason why we decided to move from HILIC to RP chromatography, which separates the GPLs primarily based on the FA constituents, resulting in very minimal overlap of these interfering species.

Utilizing the PC regioisomer standards, we observed that the FA constituents influence the fragmentation pattern of PCs, resulting in slightly different $[R_1COO]^-$ / $[R_2COO]^-$ fragment ion ratios with different FA combinations. Furthermore, utilizing the PC regioisomer standards, we have developed a machine learning-based fragmentation model, which predicts fragment ion ratios of PCs with different FA constituents (Doctoral thesis of Mikael Fabritius (Fabritius, 2023), unpublished manuscript). In addition, the unpublished work shows that the structurally informative fragment ion ratios are very stable across a wide concentration range of 0.1−100 µg/mL with the deviation only starting to somewhat increase at the two lowest concentration levels (0.1 and 0.2 µg/mL). This means that PC regioisomer ratios can be quantified in complex samples containing PCs of different abundances. While Ekroos et al. demonstrated this type of fragmentation behavior for GPLs in his pioneering work (Ekroos et al., 2003), the novelty of our work lies in generalizing the fragmentation patterns to a wide range of PCs, enabling comprehensive and untargeted analysis of PC regioisomers in complex samples.

## 4.5 Statistical analysis

The data analysis was performed using IBM SPSS statistics 25.0 software (IBM, Armonk, NY, USA). All data (Study II) were checked for normality and homogeneity of variance and are presented as a mean ± standard deviation (SD). The significance of the difference between all experimental treatments (Study II) was tested by a one-way analysis of variance (ANOVA) followed by the post hoc Tukey's HSD test. The difference between the three DHA groups was tested by post hoc LSD test. Tamhane's T2 analysis was used when the variance was not homogeneous. Statistical significance was considered when the $p < 0.05$. The Pearson correlation analysis was performed to study the correlation between the factors with two-tailed significance (Study I).

# 5 RESULTS AND DISCUSSION

## 5.1 Chiral separation of TG enantiomers (Study I)

### 5.1.1 Enantiomeric separation

In total, 33 enantiopairs were analyzed on the sample recycling HPLC. The sample peak recycler was installed in the system (Kalpio et al., 2015), which enables the TG enantiomers to be resolved by rerunning the interest compound as many times as we want between two columns. Two examples of chromatograms of O/La/P: P/La/O (60:40) and *rac*-L_O(*sn*-2)_La are shown in **Figure 7**. Seven of them did not show any enantioseparation or asymmetry in the peaks in the chromatogram with the current method, within the 8-hour analysis time. These were classified as unseparated (**Figure 8**). The remainder were baseline or partially separated. **Figure 8** shows the enantiopairs analyzed belonging to different categories. The reference compounds were separated into three groups based on the degree of the unsaturation of their FA composition. The USS' type represents the TGs that possess only one UFA, and it is located in the outer position. The UU'S type is the type of TG that has two UFA and one SFA. The SFA is in the *sn*-1 or *sn*-3 position. The SUS' and USU' types are TGs with either two UFA or SFA on the outer positions. Limited by the sample set, only three enantiopairs of USU' type TGs were involved in this study and none of them were separated until the analysis time which was around 8 hours. The result is consistent with the previous study (Kalpio et al., 2015). Similarly, some of the SUS' types were inseparable by this method. The presence of two SFAs or UFAs in the outer positions makes the molecular structure even more similar and symmetrical than the TGs, which have one SFA and one UFA in the outer positions, making the chiral chromatographic separation even more challenging.

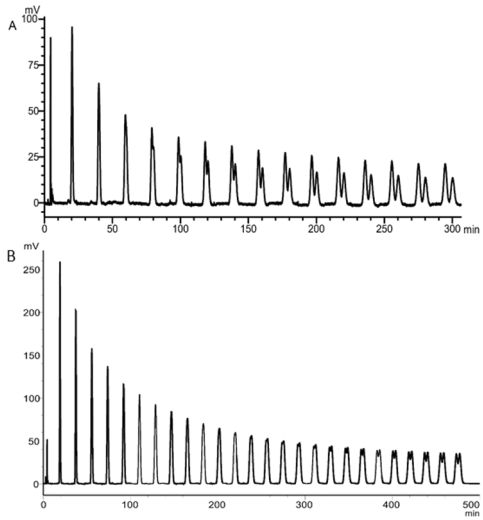


**Fig. 7** UV chromatogram of the enantiopair O/La/P: P/La/O (60:40) and *rac*-L_O(*sn*-2)_La. Chromatography conditions of recycle HPLC-UV: CHIRALCEL OD-RH (150 × 4.6 mm, 5 $\mu$m) columns; mobile phase: methanol.

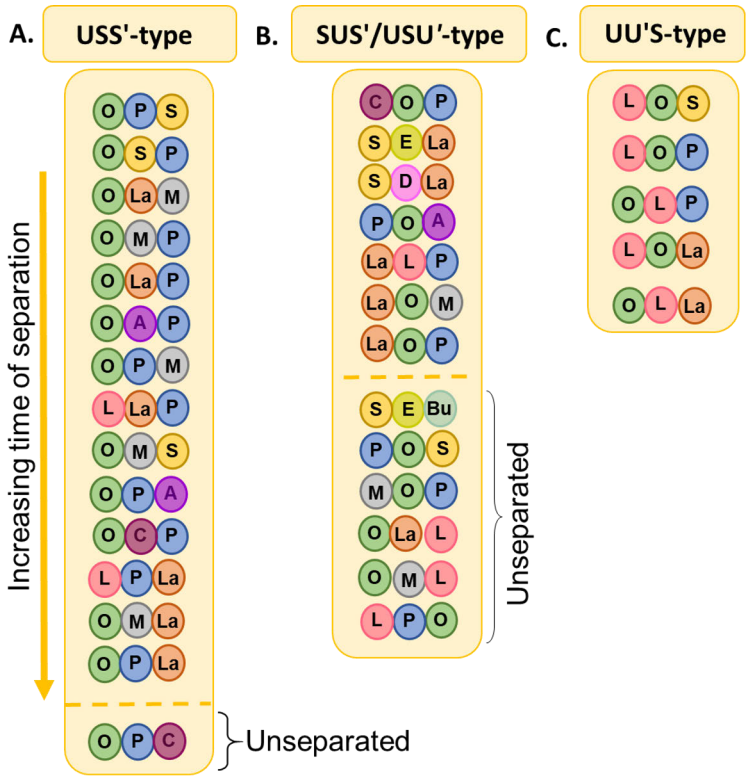


**Fig. 8** The enantioseparation results of USS' (A.), SUS'/USU' (B.), and UU'S -type TGs (C.). Modified from the original publication (Y. Zhang et al., 2024).

The separation was influenced by multiple factors, such as the carbon chain length of the FAs, the number of DBs, as well as the carbon number or DB number difference between the two positions. A Pearson correlation test was performed to determine the most important factors affecting the separation. As shown in **Table 7**, the adjusted retention time ($t'_R$) correlated significantly with the retention time ($t_R$) at separation, ECN, *sn*-3 C, ΔC *sn*-1 vs. 2, and ΔC *sn*-1 vs. 3. Among them, the ECN and *sn*-3 C are positively correlated with $t'_R$, while others are negatively correlated. The $t_R$ at separation is the time needed for the peak to valley (p/v) ratio ≥ 1, which is a parameter to evaluate the easiness of the separation of certain enantiopair. It is significantly negatively correlated with the ECN and *sn*-3 C. The ΔC *sn*-1&3 has a significant positive correlation with the $t_R$ at separation. It is well known that in RP chromatography, the larger the ECN number, the longer the retention in the stationary phase and the longer the retention time (Kalpio et al., 2015, 2020). The chromatographic separation is highly dependent on the time that the sample is retained in the stationary phase. Therefore, it is not surprising that the correlation analysis in this study again confirmed this rule that the higher the ECN value, the easier or better the separation. The result of the Pearson correlation may be limited by the data set in this study. More samples and more variation in FA composition may provide further insights.

**Table 5** The Pearson correlation analysis of the separated enantiopairs. $t'_R$ (min), adjusted retention time after the first column; $t_R$ (min) at separation, the retention time when the p/v ratio is above one. (The C represents the acyl carbon number; ΔC represents the acyl carbon number difference between different positions) Reprinted from the original publication (Y. Zhang et al., 2024) with the permission of American Chemistry Society.

| Factors | $t'_R$ (min) | $t_R$ (min) at separation |
|---|---|---|
| $t_R$ (min) at separation | -0.399* | 1 |
| ECN | 0.981** | -0.455* |
| *sn*-1 C | 0.199 | -0.253 |
| *sn*-1 DB | 0.043 | -0.12 |
| *sn*-2 C | 0.137 | 0.17 |
| *sn*-2 DB | -0.379 | 0.217 |
| *sn*-3 C | 0.737** | -0.541** |
| *sn*-3 DB | 0.074 | -0.25 |
| ΔC *sn*-1&2 | -0.416* | 0.089 |
| ΔC *sn*-1&3 | -0.519** | 0.618** |
| ΔC *sn*-2&3 | -0.368 | 0.265 |

* Correlation is significant at the 0.05 level (2-tailed).
** Correlation is significant at the 0.01 level (2-tailed).

### 5.1.2 Chiral retention behavior

**Table 6** shows the separation results of the enantiopairs analyzed in this study. The enantiomer pairs are listed according to the FA composition type and retention time at separation. The USS' type TGs are the largest group in this study. The results showed that most of the enantiopairs possessing only one UFA on the outer position of TG could be separated by the current method except the O_P(*sn*-2)_C. The first eluted enantiomer was always the one with the UFA on the *sn*-1 position. This is consistent with the previous research (Kalpio et al., 2015, 2020), where the same column-solvent combination was applied.

Lísa and Holčapek (Lísa & Holčapek, 2013) analyzed synthesized TGs with chiral HPLC/APCI-MS, and they reported that the separation of enantiomers was governed by the *sn*-1 and *sn*-3 positions. However, in this study, we found that the middle position also played an important role in the elution behavior. The series of O_P(*sn*-2)_S, O_P(*sn*-2)_M, O_P(*sn*-2)_A, O_P(*sn*-2)_La, and O_P(*sn*-2)_C is a group of enantiomer pairs that differ by only one fatty acyl. Their regioisomers O_S(*sn*-2)_P, O_M(*sn*-2)_P, O_La(*sn*-2)_P, O_A(*sn*-2)_P, and O_C(*sn*-2)_P formed a series in which only the fatty acyl on the middle position is different. Based on their chromatographic elution behavior, we observed that a smaller difference in acyl carbon chain length between the *sn*-2 and *sn*-3 positions of the first eluting enantiomer led to a shorter retention time at separation of the enantiomers. However, when this difference reached six, as observed in O_P(*sn*-2)_C, the enantiomers were no longer distinguishable.

For the UU'S type TGs, the first eluted enantiomer was always the one that possessed the SFA on the *sn*-3 position and a UFA on the *sn*-1 position. This obeyed the rule we found in the USS' group. The carbon chain length of the SFA affected the separation. The longer the carbon chain length, the faster the enantiopair was separated. The current methodology separated the P_O(*sn*-2)_L and L_O(*sn*-2)_La. However, this deviated from the previous reports. Lísa et al. (Lísa et al., 2013) analyzed the P_O(*sn*-2)_L with the stationary phase 3,5-dimethylphenylcarbamate (Lux Cellulose-1) and used hexane and hexane-2-propanol as mobile phases. They indicated that TGs with SFA and UFA with 2 or 3 DBs in the outer positions were not separable by their method. Chen and others (Y. J. Chen et al., 2020) were not able to separate enantiomers of P_O(*sn*-2)_L with a chiral column packed with cellulose *tris*-3,5-dimethylphenyl-carbamate using hexane as the mobile phase. Therefore, it is important to consider the column-solvent (mobile phase) combination before each chiral separation.

The SUS' and USU' type TGs have more similar structures between the *sn*-1 and *sn*-3 FAs. Limited by the small data set, the UFAs in the USU' type TGs are O (18:1) and L (18:2) differing in the DB number by only one. This may have been one of the reasons why none of the USU' TGs were separated in this study.

For the SUS' type, the carbon chain length of those two SFAs is a crucial factor for separations. As shown in **Table 6**, the larger the carbon chain length difference between the *sn*-1 and the *sn*-3 positions, the shorter the retention time at separation. However, some of the TGs containing very long-chain PUFA were exceptions. When there were more than 5 DBs in FAs, the elution order of TG did not follow the ECN anymore. The large number of DBs causes permanent kicks and a greater extent of bending in the carbon chain, which influences the interaction between TG molecules and the stationary phase, leading to the alteration of elution behavior. It has been previously confirmed that the high degree of unsaturation causes special behavior in the chiral HPLC analysis (Kalpio et al., 2020; Řezanka et al., 2018).

**Table 6** The results of all analyzed TG enantiopairs

| Type | Sample | First eluted enantiomer | | | $t'_R$ (min) | ECN | p/v ratio | $t_R$ (min) at separation* |
|---|---|---|---|---|---|---|---|---|
| | | *sn*-1 | *sn*-2 | *sn*-3 | | | | |
| USS' | O_P(*sn*-2)_S | O | P | S | 32.8 | 50 | 1.082 | 66.971 |
| USS' | O_S(*sn*-2)_P | O | S | P | 32.8 | 50 | 1.028 | 67.667 |
| USS' | O_La(*sn*-2)_M | O | La | M | 16.8 | 42 | 1.061 | 68.061 |
| USS' | O_M(*sn*-2)_P | O | M | P | 22.9 | 46 | 1.007 | 69.449 |
| USS' | O_La(*sn*-2)_P | O | La | P | 19.6 | 44 | 1.020 | 80.126 |
| USS' | O_A(*sn*-2)_P | O | A | P | 40.4 | 52 | 1.240 | 82.118 |
| USS' | O_P(*sn*-2)_M | O | P | M | 23.0 | 46 | 1.227 | 92.906 |
| USS' | L_La(*sn*-2)_P | L | La | P | 18.1 | 42 | 1.057 | 110.317 |
| USS' | O_M(*sn*-2)_S | O | M | S | 27.7 | 48 | 1.052 | 110.537 |
| USS' | O_P(*sn*-2)_A | O | P | A | 40.2 | 52 | 1.016 | 122.184 |
| USS' | O_C(*sn*-2)_P | O | C | P | 17.0 | 42 | 1.059 | 138.167 |
| USS' | L_P(*sn*-2)_La | L | P | La | 18.0 | 42 | 1.033 | 200.813 |
| USS' | O_M(*sn*-2)_La | O | M | La | 16.7 | 42 | 1.005 | 367.300 |
| USS' | O_P(*sn*-2)_La | O | P | La | 19.6 | 44 | 1.019 | 433.667 |
| USS' | O_P(*sn*-2)_C | O | P | C | 16.9 | 42 | unseparated | |
| UU'S | S_O(*sn*-2)_L | L | O | S | 26.3 | 48 | 1.195 | 26.955 |
| UU'S | P_O(*sn*-2)_L | L | O | P | 18.1 | 42 | 1.040 | 75.369 |
| UU'S | O_L(*sn*-2)_P | O | L | P | 16.1 | 42 | 1.015 | 123.775 |
| UU'S | La_O(*sn*-2)_L | L | O | La | 19.1 | 46 | 1.019 | 315.000 |
| UU'S | O_L(*sn*-2)_La | O | L | La | 19.1 | 46 | shoulder | |
| SUS' | C_O(*sn*-2)_P | C | O | P | 16.9 | 42 | 1.053 | 68.862 |
| SUS' | P_O(*sn*-2)_A | P | O | A | 39.8 | 52 | 1.170 | 161.641 |
| SUS' | S_E(*sn*-2)_La | S | EPA | La | 13.3 | 40 | 1.009 | 203.446 |
| SUS' | S_D(*sn*-2)_La | S | DHA | La | 14.6 | 40 | 1.078 | 219.469 |
| SUS' | La_O(*sn*-2)_M | La | O | M | 16.7 | 42 | 0.997 | 252.974 |
| SUS' | La_O(*sn*-2)_P | La | O | P | 19.7 | 44 | 1.006 | 256.667 |
| SUS' | La_L(*sn*-2)_P | La | L | P | 15.3 | 42 | 1.074 | 395.667 |
| SUS' | P_O(*sn*-2)_S | P | O | S | 34.7 | 50 | unseparated | |
| SUS' | S_E(*sn*-2)_Bu | S | EPA | Bu | 8.0 | 32 | unseparated | |

| | | | | | | | |
|---|---|---|---|---|---|---|---|
| SUS' | M_O(*sn*-2)_P | M | O | P | 21.5 | 46 | unseparated |
| USU' | O_La(*sn*-2)_L | O | La | L | 19.2 | 42 | unseparated |
| USU' | O_M(*sn*-2)_L | O | M | L | 21.7 | 44 | unseparated |
| USU' | L_P(*sn*-2)_O | L | P | O | 24.7 | 46 | unseparated |

* Separation was determined when the p/v ratio ≥ 1

## 5.2 Separation of regioisomeric TG mixtures (Study I)

By mixing three enantiopure TGs, which are regioisomers to each other, samples containing regioisomeric triplets were obtained as shown in **Table 7**. To test the applicability of chiral separation, the mixture samples were injected into the chiral column with the same chromatographic parameters. The results showed that the current method was able to partially separate the regioisomers. However, the separation was limited by the peak broadening with the increase in the analysis time. The elution order can be speculated by the retention time of the individual stereoisomers due to the stability of the system. **Figure 9** shows the chromatograms of the TG mixtures. Mixture 1 showed only a small asymmetry after 400 minutes. Mixture 2 showed two shoulders after 350 minutes. The first shoulder could be P/O/M and the second one was likely P/M/O based on the retention time. The mixture 3 tended to separate into three peaks after 400 minutes and the elution order based on the retention time was C/P/O, P/O/C, and P/C/O. The mixture 4 was separated into two peaks after 400 minutes. To sum up, the separation of regioisomeric triplets is challenging with the chiral column and solvent used in this study. Other column-solvent combinations could be tried, and mass spectrometry may be a better option to identify the regioisomeric elution order.

Despite the analytical success of this approach, its application to natural fats and oils remains challenging. Individual natural oils often require pre-fractionation into simpler TG fractions or even isolated TG species for effective enantiomer separation. Kalpio et al. (Kalpio et al., 2021) characterized the enantiomer composition of TGs in sea buckthorn oils. RP-LC was first performed on a C18 column, and three out of seven fractions were collected based on ECN values. Each collected fraction was then introduced into recycling chiral LC for further separation. Each fraction yielded two to four peaks, which were collected and analyzed. The purified fractions were subjected to direct inlet ammonia negative ion chemical ionization MS with CID, enabling the profiling of both regio- and enantiomeric TG species in complex natural samples. However, coelution of multiple TGs was still observed based on the MS results. Currently, the supercritical fluid chromatography (SFC) is intensively studied for the analysis of TG isomers. Zhang et al. (Xinghe Zhang et al., 2022) compared palmitic acid-containing TGs in mammalian milk, lard, and fish oil. Six regioisomers were analyzed using ultra-performance SFC coupled with

QTOF-MS. Masuda et al. (Masuda et al., 2021) applied SFC coupled with triple quadrupole MS and chiral column to separate the TG isomers. The method was applied to palm oil and olive oil, the concentration of O/P/O, O/O/P, and P/O/O was quantified. This method can separate the enantiomer and regioisomer at the same time. However, only TG O_P_O was resolved. Recently, Bruin et al. (De Bruin et al., 2025) developed a direct infusion cyclic ion mobility MS method for the separation of all types of TG isomers, including *sn*-positions, double bond positions, acyl chain lengths, and *cis/trans* configurations. Complex multi-isomer sets (4, 5, or 6 isomers) were successfully separated using sodium adducts. Although the method has so far only been applied to standard compounds, it shows strong potential for extension to real biological samples. Overall, continued development and integration of complementary techniques will be essential to fully elucidate TG isomer profiles in natural samples.

**Table 7** Regioisomeric triplets formed by enantiopure compounds. Reprinted from the original publication (Y. Zhang et al., 2024) with the permission of American Chemical Society.

| Sample name | Composition | Proportion % |
|---|---|---|
| Mixture 1 | M/La/O | 20 |
| | La/M/O | 30 |
| | M/O/La | 50 |
| Mixture 2 | P/M/O | 20 |
| | M/P/O | 30 |
| | P/O/M | 50 |
| Mixture 3 | P/C/O | 20 |
| | P/O/C | 30 |
| | C/P/O | 50 |
| Mixture 4 | La/P/L | 20 |
| | P/L/La | 30 |
| | P/La/L | 50 |

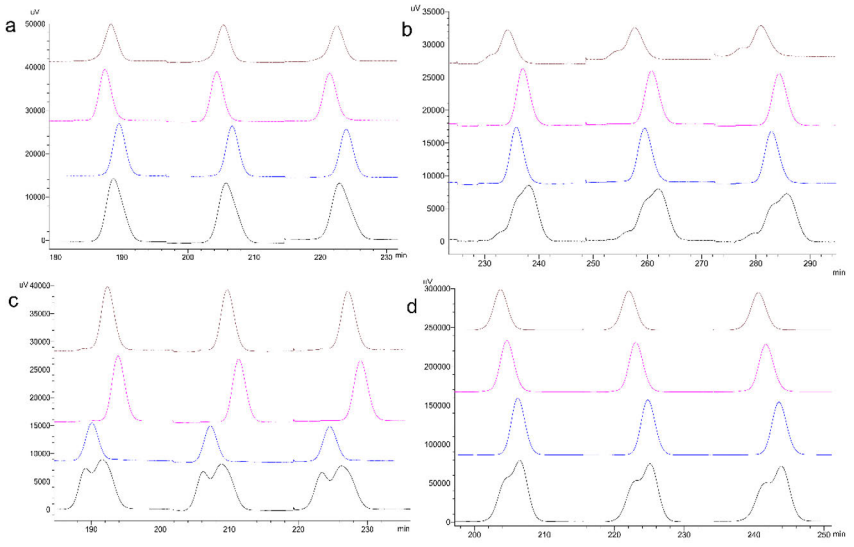


**Fig. 9** The UV chromatograms of regioisomeric mixed TGs and the individual enantiomers. All black chromatograms represent the mixture of TG samples. Mixture TG 1 (a): Pink: M/La/O, blue: La/M/O, brown: M/O/La; Mixture TG 2 (b): Pink: P/M/O, blue: M/P/O, brown: P/O/M; Mixture TG 3 (c): Pink: C/P/O,

blue: P/C/O, brown: P/O/C; Mixture TG 4 (d): Pink: P/La/L, blue: La/P/L, brown: P/L/La.

## 5.3 Effect of n-3 deficient diet and DHA supplementation from different *sn*-positions of TG molecules (Study II)

### 5.3.1 Body weight and organ weight

**Table 8** shows the body weights of the rats at the baseline and during the intervention phase. The body weights of the six groups of rats did not show any significant difference at the baseline, during the intervention, or after the intervention. This was mainly due to the free access to food and water. The body weight of all rats increased during the intervention and the increasing rate was stable all the time. At the end of the trial, the body weight was 6 times higher than the baseline body weight, which was used to determine the daily dose during each week.

**Table 9** shows the fresh organ weights of the brain, heart, lungs, liver, spleen, kidneys, and testis at the end of the intervention. The organ weights did not show any significant difference between any groups at the end of the intervention. The organ-to-body weight ratio (data not shown) also showed no difference between the groups.

**Table 8** Bodyweight (g) of the rats before and during the intervention.

| | **Control** | **Deficiency** | **Tripalmitin** | ***sn*-1 DHA** | ***sn*-2 DHA** | ***sn*-3 DHA** |
|---|---|---|---|---|---|---|
| baseline | 54.6 ± 5.5 | 54.1 ± 6.3 | 53.1 ± 5.9 | 51.9 ± 4.8 | 55.8 ± 4.4 | 53.1 ± 5.2 |
| week 1 | 95.4 ± 9.4 | 94.5 ± 12.6 | 91.81 ± 7.6 | 88.3 ± 6.1 | 96.1 ± 7.7 | 90.6 ± 7.1 |
| week 2 | 169.3 ± 12.3 | 165.5 ± 20.6 | 166.0 ± 9.6 | 158.4 ± 9.7 | 172.7 ± 10.9 | 161.7 ± 10.9 |
| week 3 | 223.4 ± 13.9 | 220.2 ± 23.4 | 221.9 ± 12.4 | 216.2 ± 13.9 | 223.6 ± 16.8 | 216.7 ± 12.7 |
| week 4 | 279.8 ± 18.1 | 281.1 ± 29.3 | 280.0 ± 14.0 | 274.1 ± 19.5 | 283.5 ± 19.0 | 272.6 ± 20.3 |

**Table 9** Weight (g) of rat organs after the intervention phase. Reprinted from the original publication (Y. Zhang et al., 2023) with the permission of Elsevier.

| | **Groups** | | | | | |
|---|---|---|---|---|---|---|
| **Organs** | **Normal feed** | **Deficiency** | **Tripalmitin** | ***sn*-1 DHA** | ***sn*-2 DHA** | ***sn*-3 DHA** |
| Brain | 1.67 ± 0.17 | 1.70 ± 0.19 | 1.75 ± 0.14 | 1.74 ± 0.17 | 1.85 ± 0.15 | 1.82 ± 0.15 |
| Heart | 1.12 ± 0.06 | 1.16 ± 0.15 | 1.16 ± 0.14 | 1.12 ± 0.18 | 1.11 ± 0.08 | 1.11 ± 0.16 |
| Lung | 1.41 ± 0.25 | 1.33 ± 0.26 | 1.39 ± 0.10 | 1.38 ± 0.14 | 1.29 ± 0.16 | 1.30 ± 0.11 |
| Liver | 14.84 ± 1.66 | 15.76 ± 2.11 | 14.79 ± 1.70 | 14.24 ± 1.46 | 14.9 ± 1.30 | 14.35 ± 1.77 |
| Spleen | 0.73 ± 0.11 | 0.68 ± 0.14 | 0.76 ± 0.15 | 0.76 ± 0.11 | 0.75 ± 0.11 | 0.76 ± 0.10 |
| Kidney | 2.54 ± 0.20 | 2.44 ± 0.27 | 2.64 ± 0.23 | 2.52 ± 0.27 | 2.41 ± 0.14 | 2.45 ± 0.20 |
| Testis | 2.63 ± 0.16 | 2.56 ± 0.23 | 2.61 ± 0.17 | 2.58 ± 0.19 | 2.68 ± 0.16 | 2.54 ± 0.20 |

### 5.3.2 Lipid content in rat tissue and organs

The lipid contents in different organs are shown in **Table 10**. The plasma and liver total lipids were fractionated into polar lipids and neutral lipids, which are mainly GPL and TG fractions. Evidently, the visceral fat shows the highest level of lipid content. There is more GPL than TG in the liver. The lipid content did not show a significant difference between the six groups, likely because of the

free access to food and water. This is also reflected in the consistent body weight, although DHA is believed to have an effect of decreasing the TG content and anti-obesity (J. J. Li et al., 2008). Previous studies indicated that the dietary DHA showed little effect on body weight in rats (Shirouchi et al., 2007), but the supplementation decreased the content of adipose tissue (Wei et al., 2021). In this study, the TG content or the body weight of the animals did not show any significant differences between the DHA groups and others.

**Table 10** The lipid contents in different organs and tissues in rats (% percentage of wet tissue)

| **Organs** | **Normal feed** | **Deficiency** | **Tripalmitin** | ***sn*-1 DHA** | ***sn*-2 DHA** | ***sn*-3 DHA** |
|---|---|---|---|---|---|---|
| Plasma TG | 0.18±0.02 | 0.22±0.04 | 0.16±0.04 | 0.19±0.04 | 0.20±0.03 | 0.18±0.03 |
| Plasma GPL | 0.16±0.02 | 0.17±0.02 | 0.15±0.03 | 0.16±0.02 | 0.16±0.02 | 0.15±0.02 |
| Liver TG | 1.65±0.45 | 2.21±0.69 | 1.73±0.40 | 1.54±0.54 | 1.71±0.48 | 1.68±0.36 |
| Liver GPL | 2.62±0.16 | 2.51±0.15 | 2.64±0.13 | 2.69±0.14 | 2.71±0.17 | 2.72±0.15 |
| Brain | 4.23±0.25 | 4.21±0.19 | 4.39±0.22 | 4.19±0.08 | 4.34±0.23 | 4.14±0.22 |
| Visceral fat | 72.06±3.80 | 71.07±2.96 | 70.02±2.92 | 68.90±2.68 | 72.68±3.24 | 70.93±4.05 |
| Testis | 3.09±0.43 | 3.92±1.85 | 2.73±0.26 | 2.44±0.15 | 2.81±1.01 | 2.79±1.05 |
| Lung | 5.65±1.57 | 6.09±2.59 | 5.96±1.49 | 5.29±1.12 | 5.60±0.84 | 4.65±0.62 |
| Kidney | 5.09±0.78 | 5.59±1.41 | 5.43±1.95 | 5.65±1.53 | 6.85±2.74 | 6.61±1.82 |
| Spleen | 3.74±1.35 | 3.15±1.73 | 3.54±1.54 | 4.51±1.16 | 5.19±1.99 | 3.60±1.07 |
| Heart | 4.40±0.68 | 4.75±0.38 | 3.90±1.23 | 4.44±1.70 | 3.98±0.67 | 4.35±0.47 |
| Eye | 2.67±0.20 | 2.66±0.17 | 2.68±0.31 | 2.21±0.21 | 3.10±0.96 | 2.46±0.27 |

### 5.3.3 Fatty acid composition of organs

**Figure 10** displays the relative levels of major n-3 and n-6 FAs, including total n-3 and n-6 FAs, across six groups. The ALA content in the organs mirrored the dietary variations resulting from soybean oil and peanut oil. Notably, the normal feed group exhibited significantly higher ALA levels compared to other groups, except in the brain.

The EPA content in the tested organs and tissue is relatively low. There was no significant difference in the visceral fat. The ALA is not only the precursor to the synthesis of DHA but also EPA. The EPA content of three DHA groups in the liver and the brain showed a significantly higher amount than the deficiency and the tripalmitin group. This could have been due to either reduced conversion of EPA to DHA because of feedback inhibition or the retro conversion from DHA to EPA because the ALA in the deficiency diet was very low.

Compared to the normal feed group, DHA levels were lower in both the deficiency and tripalmitin groups. The DHA content increased significantly in the three DHA groups compared to the other groups. The exception was in the brain, where no significant difference was found between the normal feed group and the DHA groups. This is consistent with the previous research. Valentini et al. (Valentini et al., 2018) reported the DHA content in the brain was not affected by the dietary DHA in normal mice. Gerbi et al. (Gerbi et al., 1994) found there were no changes in the brain DHA content after feeding fish oil to rats on normal feed. Brain DHA synthesis occurs at approximately 1% of its consumption rate (Rapoport et al., 2007). This indicates that the brain is not the main place where the DHA is synthesized, but the DHA consumed there is transported from the other organs, mostly from the liver (Igarashi et al., 2007). The results suggest that when there is a limited supply of DHA in the body, the brain is the most prioritized in the DHA distribution.

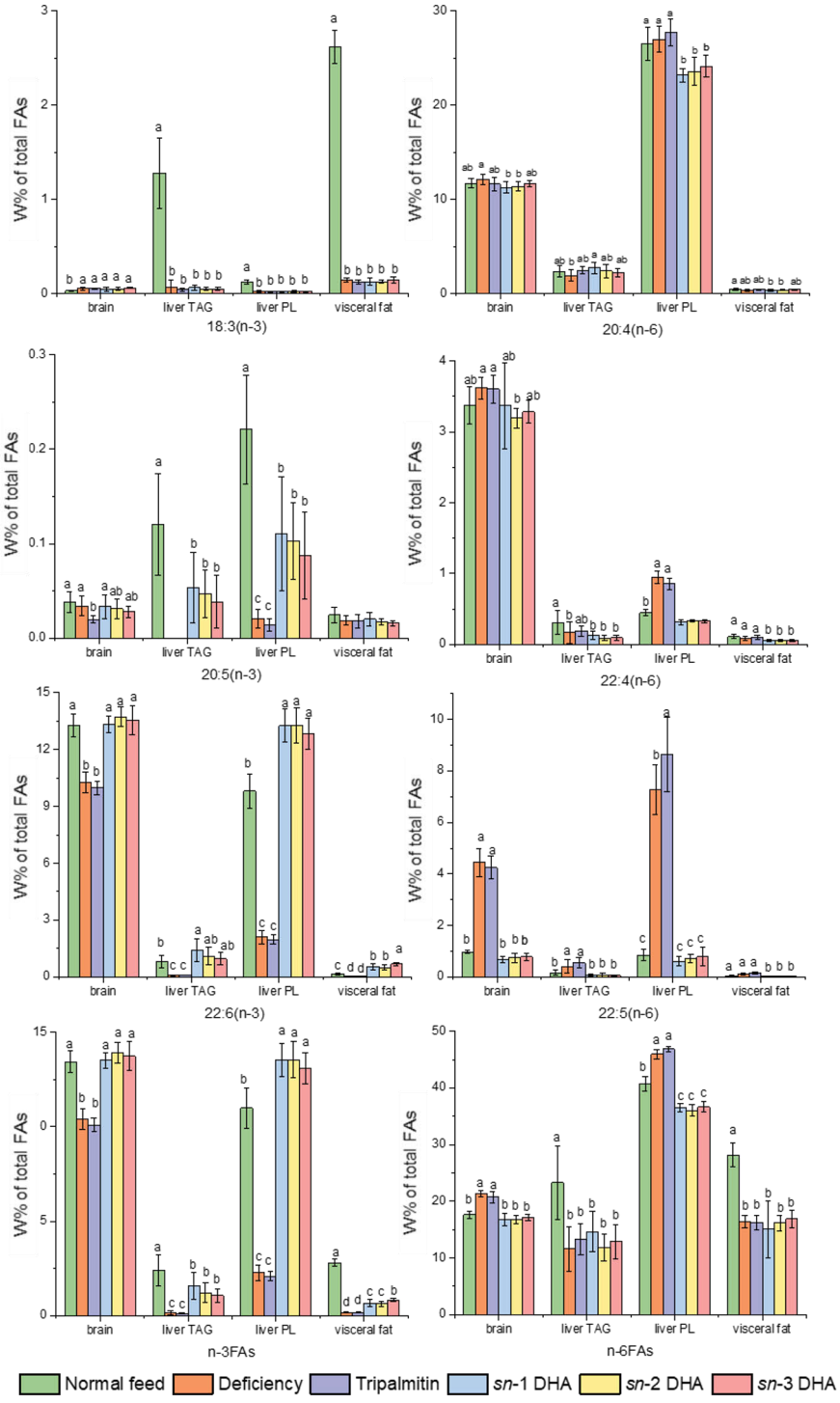


**Fig. 10** Relative content (w %) of major n-3 and n-6 FAs in rat tissue and organs in different groups (Values marked with different letters differ statistically significantly.)

Among the three DHA groups, a difference in DHA content was observed only in visceral fat. The *sn*-3 DHA group exhibited a significantly higher DHA content compared to the *sn*-1 ($p$=0.019) and *sn*-2 ($p$=0.01) groups. The DHA content in the *sn*-1, *sn*-2, and *sn*-3 groups was 377.95 ± 105.16, 356.78 ± 86.54, and 481.86 ± 82.59 μg/100 mg tissue, respectively. The relative content of DHA in the visceral fat is lower compared to the other organs because the visceral fat has TG as the dominating lipid and is usually considered as storage fat, while the DHA as a functional FA is mostly located in GPLs playing many crucial rules in the whole body. However, visceral fat exhibited the highest lipid content among the tissues and organs analyzed. As a result, despite its low percentage of total lipids, the absolute DHA amount in visceral fat remained relatively high. Overall, the impact of the positional distribution of the DHA on the TG has limited influence on the DHA bioavailability or distribution. Christensen and Høy (M. M. Christensen & Høy, 1997) investigated the impact of structured *sn*-2 DHA-containing TG and randomized oil with DHA evenly distributed across all three positions on newborn rats. The results showed that DHA in the outer position led to greater visceral fat accumulation compared to DHA in the middle position. However, studies related to this topic are limited so far, and the results were contradictory. Ikeda et al. (Ikeda et al., 1998) performed the comparison between seal oil and squid oil to compare between n-3 FAs at the outer positions and middle positions. Because DHA is mostly located in the outer positions in seal oil but predominantly in the *sn*-2 position in squid oil. The relative content of DHA and EPA in rat liver TG was significantly lower in the seal oil group compared to the squid oil group. Yoshinaga and coworkers (Yoshinaga et al., 2015) compared the effects of the positional distribution of DHA and EPA in mice. They concluded that the FAs on the *sn*-2 position have the highest bioavailability, which is consistent with Ikeda and others. Another 12-week study on hamsters reported the DHA located in the middle position accumulated more in the brain than DHA at the *sn*-1/3 positions (Bandarra et al., 2016).

The relative content of 22:4(7,10,13,16) in the deficiency and tripalmitin groups increased in most organs following the intervention. Likewise, 22:5(4,7,10,13,16) levels showed a substantial rise, particularly in liver GPL and the brain. This increase of n-6 FAs is related to the compensation for the lack of DHA. The DBs create small kinks in the GPL molecules which influence the fluidity of the bio membrane (BarCba-Bon et al., 2020). As **Figure 10** shows the 22:5(4,7,10,13,16) is more abundant in the GPL fraction in the liver. This may indicate the increased elongation and desaturation of the 18:2(9,12) in response to the n-3 deficient status (Kulkarni et al., 2022). The increase of the n-6 PUFAs is also related to the inflammatory and immune responses (Gorczyca et al., 2022).

The results of the total n-3 FA content are similar to that of the DHA content since DHA was the most abundant n-3 FAs in this study. The findings from the

deficiency and tripalmitin groups suggest that a four-week deficiency diet was sufficient to induce a mild n-3 deficiency, characterized by significantly lower n-3 FA levels compared to normal, yet without noticeable clinical symptoms. The significant increase in the n-6 FAs was also reflected in the results of the total n-6 FAs content in the brain and the liver GPL fraction. The deficiency and tripalmitin groups exhibited significantly higher n-6 FA levels compared to the other groups.

### 5.3.4 Fatty acid composition of plasma TG and GPL

The FA composition of plasma TG and GPL fractions are shown in **Tables 11 and 12**. Consistent with the results of the organs, the DHA content in the deficiency and tripalmitin groups was significantly lower than in the normal feed group. Other n-3 FAs were either not detected or in trace amounts, such as the EPA, which was not detected in the TG fraction. DHA supplementation for four weeks significantly increased the DHA content in all three DHA groups, indicating that the supplementation not only compensated for the dietary deficiency but also effectively increased the DHA level. The DHA content in the *sn*-1 DHA group in the TG fraction was significantly higher than the level in the *sn*-3 DHA group. Many stereoselective enzymes are involved in the process of fat digestion (Bakala-N'Goma et al., 2022; Park & Park, 2022). For example, the gastric lipase preferentially cleaves *sn*-3 FAs from TGs (Mackie et al., 2020), while the pancreatic lipase prefers the *sn*-1 position (Carrière et al., 1997). The stereoselectivity of the lipases as well as the regio- and stereospecific structure of TG affect the digestion and absorption of TGs. Panzoldo and coworkers (Panzoldo et al., 2011) found that the rat plasma TG levels remained high after 10 hours of fat ingestion. This indicates a markedly prolonged postprandial lipemia duration compared to humans. Therefore, the higher DHA level shown in this study may be because of the delay of absorption or the slower clearance of TGs compared to the *sn*-2 and *sn*-3 DHA groups. These findings, along with variations in visceral fat, suggest differences in the bioavailability and metabolic fate of DHA based on its positional distribution in TG molecules.

The deficiency and tripalmitin groups had significantly elevated n-6 FA levels relative to the other groups. Even though the palmitic acid was supplemented in the tripalmitin group, the content of the palmitic acid was not increased in the plasma or other organs. This is due to the effective counterbalance of palmitic acid by regulating the endogenous biosynthesis via *de novo* lipogenesis (X. Song et al., 2017). The differences between the normal diet and the deficient diet caused by soybean oil and peanut oil were reflected in the FA composition. The TG fraction of plasma in the normal feed group contained significantly higher levels of 18:3(9,12,15) and 18:2(9,12). This finding also accounts for the elevated n-3 FA content in the normal feed group compared to the deficiency and

tripalmitin groups. The long-chain SFA such as 22:0 also showed a clear difference in the TG fraction of plasma among the groups.

Consisted with the organ and tissue results, the 22:5(4,7,10,13,16) content increased 10-fold in the deficiency and tripalmitin groups compared to the level in the other groups. The value of 22:4(7,10,13,16) was significantly increased as well. These changes result in the compensation for the n-3 PUFA deficiency to maintain the homeostasis of the PUFA pool needed for cell membrane fluidity. However, the shift in the n-3/n-6 FAs ratio likely results in changes in the profile of lipid mediators contributing to the resolution of inflammation (Saini & Keum, 2018), which deserves further investigation.

**Table 11** The proportion of fatty acids (weight percentage of total fatty acids) in the rat plasma TG fraction of the different groups. Reprinted from the original publication (Y. Zhang et al., 2023) with the permission of Elsevier.

| Fatty acid | Normal | Deficiency | Tripalmitin | *sn*-1 DHA | *sn*-2 DHA | *sn*-3 DHA |
|---|---|---|---|---|---|---|
| 14:0 | 0.85±0.23 | 0.80±0.18 | 0.86±0.14 | 0.79±0.24 | 0.80±0.15 | 0.78±0.17 |
| 15:0 | 0.15±0.03 | 0.16±0.02 | 0.17±0.08 | 0.17±0.04 | 0.15±0.03 | 0.16±0.02 |
| 15:1 | 1.28±0.85 | 0.81±0.56 | 1.56±0.84 | 1.32±0.83 | 1.24±0.50 | 1.32±0.60 |
| 16:0 | $20.7±2.56^{b}$ | $23.48±2.67^{a}$ | $21.6±1.94^{ab}$ | $21.29±1.48^{ab}$ | $22.28±1.88^{ab}$ | $21.8±1.71^{ab}$ |
| 16:1(9) | 2.69±0.80 | 3.23±1.12 | 2.39±0.95 | 2.38±0.86 | 2.95±1.02 | 2.69±1.06 |
| 18:0 | 6.22±0.64 | 5.51±1.19 | 6.42±1.65 | 5.77±0.88 | 6.01±0.75 | 6.12±1.06 |
| 18:1(9) | $15.69±2.28^{b}$ | $27.40±3.57^{a}$ | $23.13±4.86^{a}$ | $25.9±3.14^{a}$ | $27.16±3.01^{a}$ | $25.45±3.11^{a}$ |
| 18:1(11) | 2.35±0.48 | 2.61±0.57 | 2.28±0.82 | 2.53±0.66 | 2.87±0.76 | 2.68±0.74 |
| 18:2(9,12) | $20.36±2.30^{a}$ | $13.67±1.69^{bc}$ | $12.27±1.45^{c}$ | $14.96±1.07^{b}$ | $13.12±1.11^{bc}$ | $13.71±1.68^{bc}$ |
| 18:3(6,9,12) | 0.51±0.09 | 0.47±0.07 | 0.53±0.17 | 0.46±0.07 | 0.50±0.05 | 0.52±0.09 |
| 18:3(9,12,15) | $1.55±0.30^{a}$ | $0.09±0.10^{b}$ | $0.07±0.03^{b}$ | $0.07±0.01^{b}$ | $0.05±0.01^{b}$ | $0.06±0.01^{b}$ |
| 20:0 | $0.12±0.05^{b}$ | $0.22±0.07^{a}$ | $0.17±0.03^{ab}$ | $0.15±0.04^{b}$ | $0.16±0.06^{ab}$ | $0.18±0.05^{ab}$ |
| 20:1(11) | $0.20±0.04^{c}$ | $0.40±0.04^{a}$ | $0.31±0.09^{b}$ | $0.37±0.08^{ab}$ | $0.38±0.06^{ab}$ | $0.36±0.05^{ab}$ |
| 20:2(11,14) | $0.33±0.07^{ab}$ | $0.40±0.08^{ab}$ | $0.41±0.11^{a}$ | $0.31±0.08^{b}$ | $0.31±0.06^{ab}$ | $0.32±0.10^{ab}$ |
| 20:3(8,11,14) | $0.51±0.12^{a}$ | $0.31±0.07^{b}$ | $0.32±0.07^{b}$ | $0.47±0.03^{a}$ | $0.49±0.09^{a}$ | $0.44±0.07^{a}$ |
| 20:4(5,8,11,14) | $22.75±5.79^{ab}$ | $18.49±4.23^{b}$ | $25.12±5.55^{a}$ | $18.96±3.55^{b}$ | $17.75±3.58^{b}$ | $19.86±3.98^{ab}$ |
| 20:3(11,14,17) | $0.07±0.02^{ab}$ | $0.05±0.01^{bc}$ | $0.08±0.03^{a}$ | $0.06±0.01^{bc}$ | $0.04±0.01^{c}$ | $0.06±0.02^{abc}$ |
| 20:5(5,8,11,14,17) | $0.66±0.16^{a}$ | nd[1] | nd | $0.22±0.08^{b}$ | $0.23±0.09^{b}$ | $0.21±0.11^{b}$ |
| 22:0 | $0.06±0.02^{c}$ | $0.16±0.05^{a}$ | $0.11±0.03^{b}$ | $0.13±0.03^{ab}$ | $0.13±0.06^{ab}$ | $0.15±0.02^{ab}$ |
| 22:2(13,16) | $0.06±0.01^{ab}$ | $0.05±0.02^{b}$ | $0.08±0.04^{a}$ | $0.06±0.01^{ab}$ | $0.05±0.01^{b}$ | $0.06±0.01^{ab}$ |

| Fatty acid | Normal | Deficiency | Tripalmitin | *sn*-1 DHA | *sn*-2 DHA | *sn*-3 DHA |
|---|---|---|---|---|---|---|
| 22:4(7,10,13,16) | 0.35±0.08$^{a}$ | 0.29±0.15$^{ab}$ | 0.34±0.21$^{a}$ | 0.19±0.04$^{b}$ | 0.17±0.06$^{b}$ | 0.17±0.04$^{b}$ |
| 22:5(4,7,10,13,16) | 0.24±0.05$^{c}$ | 0.92±0.42$^{b}$ | 1.25±0.37$^{a}$ | 0.15±0.06$^{c}$ | 0.15±0.05$^{c}$ | 0.17±0.07$^{c}$ |
| 22:5(3,6,9,12,15) | 0.26±0.08$^{a}$ | nd | nd | 0.08±0.04$^{b}$ | 0.07±0.03$^{b}$ | 0.06±0.05$^{b}$ |
| 24:0 | 0.16±0.07$^{b}$ | 0.29±0.08$^{a}$ | 0.28±0.08$^{a}$ | 0.25±0.07$^{ab}$ | 0.26±0.09$^{a}$ | 0.30±0.07$^{a}$ |
| 22:6(4,7,10,13,16,19) | 1.87±0.48$^{c}$ | 0.19±0.06$^{d}$ | 0.23±0.09$^{d}$ | 2.96±0.73$^{a}$ | 2.65±0.52$^{ab}$ | 2.37±0.57$^{bc}$ |
| total SFA | 28.27±2.36 | 30.62±3.18 | 29.62±2.51 | 28.55±1.10 | 29.80±1.45 | 29.49±1.95 |
| total MUFA | 22.21±2.98$^{b}$ | 34.46±4.47$^{a}$ | 29.68±5.99$^{a}$ | 32.50±3.52$^{a}$ | 34.61±3.50$^{a}$ | 32.50±4.04$^{a}$ |
| total PUFA | 49.52±5.05$^{a}$ | 34.92±5.37$^{b}$ | 40.70±5.44$^{b}$ | 39.12±3.76$^{b}$ | 35.78±4.35$^{b}$ | 38.25±4.31$^{b}$ |
| total n-3 | 4.41±0.60$^{a}$ | 0.33±0.15$^{c}$ | 0.37±0.13$^{c}$ | 3.39±0.83$^{b}$ | 3.05±0.60$^{b}$ | 2.76±0.71$^{b}$ |
| total n-6 | 45.11±4.90$^{a}$ | 34.59±5.24$^{bc}$ | 40.32±5.33$^{ab}$ | 35.57±3.72$^{bc}$ | 32.54±4.16$^{c}$ | 35.25±3.81$^{bc}$ |

[1] Not detected.
Values are mean ± SD, n=12, except for the normal feed group (n=11) and *sn*-1 DHA group (n=11). Different superscript letters within the same row indicate statistically significant differences ($p$<0.05).

**Table 12** The proportion of fatty acids (weight percentage of total fatty acids) in the rat plasma GPL fraction of the different groups. Reprinted from the original publication (Y. Zhang et al., 2023) with the permission of Elsevier.

| Fatty acids | Normal feed | Deficiency | Tripalmitin | *sn*-1 DHA | *sn*-2 DHA | *sn*-3 DHA |
|---|---|---|---|---|---|---|
| 14:0 | 0.35±0.04$^{a}$ | 0.32±0.03$^{ab}$ | 0.32±0.03$^{ab}$ | 0.28±0.04$^{b}$ | 0.29±0.05$^{b}$ | 0.29±0.06$^{b}$ |
| 16:0 | 24.21±1.54 | 23.98±1.42 | 24.97±1.56 | 23.97±1.36 | 24.08±1.11 | 24.13±1.63 |
| 16:1(9) | 0.51±0.12 | 0.60±0.17 | 0.53±0.14 | 0.49±0.17 | 0.64±0.19 | 0.55±0.20 |
| 18:0 | 23.62±1.41 | 22.94±1.67 | 22.53±1.66 | 22.49±1.19 | 22.23±1.96 | 22.01±1.33 |
| 18:1(9) | 4.28±0.43$^{b}$ | 7.42±0.66$^{a}$ | 7.42±0.78$^{a}$ | 7.02±0.47$^{a}$ | 7.40±0.48$^{a}$ | 7.09±0.52$^{a}$ |
| 18:1(11) | 1.92±0.40 | 1.71±0.32 | 1.95±0.57 | 2.00±0.31 | 2.19±0.38 | 2.07±0.40 |
| 18:2(9,12) | 16.27±1.92$^{a}$ | 14.99±1.11$^{ab}$ | 12.65±2.16$^{c}$ | 14.46±1.17$^{abc}$ | 13.48±1.25$^{bc}$ | 13.93±1.40$^{bc}$ |
| 20:0 | 0.15±0.02$^{b}$ | 0.18±0.02$^{ab}$ | 0.19±0.03$^{a}$ | 0.17±0.02$^{ab}$ | 0.16±0.03$^{ab}$ | 0.17±0.02$^{ab}$ |
| 20:1(11) | 0.13±0.03$^{b}$ | 0.22±0.06$^{a}$ | 0.26±0.06$^{a}$ | 0.27±0.05$^{a}$ | 0.25±0.05$^{a}$ | 0.23±0.04$^{a}$ |
| 20:2(11,14) | 0.42±0.06$^{b}$ | 0.51±0.08$^{ab}$ | 0.54±0.11$^{a}$ | 0.56±0.08$^{a}$ | 0.59±0.09$^{a}$ | 0.58±0.07$^{a}$ |
| 20:3(8,11,14) | 1.24±0.40$^{bc}$ | 1.23±0.35$^{c}$ | 1.04±0.35$^{c}$ | 1.71±0.22$^{a}$ | 2.00±0.40$^{a}$ | 1.66±0.21$^{ab}$ |
| 20:4(5,8,11,14) | 16.97±2.00$^{ab}$ | 16.98±1.06$^{ab}$ | 17.41±2.21$^{a}$ | 15.13±1.14$^{b}$ | 15.24±1.21$^{b}$ | 16.27±1.58$^{ab}$ |
| 20:5(5,8,11,14,17) | 0.22±0.06$^{a}$ | 0.08±0.01$^{c}$ | 0.10±0.02$^{bc}$ | 0.13±0.05$^{bc}$ | 0.14±0.04$^{b}$ | 0.12±0.04$^{bc}$ |
| 22:0 | 0.25±0.02$^{c}$ | 0.31±0.06$^{ab}$ | 0.34±0.06$^{a}$ | 0.31±0.03$^{ab}$ | 0.28±0.04$^{bc}$ | 0.28±0.04$^{bc}$ |
| 22:2(13,16) | 0.28±0.04$^{a}$ | 0.13±0.03$^{b}$ | 0.15±0.05$^{b}$ | 0.13±0.03$^{b}$ | 0.13±0.02$^{b}$ | 0.12±0.01$^{b}$ |

| Fatty acid | Normal feed | Deficiency | Tripalmitin | *sn*-1 DHA | *sn*-2 DHA | *sn*-3 DHA |
|---|---|---|---|---|---|---|
| 22:4(7,10,13,16) | 0.39±0.04$^{b}$ | 0.70±0.05$^{a}$ | 0.71±0.11$^{a}$ | 0.25±0.03$^{c}$ | 0.28±0.02$^{c}$ | 0.25±0.05$^{c}$ |
| 22:5(4,7,10,13,16) | 0.63±0.11$^{c}$ | 4.55±0.68$^{b}$ | 5.57±0.77$^{a}$ | 0.48±0.12$^{c}$ | 0.54±0.12$^{c}$ | 0.63±0.33$^{c}$ |
| 22:5(3,6,9,12,15) | 0.45±0.09$^{a}$ | 0.10±0.03$^{b}$ | 0.09±0.02$^{b}$ | 0.12±0.03$^{b}$ | 0.13±0.04$^{b}$ | 0.12±0.03$^{b}$ |
| 24:0 | 0.93±0.15$^{c}$ | 1.17±0.22$^{ab}$ | 1.32±0.23$^{a}$ | 1.16±0.11$^{ab}$ | 1.05±0.16$^{bc}$ | 1.07±0.15$^{bc}$ |
| 22:6(4,7,10,13,16,19) | 5.75±0.68$^{b}$ | 1.17±0.21$^{c}$ | 1.13±0.19$^{c}$ | 8.01±0.71$^{a}$ | 8.20±0.93$^{a}$ | 7.72±0.83$^{a}$ |
| 24:1(15) | 0.72±0.08$^{a}$ | 0.46±0.09$^{b}$ | 0.50±0.11$^{b}$ | 0.54±0.09$^{b}$ | 0.44±0.11$^{b}$ | 0.45±0.07$^{b}$ |
| total SFA | 49.67±1.28$^{ab}$ | 49.02±0.69$^{ab}$ | 49.81±1.93$^{a}$ | 48.54±1.04$^{ab}$ | 48.22±1.44$^{ab}$ | 48.08±1.16$^{b}$ |
| total MUFA | 7.73±0.60$^{b}$ | 10.54±0.84$^{a}$ | 10.79±0.96$^{a}$ | 10.46±0.77$^{a}$ | 11.04±0.82$^{a}$ | 10.52±0.83$^{a}$ |
| total PUFA | 43.09±0.93$^{a}$ | 41.50±0.71$^{bc}$ | 40.63±1.17$^{c}$ | 42.03±0.82$^{ab}$ | 41.65±0.95$^{bc}$ | 42.35±1.20$^{ab}$ |
| total n-3 | 6.43±0.62$^{b}$ | 1.35±0.23$^{c}$ | 1.32±0.20$^{c}$ | 8.26±0.72$^{a}$ | 8.48±0.95$^{a}$ | 7.96±0.83$^{a}$ |
| total n-6 | 36.18±0.80$^{b}$ | 39.08±0.81$^{a}$ | 38.07±1.24$^{a}$ | 32.73±0.85$^{c}$ | 32.26±1.04$^{c}$ | 33.43±1.05$^{c}$ |

Values are mean ± SD, n=12, except for the normal feed group (n=11) and *sn*-1 DHA group (n=11). Different superscript letters within the same row indicate statistically significant differences ($p$<0.05).

## 5.4 Effect of n-3 deficiency on the PC molecular species distribution in rat organs

**Figure 11** shows the PC molecular species that represent more than 1% relative abundance of the total PC species. It was obvious that the deficient diet changed the composition and the relative abundance of PC molecules after four weeks of intervention. Previous research on n-3 deficiency has mainly concentrated on changes in FA composition changes. This is the first study that compares the PC molecular species and regioisomer compositions between normal and n-3 deficient rats. However, there were no significant differences regarding the ratio within each regioisomer pair (data not shown).

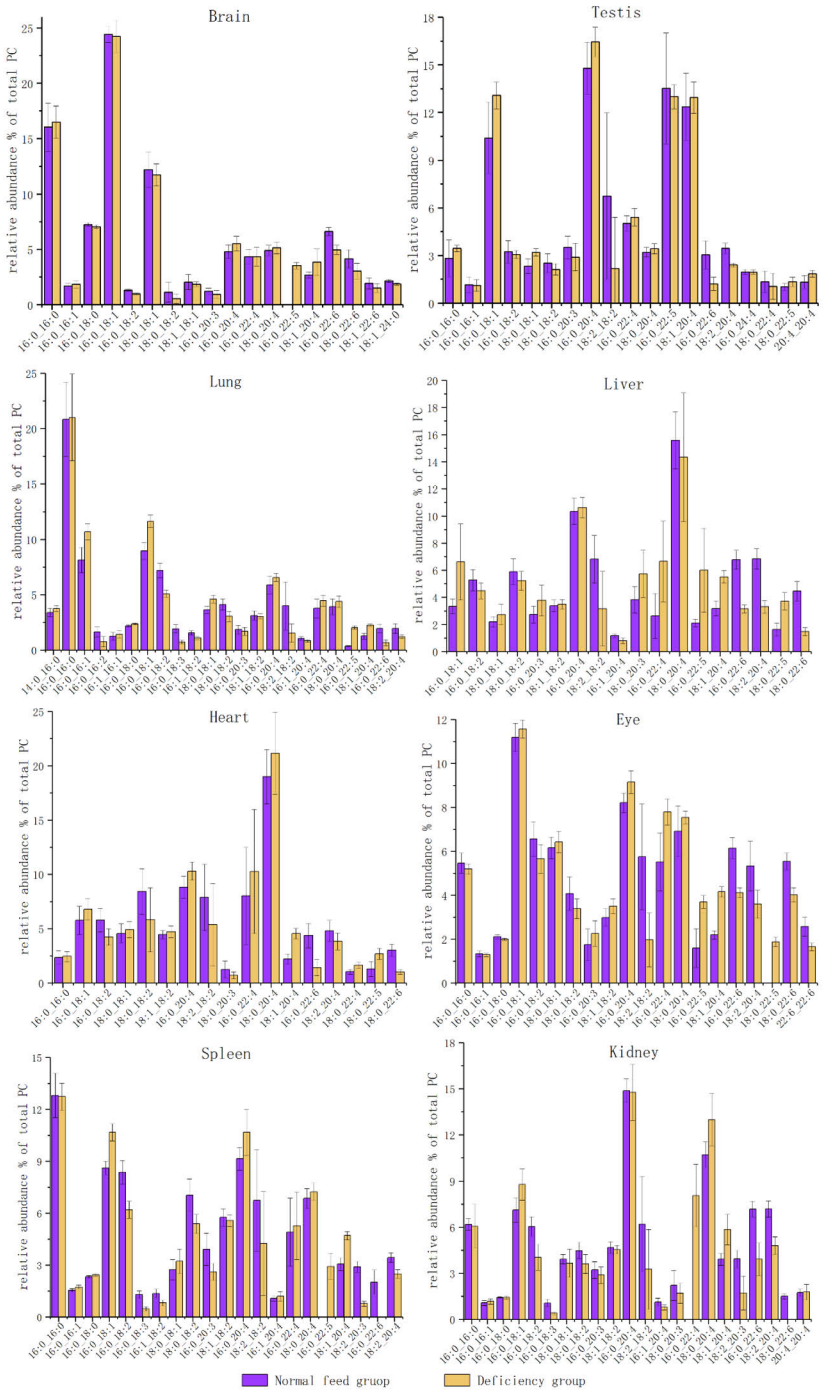


**Fig. 11** The relative abundances of the major PC molecular species in the normal feed and the n-3 FA deficiency groups.

The deficient diet not only reduced the abundance of n-3 FA-containing molecular species but also depleted some species entirely, such as PC 16:0_22:6

in the spleen and PC 18:0_22:6 in the kidney. Consistent with FA composition results from Study II, the levels of n-6 FAs increased significantly in the n-3-deficient groups. This was reflected in the PC molecular species, with a dramatic increase in n-6-containing species, particularly those with 22:4(7,10,13,16) and 22:5(4,7,10,13,16). In organs such as the brain, spleen, kidney, and eye, the deficiency groups exhibited a notable rise in PC 16:0_22:5 and PC 16:0_22:4 compared to the normal feed group. However, molecular species containing another n-6 PUFA, AA, did not show a significant increase in the deficiency group. These findings align with previous studies. For instance, Murthya et al. (Murthya et al., 2002) examined the effects of n-3 FA deficiency on the GPL molecular species composition in rat hippocampus. The rats were raised for two generations on the n-3 FA deficiency diet. The GPL molecular species were analyzed by RP-HPLC-ESI-MS. The results showed the PC 16:0_22:6(n-3) specie was replaced by PC 16:0_22:5(n-6) and PC 18:0_22:5(n-6), while the 20:4 containing PC species were not affected by the deficient diet. Similarly, a recent study on mice examined the recovery of DHA and EPA in PC FA composition after supplementation with either EPA or DHA (Cui et al., 2022). The n-3 deficiency was induced by maternal deprivation of n-3 PUFAs during pregnancy and lactation. The results showed that within 14 days of supplementation, the levels of 22:5(n-6) decreased dramatically during the first 3 days and then stabilized across the tested organs, including the liver, brain, heart, bone marrow, and spleen, regardless of whether DHA or EPA was supplemented.

Notably, a pilot study (M. J. Khan et al., 2022) observed significant alterations in plasma PC 16:0_22:6 and PC 18:0_22:6 in AD patients compared to the cognitively normal group. Consistent with previous findings, PC classes showed an overall decrease in AD patients (Proitsi et al., 2017). Along with changes in specific molecular species, these lipids have been evaluated as potential AD biomarkers in plasma. The results suggest that if the deficiency persists, it may increase the risk of AD. Similarly, lipid profiling of gallbladder cancer-derived biliary extracellular vesicles revealed that GPL levels were downregulated in biliary exosomes, with PC 16:0/20:5 and PC 16:0/22:6 showing a significant decrease (Kong et al., 2024). This aligns with earlier findings that cancer patients tend to have lower plasma n-3 PUFA levels (Murphy et al., 2012). Although the deficiency observed in this study was mild and no obvious symptoms were present, the decrease in certain molecular species may indicate an elevated risk for various diseases.

As the primary component of biological membranes, PC plays a critical role in maintaining membrane fluidity, a function facilitated by long-chain PUFAs, as discussed in Study II. Both the FA composition and PC molecular composition findings indicate that four weeks of peanut oil-based feeding was sufficient to induce n-3 FA deficiency in all studied organs and tissues. These results

emphasize the significant impact of dietary n-3 PUFA deficiency on membrane composition and its potential functional consequences. On the other hand, the molecular species of GPLs vary not only among different GPL classes (Phillips et al., 2022) but also across different regions within the same organ, such as the white cortex, grey cortex, and cerebellum of the brain (Hopiavuori et al., 2017). This highlighted the importance of fully revealing the lipid structure profile in organs.

## 5.5 Effect of n-3 deficiency and positional distribution of DHA in dietary TG molecules on PC species and regioisomers in rat organs (Study III)

### 5.5.1 The molecular weight species distribution of PC in rat organs

Phosphatidylcholine (PC) is the major GPL in cell membranes (Z. Li et al., 2006). **Figure 12** shows the PC species distribution or so-called molecular weight distribution in normal rats. As it shows, the distribution of PC species differs among different organs. There were 37 different ACN: DB species detected in all organs. Among them, 13 of them were common in all organs, such as PC 34:1, PC 36:4, PC 38:4, and PC 38:6 being major species. Some of the species were only detected in certain organs, such as PC 30:1 and PC 32:3 in the lung, PC 36:0 in the spleen, PC 38:1 in the eyes, PC 38:2 in the liver, and PC 42:9, PC 44:8 in the testis. The most dominating species in the lung was the 32:0. The FA composition of the lung also revealed a higher presence of 14:0 and 16:0 compared to other organs (Kulkarni et al., 2022). The most abundant species in the brain was 34:1. The PC 36:4 is highly prevalent in various organs, making up at least 13.96% of the total PC in the eye lipids. The results of testicles showed abundant amounts of PC 38:5 and PC 36:4, together accounting for almost half of the total PC. Recently, many studies have shown that changes in PC composition in rodent tissues indicate various diseases, such as cancer (Tang et al., 2022) and non-alcoholic steatohepatitis (Z. Li et al., 2006). As the major components of cell membranes, the distinct PC composition in different organs may lead to different biological properties. Revealing the profile of PC composition in different organs contributes to the understanding of the functions of PC and the mechanisms responsible for these functions.

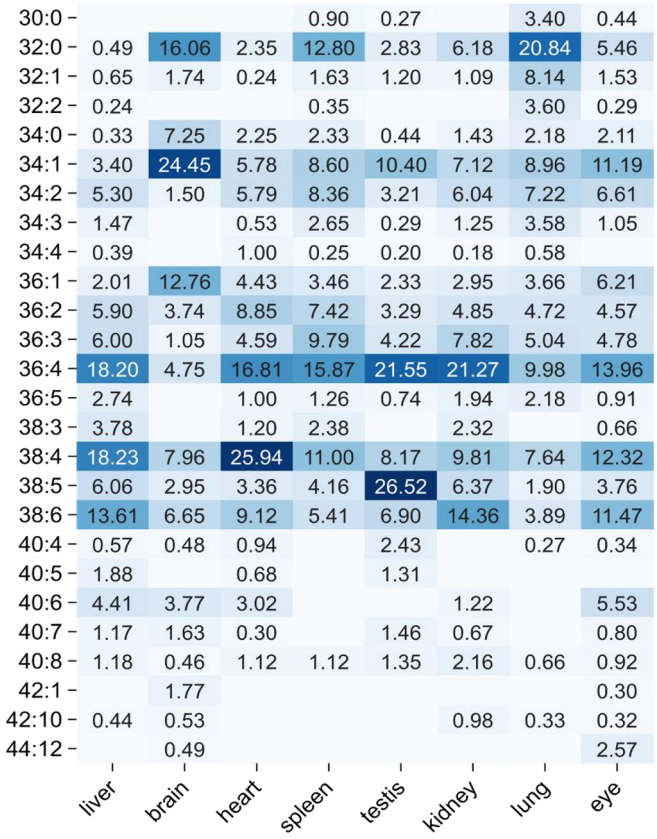


**Fig. 12** Heat map of the major PC species in different organs of Sprague-Dawley rats in the normal feed group (the numbers show the percentage of all the species)

### 5.5.2 Molecular species and positional distribution of FAs in PC molecules

**Figure 13** shows the major molecular species composition and the ratio of the regioisomer pairs in the normal feed group in different organs. This is the first time that the PC molecular composition profile at the *sn*-position level has been revealed in rat organs. The molecular species composition varied a lot between different organs. The molecular species containing 16:0, 18:0, 18:1, and 18:2, in combination with each other or one of them with a longer chain PUFAs, were the most common ones. This is consistent with the molecular weight distribution. It is commonly suggested that PC diversity is acquired through acyl-chain remodeling, and the lysophospholipid acyltransferases (LPLAT) play essential roles in this process by regulating the *de novo* and remodeling pathways (Harayama et al., 2014). In line with the molecular weight distribution result, the SFA is relatively more abundant in the lung than in the other organs, especially the PC 16:0/16:0. Because the dipalmitoyl-PC is the major component of

pulmonary surfactant. It is biosynthesized by the lysophosphatidylcholine acyltransferase 1 (LPCAT1) in the Lands cycle, while the LPCAT1 is mainly expressed in the lung (X. Chen et al., 2006). In the brain, the most abundant molecular species was the PC 16:0_18:1. The 34:1 species in **Figure 12** was also the most abundant in the brain. The PC 16:0_20:4 contributed a large share of the PC 36:4, which was one of the dominant species in many organs. The most abundant DHA-containing species was PC 16:0_22:6 in PC 38:6 in all organs, especially in the liver, kidney, and eye. This indicates that the DHA showed a preference for accumulation in these organs. However, the DHA-containing molecular species was detected in all organs indicating DHA's important role in these organs.

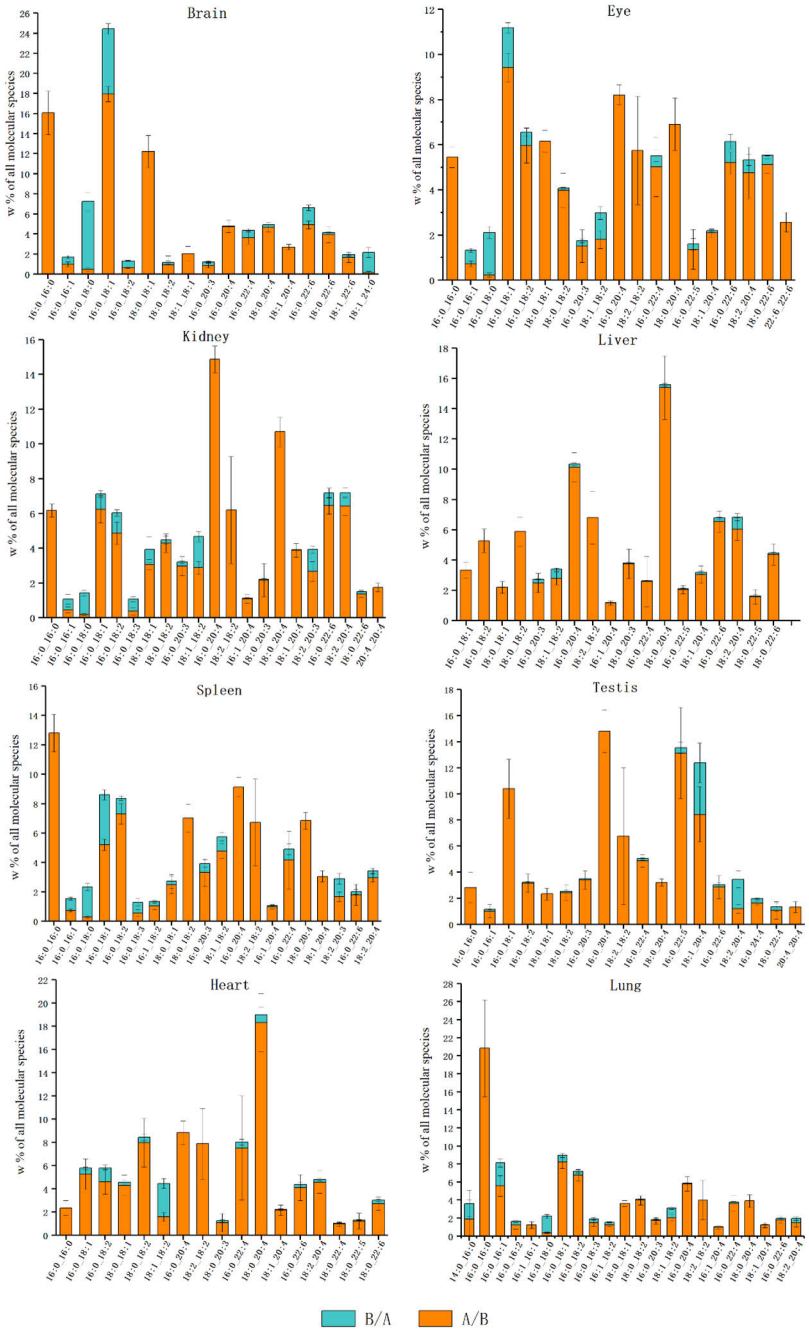


**Fig. 13** The profile of major PC molecular species of rat organs (% of all molecular species).

**Figure 14** shows the regioisomer ratio of the major molecular species in the normal feed, deficient, and DHA groups in eight organs. Only the *sn*-1 DHA group was included in this figure because no significant differences in

regioisomer ratio were found between the three DHA groups. This indicates that the positional distribution of dietary DHA has limited influence on the organ PC regioisomer ratio after the intervention. This was not surprising as the lipid structure is mainly determined genetically and related to the activity of the enzymes involved in the metabolic pathways. According to limited research in the past, it was believed that the UFAs prefer to be located in the *sn*-2 position (Beppu et al., 2017; Ruiz-Lopez et al., 2015). However, in this study, we discussed all the possible combinations of FAs and systematically concluded the positional preference. The FA composition of GPL can be divided into three categories: two SFAs, two UFAs, and SFA+UFA. There were few molecular species in the rat organs possessing two SFAs, for example, PC 16:0_18:0 in the brain, eye, and kidney. However, there was no clear pattern that the carbon chain length affects the regioisomer ratio. When there are both SFA and UFA on the PC molecule, the UFA tends to esterify on the *sn*-2 position no matter the degree of unsaturation. Some of the regioisomer pairs showed extreme ratios, with almost 100% of the regioisomer with UFA on the *sn*-2 position, such as PC 18:0_20:4 and PC 18:0_18:1. However, it becomes complex when the two FAs on the PC molecule are both UFAs. In this case, the number of the DB is important. If the difference in the number of DB of those two UFAs is larger than 3, then the FA with more DBs is dominating on the *sn*-2 position. If the DB difference is less than 3, there were no clear rules shown in the current study. For instance, the PC 18:2/20:4 is dominant in the spleen, but the ratio is opposite in the testis. The regioisomer pair PC 18:1_18:2 also showed different ratios in different organs. GPLs can be synthesized *de novo* and subsequently undergo remodeling through the Lands cycle. Because of the substrate specificity, the remodeling process enriched the diversity of the GPL molecules. The lysophosphatidylcholine acyltransferase (LPCAT) family is believed to be critical for the regulation of PC composition. For example, the LPCAT 3 preferentially bonds the UFA on the *sn*-2 position, especially the AA and the 18:2(9,12) (Rong et al., 2013). However, there were many other enzymes involved in the metabolic pathways. Nevertheless, the mechanisms remain unclear and need further investigation.

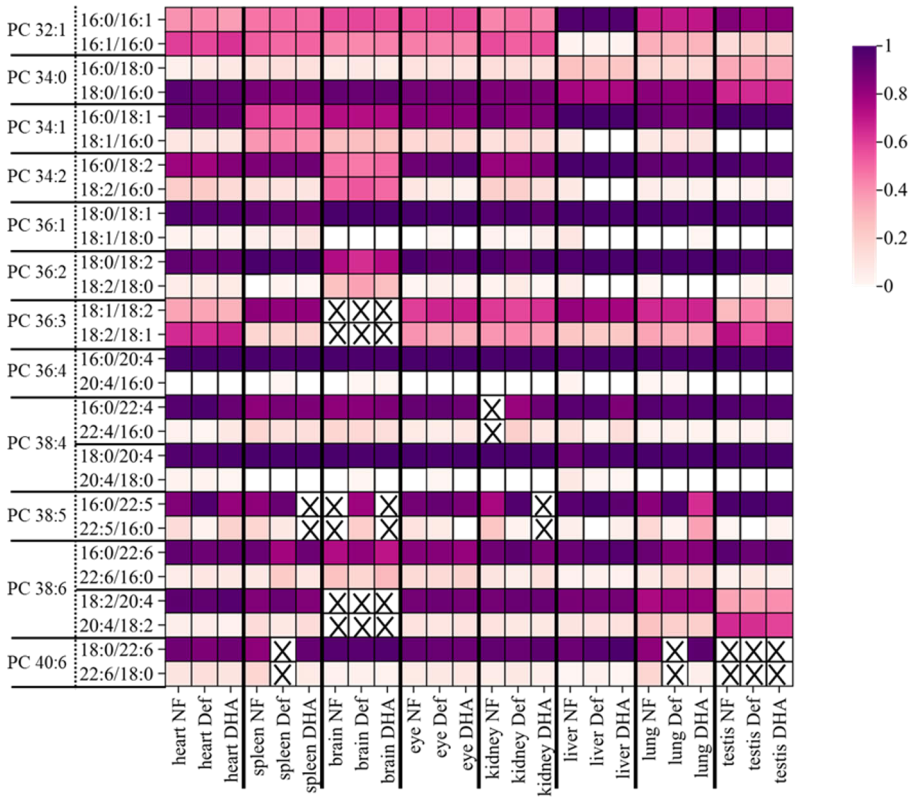


**Fig. 14** The positional distribution of FAs on the major PC molecular species. (The DHA group in this figure is the *sn*-1 DHA group. The X represents the PC regioisomer pair was not detected at all)

# 6 SUMMARY AND CONCLUSION

This thesis investigated the chiral separation of TG enantiomers and the effects of TG structure on the bioavailability of DHA. Thanks to a collaboration with the University of Iceland, regio- and enantiopure TGs were synthesized, enabling chromatographic behavior analysis and rat feeding trial. A chiral LC system equipped with a sample recycling feature was employed to study the chiral separation of a wide range of TG enantiomer pairs (Study I). The impact of n-3 deficient diet and DHA supplementation from different positions in TG molecules' lipid composition in tissues and organs was studied in a four-week feeding trial in Sprague-Dawley rats. The FA composition (Study II) and PC molecular species and regioisomer composition (Study III) were analyzed in tissues and organs at the end of the feeding, representing a novel approach to bioavailability research.

Separation of TG enantiomers is a complex but essential task for determining the composition of individual TG molecules. Limited access to standard compounds has slowed methodological development in this area. This study represents the first systematic analysis of the enantiomer separation and elution behavior of 33 ABC-type TG enantiomer pairs. The findings demonstrated that the separation of enantiomer pairs is influenced by ECN, retention time, carbon chain length, and the number of DBs at all three positions. These retention behaviors and elution patterns provide valuable insights for elucidating the specific structures of complex natural lipids.

The lack of structured TGs has stunted the understanding of the effects of the positional distribution of FAs on the glycerol backbone of TGs. In this thesis a four-week feeding intervention in rats was conducted to investigate tissue- and organ-specific differences for the first time. Comprehensive analyses covered FA composition, PC molecular species, and PC regioisomer profiles. Four weeks of an n-3 deficient diet in rats resulted in changes in FA composition and GPL regioisomer composition. The DHA content and total n-3 FA content showed a dramatic decrease accompanied by an increase of n-6 FAs. The PC molecular species showed corresponding changes, especially a decrease in content of PC 16:0/22:6 and PC 18:0/22:6, accompanied by an increase in PC 16:0/22:5 and PC 18:0/22:5. Feeding with DHA at the *sn*-1 position of TG led to a significantly higher DHA content in the plasma TG fraction compared to DHA at the *sn*-3 position. However, supplementation with *sn*-3 DHA led to the highest level of DHA in visceral fat. The n-3 deficiency-induced changes in PC molecular species and regioisomers were all reverted by supplementation with DHA, although the *sn*-position of DHA in dietary TG molecules did not show a significant impact on the PC species and isomers in the tissues and organs. These

findings confirmed the differential accumulation of DHA in tissues from the different positions of TG.

This thesis revealed the rat PC composition profile of almost all organs to the *sn*-regioisomer level, which is crucial for understanding lipid metabolism. The results of this thesis provide references for natural glycerol lipids regioisomer analysis. The findings expand our understanding of the bioavailability and metabolic pathways of dietary DHA, especially regarding the significance of its position in TGs. The results of this research contribute valuable references for analyzing the composition of TGs and GPLs in natural fats and oils. These insights hold potential applications in food science, nutrition, health, and disease research, paving the way for advancements in developing functional foods and nutraceuticals targeting DHA bioavailability and metabolic health.

# ACKNOWLEDGEMENTS

First of all, I would like to express my heartfelt gratitude to the experimental animals who sacrificed their precious lives for science in this thesis. This work was primarily conducted at the Food Science unit, Department of Life Technologies, University of Turku, with the animal trials performed at the School of Public Health, Peking University, China. The reference compounds were synthesized at the University of Iceland. I am deeply grateful to our collaborators, Prof. Yumei Zhang's group and Prof. Guðmundur Haraldsson and Haraldur Guðmundsson's group, for their invaluable contributions.

I would also like to thank the Doctoral Program of Technology (DPT) and the former Doctoral Program of Molecular Life Science (DPMLS) for the opportunity to pursue my doctoral studies. My sincere gratitude goes to the Turku University Foundation, the Finland-China Food and Health Network, the Finnish Food Research Foundation, the Magnus Ehrnrooth Foundation, and the Doctoral Program of Technology for their generous financial support.

A special acknowledgment goes to my supervisors, Baoru Yang, Marika Kalpio, and Mikael Fabritius. Thank you, Baoru, for your care, trust, and inspiring passion for scientific research, which has deeply influenced me. Marika, as my office mate and mentor, you have always been my first point of contact for both scientific and personal matters. Your patience and willingness to help, even when you are exceptionally busy, mean the world to me. Mikael, thank you for being with me from the very beginning, guiding me in the lab, and collaborating on publications, and taking care of my internet cable. Your kindness and teamwork have been invaluable. I am deeply grateful to my advisory committee members, Professor Emeritus Heikki Kallio and Professor Kaisa Linderborg, whose enthusiasm for science has been a constant source of encouragement.

I would also like to extend my gratitude to my coauthors and colleagues, Hafdis Haraldsdottir, Jukka-Pekka Suomela, Maaria Kortesniemi, Oskar Laaksonen, Annelie Damerau, Anna Puganen, Eija Ahonen, Mohammed Sazzad, Tanja Seppälä, Amruta Kulkarni, Timo Seitz, Henri Avela, Hany Ahmed, and other present and former colleagues, for your friendship and support over the years. Special thanks to the master's thesis students I had the privilege to guide, Xiangrong Fang and Mika Tuominen—working with you taught me valuable lessons as well. I am also grateful to the technical and administrative personnel of the Department of Life Technologies, including Anu Hirvensalo, Heli Kuusela, Tapio Ronkainen, and Leena Neuvonen. My warm thanks go to Qizhu Zhao, Ye Tian, Ying Zhou, Qizai Wang, Cong Ding, Kang Chen, Fan Luo, and Mrunalini Lotankar for their friendship and support, as well as Heli and Sami, Keith, Arina, Aleksi, Magdalana, Olena and other friends from the biochemistry unit.

Finally, my deepest gratitude is reserved for my family. Thank you to my entire family, especially my parents, for your unconditional and eternal love. A special acknowledgment goes to my cat, Panghu, for always being by my side and reminding me to take breaks. To my husband, Rongbin Wang, your unwavering support and care have been my greatest source of strength. You are not just my partner but also my best coworker and friend. This doctoral journey has been transformative, and I have grown into a better version of myself.

Turku, April 2025

Yuqing Zhang

# REFERENCES


Aguirre, G. A., Goulart, M. R., Dalli, J., & Kocher, H. M. (2023). Arachidonate 15-lipoxygenase-mediated production of Resolvin D5n-3 DPA abrogates pancreatic stellate cell-induced cancer cell invasion. *Frontiers in Immunology*, *14*(November), 1–17. https://doi.org/10.3389/fimmu.2023.1248547

Ahmed Nasef, N., Zhu, P., Golding, M., Dave, A., Ali, A., Singh, H., & Garg, M. (2021). Salmon food matrix influences digestion and bioavailability of long-chain omega-3 polyunsaturated fatty acids. *Food and Function*, *12*(14), 6588–6602. https://doi.org/10.1039/d1fo00475a

Akanbi, T. O., Sinclair, A. J., & Barrow, C. J. (2014). Pancreatic lipase selectively hydrolyses DPA over EPA and DHA due to location of double bonds in the fatty acid rather than regioselectivity. *Food Chemistry*, *160*, 61–66. https://doi.org/10.1016/j.foodchem.2014.03.092

Alfieri, A., Imperlini, E., Nigro, E., Vitucci, D., Orrù, S., Daniele, A., Buono, P., & Mancini, A. (2018). Effects of plant oil interesterified triacylglycerols on lipemia and human health. *International Journal of Molecular Sciences*, *19*(1), 1–11. https://doi.org/10.3390/ijms19010104

Araujo, P., Tilahun, E., & Zeng, Y. (2018). A novel strategy for discriminating marine oils by using the positional distribution (sn-1, sn-2, sn-3) of omega-3 polyunsaturated fatty acids in triacylglycerols. *Talanta*, *182*(January), 32–37. https://doi.org/10.1016/j.talanta.2018.01.030

Bakala-N'Goma, J.-C., Couëdelo, L., Vaysse, C., Letisse, M., Pierre, V., Géloen, A., Michalski, M.-C., Lagarde, M., Leao, J.-D., & Carrière, F. (2022). The digestion of diacylglycerol isomers by gastric and pancreatic lipases and its impact on the metabolic pathways for TAG re-synthesis in enterocytes. *Biochimie*, *203*, 106–117. https://doi.org/10.1016/j.biochi.2022.01.003

Balgoma, D., Guitton, Y., Evans, J. J., Le Bizec, B., Dervilly-Pinel, G., & Meynier, A. (2019). Modeling the fragmentation patterns of triacylglycerides in mass spectrometry allows the quantification of the regioisomers with a minimal number of standards. *Analytica Chimica Acta*, *1057*, 60–69. https://doi.org/10.1016/j.aca.2019.01.017

Bandarra, N. M., Lopes, P. A., Martins, S. V., Ferreira, J., Alfaia, C. M., Rolo, E. A., Correia, J. J., Pinto, R. M. A., Ramos-Bueno, R. P., Batista, I., Prates, J. A. M., & Guil-Guerrero, J. L. (2016). Docosahexaenoic acid at the sn-2 position of structured triacylglycerols improved n-3 polyunsaturated fatty acid assimilation in tissues of hamsters. *Nutrition Research*,

*36*(5), 452–463. https://doi.org/10.1016/j.nutres.2015.12.015

Bar-Yoseph, F., Lifshitz, Y., & Cohen, T. (2013). Review of sn-2 palmitate oil implications for infant health. *Prostaglandins Leukotrienes and Essential Fatty Acids*, *89*(4), 139–143. https://doi.org/10.1016/j.plefa.2013.03.002

Barba-Bon, A., Nilam, M., & Hennig, A. (2020). Supramolecular Chemistry in the Biomembrane. *ChemBioChem*, *21*(7), 886–910. https://doi.org/10.1002/cbic.201900646

Beppu, F., Yasuda, K., Okada, A., Hirosaki, Y., Okazaki, M., & Gotoh, N. (2017). Comparison of the distribution of unsaturated fatty acids at the Sn-2 position of phospholipids and triacylglycerols in marine fishes and mammals. *Journal of Oleo Science*, *66*(11), 1217–1227. https://doi.org/10.5650/jos.ess17132

Bernback, S., Blackberg, L., & Hernell, O. (1990). The complete digestion of human milk triacylglycerol in vitro requires gastric lipase, pancreatic colipase-dependent lipase, and bile salt-stimulated lipase. *Journal of Clinical Investigation*, *85*(4), 1221–1226. https://doi.org/10.1172/JCI114556

Bottino, N. R., Vandenburg, G. A., & Reiser, R. (1967). Resistance of certain long-chain polyunsaturated fatty acids of marine oils to pancreatic lipase hydrolysis. *Lipids*, *2*(6), 489–493. https://doi.org/10.1007/BF02533177

Brink, E. J., Haddeman, E., De Fouw, N. J., & Weststrate, J. A. (1995). Positional distribution of stearic acid and oleic acid in a triacylglycerol and dietary calcium concentration determines the apparent absorption of these fatty acids in rats. *Journal of Nutrition*, *125*(9), 2379–2387. https://doi.org/10.1093/jn/125.9.2379

Campbell, J. L., & Baba, T. (2015). Near-complete structural characterization of phosphatidylcholines using electron impact excitation of ions from organics. *Analytical Chemistry*, *87*(11), 5837–5845. https://doi.org/10.1021/acs.analchem.5b01460

Cao, W., Cheng, S., Yang, J., Feng, J., Zhang, W., Li, Z., Chen, Q., Xia, Y., Ouyang, Z., & Ma, X. (2020). Large-scale lipid analysis with C=C location and sn-position isomer resolving power. *Nature Communications*, *11*(1), 1–11. https://doi.org/10.1038/s41467-019-14180-4

Carrière, F., Rogalska, E., Cudrey, C., Ferrato, F., Laugier, R., & Verger, R. (1997). In vivo and in vitro studies on the stereoselective hydrolysis of tri- and diglycerides by gastric and pancreatic lipases. *Bioorganic and Medicinal Chemistry*, *5*(2), 429–435. https://doi.org/10.1016/S0968-0896(96)00251-9

Carta, G., Murru, E., Banni, S., & Manca, C. (2017). Palmitic acid: Physiological role, metabolism

and nutritional implications. *Frontiers in Physiology*, *8*(NOV), 1–14. https://doi.org/10.3389/fphys.2017.00902

Chen, X., Hyatt, B. A., Mucenski, M. L., Mason, R. J., & Shannon, J. M. (2006). Identification and characterization of a lysophosphatidylcholine acyltransferase in alveolar II cells. *Proceedings of the National Academy of Sciences of the United States of America*, *103*(31), 11724–11729. https://doi.org/10.1073/pnas.0604946103

Chen, Y. J., Zhou, X. H., Han, B., Yu, Z., Yi, H. X., Jiang, S. L., Li, Y. Y., Pan, J. C., & Zhang, L. W. (2020). Regioisomeric and enantiomeric analysis of primary triglycerides in human milk by silver ion and chiral HPLC atmospheric pressure chemical ionization-MS. *Journal of Dairy Science*, *103*(9), 7761–7774. https://doi.org/10.3168/jds.2019-17353

Choi, Y., Park, J. Y., & Chang, P. S. (2021). Integral Stereoselectivity of Lipase Based on the Chromatographic Resolution of Enantiomeric/Regioisomeric Diacylglycerols. *Journal of Agricultural and Food Chemistry*, *69*(1), 325–331. https://doi.org/10.1021/acs.jafc.0c07430

Christensen, M., Høy, C., Becker, C., & Redgrave, T. (1995). Intestinal absorption and lymphatic transport of eicosapentaenoic (EPA), docosahexaenoic (DHA), and decanoic acids: dependence on intramolecular triacylglycerol structure. *The American Journal of Clinical Nutrition*, *61*(1), 56–61. https://doi.org/10.1093/ajcn/61.1.56

Christensen, M. M., & Høy, C. (1997). Early dietary intervention with structured triacylglycerols containing docosahexaenoic acid. Effect on brain, liver, and adipose tissue lipids. *Lipids*, *32*(2), 185–191. https://doi.org/10.1007/s11745-997-0023-2

Claes, B. S. R., Bowman, A. P., Poad, B. L. J., Young, R. S. E., Heeren, R. M. A., Blanksby, S. J., & Ellis, S. R. (2021). Mass Spectrometry Imaging of Lipids with Isomer Resolution Using High-Pressure Ozone-Induced Dissociation. *Analytical Chemistry*, *93*(28), 9826–9834. https://doi.org/10.1021/acs.analchem.1c01377

Cornish, S. M., Cordingley, D. M., Shaw, K. A., Forbes, S. C., Leonhardt, T., Bristol, A., Candow, D. G., & Chilibeck, P. D. (2022). Effects of Omega-3 Supplementation Alone and Combined with Resistance Exercise on Skeletal Muscle in Older Adults: A Systematic Review and Meta-Analysis. *Nutrients*, *14*(11), 2221. https://doi.org/10.3390/nu14112221

Costenbader, K. H., Cook, N. R., Lee, I. M., Hahn, J., Walter, J., Bubes, V., Kotler, G., Yang, N., Friedman, S., Alexander, E. K., & Manson, J. A. E. (2024). Vitamin D and Marine n-3 Fatty Acids for Autoimmune Disease

Prevention: Outcomes Two Years After Completion of a Double-Blind, Placebo-Controlled Trial. *Arthritis and Rheumatology*, *76*(6), 973–983. https://doi.org/10.1002/art.42811

Craven, R. J., & Lencki, R. W. (2012). Triacylglycerol polymorphism is a stereochemical phenomenon. *Lipid Technology*, *24*(9), 204–207. https://doi.org/10.1002/lite.201200221

Cubero Herrera, L., Ramaley, L., Potvin, M. A., & Melanson, J. E. (2013). A method for determining regioisomer abundances of polyunsaturated triacylglycerols in omega-3 enriched fish oils using reversed-phase liquid chromatography and triple-stage mass spectrometry. *Food Chemistry*, *139*(1), 655–662. https://doi.org/https://doi.org/10.1016/j.foodchem.2012.12.059

Cuenoud, B., Rochat, I., Gosoniu, M., Dupuis, L., Berk, E., Jaudszus, A., Mainz, J., Hafen, G., Beaumont, M., & Cruz-Hernandez, C. (2020). Monoacylglycerol Form of Omega-3s Improves Its Bioavailability in Humans Compared to Other Forms. *Nutrients*, *12*(4), 1014. https://doi.org/10.3390/nu12041014

Cui, X. Y., Jiang, S., Wang, C. C., Yang, J. Y., Zhao, Y. C., Xue, C. H., Wang, Y. M., & Zhang, T. T. (2022). Comparative Analyses of EPA-Phosphatidylcholine, EPA-Lysophosphatidylcholine, and DHA-Lysophosphatidylcholine on DHA and EPA Repletion in n-3 PUFA-Deficient Mice. *Journal of Agricultural and Food Chemistry*. https://doi.org/10.1021/acs.jafc.2c06462

Dawczynski, C., Dittrich, M., Neumann, T., Goetze, K., Welzel, A., Oelzner, P., Völker, S., Schaible, A. M., Troisi, F., Thomas, L., Pace, S., Koeberle, A., Werz, O., Schlattmann, P., Lorkowski, S., & Jahreis, G. (2018). Docosahexaenoic acid in the treatment of rheumatoid arthritis: A double-blind, placebo-controlled, randomized cross-over study with microalgae vs . sunflower oil. *Clinical Nutrition*, *37*(2), 494–504. https://doi.org/10.1016/j.clnu.2017.02.021

De Bruin, C. R., De Bruijn, W. J. C., Hemelaar, M. A., Vincken, J. P., & Hennebelle, M. (2025). Separation of triacylglycerol (TAG) isomers by cyclic ion mobility mass spectrometry. *Talanta*, *281*(September 2024), 126804. https://doi.org/10.1016/j.talanta.2024.126804

De Toro, V., Alberti, G., Dominguez, A., Carrasco-Negüe, K., Ferrer, P., Valenzuela, R., Garmendia, M. L., & Casanello, P. (2024). Growth patterns in infants born to women with pregestational overweight/obesity supplemented with docosahexaenoic acid during pregnancy. *Journal of Pediatric Gastroenterology and Nutrition*, *79*(2), 371–381.

https://doi.org/10.1002/jpn3.12294

Dempsey, M., Rockwell, M. S., & Wentz, L. M. (2023). The influence of dietary and supplemental omega-3 fatty acids on the omega-3 index: A scoping review. *Frontiers in Nutrition*, *10*(1). https://doi.org/10.3389/fnut.2023.1072653

Ding, W., Zhang, X., Xiao, D., & Chang, W. (2023). Decreased in n-3 DHA enriched triacylglycerol in small extracellular vesicles of diabetic patients with cardiac dysfunction. *Journal of Diabetes*, *15*(12), 1070–1080. https://doi.org/10.1111/1753-0407.13457

Dou, Y., Wang, Y., Chen, Z., Yu, X., & Ma, D. (2022). Effect of n-3 polyunsaturated fatty acid on bone health: A systematic review and meta-analysis of randomized controlled trials. *Food Science and Nutrition*, *10*(1), 145–154. https://doi.org/10.1002/fsn3.2655

Dyall, S. C., Balas, L., Bazan, N. G., Brenna, J. T., Chiang, N., da Costa Souza, F., Dalli, J., Durand, T., Galano, J. M., Lein, P. J., Serhan, C. N., & Taha, A. Y. (2022). Polyunsaturated fatty acids and fatty acid-derived lipid mediators: Recent advances in the understanding of their biosynthesis, structures, and functions. *Progress in Lipid Research*, *86*(April), 101165. https://doi.org/10.1016/j.plipres.2022.101165

Ekroos, K., Ejsing, C. S., Bahr, U., Karas, M., Simons, K., & Shevchenko, A. (2003). Charting molecular composition of phosphatidylcholines by fatty acid scanning and ion trap MS3 fragmentation. *Journal of Lipid Research*, *44*(11), 2181–2192. https://doi.org/10.1194/jlr.D300020-JLR200

Engelen, M. P., Jonker, R., Sulaiman, H., Fisk, H. L., Calder, P. C., & Deutz, N. E. (2022). Ω-3 Polyunsaturated Fatty Acid Supplementation Improves Postabsorptive and Prandial Protein Metabolism in Patients With Chronic Obstructive Pulmonary Disease: a Randomized Clinical Trial. *American Journal of Clinical Nutrition*, *116*(3), 686–698. https://doi.org/10.1093/ajcn/nqac138

Fabritius, M. (2023). Mass spectrometric methodologies for analysis of triacylglycerol and phospholipid regioisomers in natural fats and oils. *Doctoral Thesis in Food Sciences, University of Turku*, Turku, Finland.

Fabritius, M., Linderborg, K. M., Tarvainen, M., Kalpio, M., Zhang, Y., & Yang, B. (2020). Direct inlet negative ion chemical ionization tandem mass spectrometric analysis of triacylglycerol regioisomers in human milk and infant formulas. *Food Chemistry*, *328*, 126991. https://doi.org/10.1016/j.foodchem.2020.126991

Fahy, E., Subramaniam, S., Brown, H. A., Glass, C. K., Merrill, A. H., Murphy, R. C., Raetz, C. R. H., Russell, D. W., Seyama, Y., Shaw, W., Shimizu, T., Spener,

F., van Meer, G., VanNieuwenhze, M. S., White, S. H., Witztum, J. L., & Dennis, E. A. (2005). A comprehensive classification system for lipids. *European Journal of Lipid Science and Technology*, *107*(5), 337–364. https://doi.org/10.1002/ejlt.200405001

Fahy, E., Subramaniam, S., Murphy, R. C., Nishijima, M., Raetz, C. R. H., Shimizu, T., Spener, F., Van Meer, G., Wakelam, M. J. O., & Dennis, E. A. (2009). Update of the LIPID MAPS comprehensive classification system for lipids. *Journal of Lipid Research*, *50*(SUPPL.), S9–S14. https://doi.org/10.1194/jlr.R800095-JLR200

Feehan, O., Magee, P. J., Pourshahidi, L. K., Armstrong, D. J., Slevin, M. M., Allsopp, P. J., Conway, M. C., Strain, J. J., & McSorley, E. M. (2023). Associations of long chain polyunsaturated fatty acids with bone mineral density and bone turnover in postmenopausal women. *European Journal of Nutrition*, *62*(1), 95–104. https://doi.org/10.1007/s00394-022-02933-9

Foubert, I., Dewettinck, K., Van de Walle, D., Dijkstra, A. J., & Quinn, P. J. (2007). Physical properties: structural and physical characteristics. *The Lipid Handbook*, 471–534.

Georgiou, M., & Prokopiou, E. (2023). Diabetic retinopathy and the role of Omega-3 PUFAs: A narrative review. *Experimental Eye Research*, *231*(December 2022), 109494. https://doi.org/10.1016/j.exer.2023.109494

Gerbi, A., Zérouga, M., Debray, M., Durand, G., Chanez, C., & Bourre, J. -M. (1994). Effect of Fish Oil Diet on Fatty Acid Composition of Phospholipids of Brain Membranes and on Kinetic Properties of Na+, K+-ATPase Isoenzymes of Weaned and Adult Rats. *Journal of Neurochemistry*, *62*(4), 1560–1569. https://doi.org/10.1046/j.1471-4159.1994.62041560.x

Ghasemifard, S., Hermon, K., Turchini, G. M., & Sinclair, A. J. (2015). Metabolic fate (absorption, β-oxidation and deposition) of long-chain n-3 fatty acids is affected by sex and by the oil source (krill oil or fish oil) in the rat. *British Journal of Nutrition*. https://doi.org/10.1017/S0007114515002457

Ghide, M. K., & Yan, Y. (2021). 1,3-Dioleoyl-2-palmitoyl glycerol (OPO)-Enzymatic synthesis and use as an important supplement in infant formulas. *Journal of Food Biochemistry*, *45*(7), e13799. https://doi.org/10.1111/jfbc.13799

Gorczyca, D., Szponar, B., Paściak, M., Czajkowska, A., & Szmyrka, M. (2022). Serum levels of n-3 and n-6 polyunsaturated fatty acids in patients with systemic lupus erythematosus and their association with disease activity: a pilot study. *Scandinavian Journal of Rheumatology*, *51*(3), 230–236. https://doi.org/10.1080/030097

42.2021.1923183

Gouk, S. W., Cheng, S. F., Mok, J. S. L., Ong, A. S. H., & Chuah, C. H. (2013). Long-chain SFA at the sn-1, 3 positions of TAG reduce body fat deposition in C57BL/6 mice. *British Journal of Nutrition*, *110*(11), 1987–1995. https://doi.org/10.1017/S0007114513001475

Gould, J. F., Anderson, P. J., Yelland, L. N., Gibson, R. A., & Makrides, M. (2021). The Influence of Prenatal DHA Supplementation on Individual Domains of Behavioral Functioning in School-Aged Children: Follow-Up of a Randomized Controlled Trial. *Nutrients*, *13*(9), 2996. https://doi.org/10.3390/nu13092996

Gudmundsson, H. G., Linderborg, K. M., Kallio, H., Yang, B., & Haraldsson, G. G. (2020). Synthesis of enantiopure ABC-type triacylglycerols. *Tetrahedron*, *76*(2), 130813. https://doi.org/10.1016/j.tet.2019.130813

Halldorsson, A., Magnusson, C. D., & Haraldsson, G. G. (2003). Chemoenzymatic synthesis of structured triacylglycerols by highly regioselective acylation. *Tetrahedron*, *59*(46), 9101–9109. https://doi.org/10.1016/j.tet.2003.09.059

Hamosh, M., & Scow, R. O. (1973). Lingual Lipase and Its Role in the Digestion of Dietary Lipid. *Journal of Clinical Investigation*, *52*(1), 88–95. https://doi.org/10.1172/JCI107177

Han, X., & Gross, R. W. (2001). Quantitative analysis and molecular species fingerprinting of triacylglyceride molecular species directly from lipid extracts of biological samples by electrospray ionization tandem mass spectrometry. *Analytical Biochemistry*, *295*(1), 88–100. https://doi.org/10.1006/abio.2001.5178

Han, X., & Ye, H. (2021). Overview of Lipidomic Analysis of Triglyceride Molecular Species in Biological Lipid Extracts. *Journal of Agricultural and Food Chemistry*, *69*(32), 8895–8909. https://doi.org/10.1021/acs.jafc.0c07175

Haraldsdottir, H., Gudmundsson, H. G., Linderborg, K. M., Yang, B., & Haraldsson, G. G. (2024). Chemoenzymatic Synthesis of ABC-Type Enantiostructured Triacylglycerols by the Use of the p-Methoxybenzyl Protective Group. *Molecules*, *29*(7), 1633. https://doi.org/10.3390/molecules29071633

Haraldsson, G. G., Halldorsson, A., & Kuls, E. (2000). Chemoenzymatic synthesis of structured triacylglycerols containing eicosapentaenoic and docosahexaenoic acids. *JAOCS, Journal of the American Oil Chemists' Society*, *77*(11), 1139–1145. https://doi.org/10.1007/s11746-000-0179-1

Harayama, T., Eto, M., Shindou, H., Kita, Y., Otsubo, E., Hishikawa, D., Ishii, S., Sakimura, K., Mishina, M., & Shimizu, T.

(2014). Lysophospholipid acyltransferases mediate phosphatidylcholine diversification to achieve the physical properties required in vivo. *Cell Metabolism*, *20*(2), 295–305. https://doi.org/10.1016/j.cmet.2014.05.019

Harvey, D. J. (2005). A new charge-associated mechanism to account for the production of fragment ions in the high-energy CID spectra of fatty acids. *Journal of the American Society for Mass Spectrometry*, *16*(2), 280–290. https://doi.org/10.1016/j.jasms.2004.11.008

Holčapek, M., Dvořáková, H., Lísa, M., Girón, A. J., Sandra, P., & Cvačka, J. (2010). Regioisomeric analysis of triacylglycerols using silver-ion liquid chromatography-atmospheric pressure chemical ionization mass spectrometry: Comparison of five different mass analyzers. *Journal of Chromatography A*, *1217*(52), 8186–8194. https://doi.org/10.1016/j.chroma.2010.10.064

Holčapek, M., & Ekroos, K. (2023). Introduction to Lipidomics. In *Mass Spectrometry for Lipidomics (Volume 1)* (pp. 1–12). Wiley-VCH. https://doi.org/https://doi.org/10.1002/9783527836512.ch1

Hopiavuori, B. R., Agbaga, M. P., Brush, R. S., Sullivan, M. T., Sonntag, W. E., & Anderson, R. E. (2017). Regional changes in CNS and retinal glycerophospholipid profiles with age: A molecular blueprint. *Journal of Lipid Research*, *58*(4), 668–680. https://doi.org/10.1194/jlr.M070714

Igarashi, M., Ma, K., Chang, L., Bell, J. M., & Rapoport, S. I. (2007). Dietary n-3 PUFA deprivation for 15 weeks upregulates elongase and desaturase expression in rat liver but not brain. *Journal of Lipid Research*, *48*(11), 2463–2470. https://doi.org/10.1194/jlr.M700315-JLR200

Ikeda, I., Yoshida, H., Tomooka, M., Yosef, A., Imaizumi, K., Tsuji, H., & Seto, A. (1998). Effects of long-term feeding of marine oils with different positional distribution of eicosapentaenoic and docosahexaenoic acids on lipid metabolism, eicosanoid production, and platelet aggregation in hypercholesterolemic rats. *Lipids*. https://doi.org/10.1007/s11745-998-0286-7

Innes, J. K., & Calder, P. C. (2020). Marine Omega-3 (N-3) Fatty Acids for Cardiovascular Health: An Update for 2020. *International Journal of Molecular Sciences*, *21*(4), 1362. https://doi.org/10.3390/ijms21041362

Jensen, R. G., Dejong, F. A., Clark, R. M., Palmgren, L. G., Liao, T. H., & Hamosh, M. (1982). Stereospecificity of premature human infant lingual lipase. *Lipids*, *17*(8), 570–572. https://doi.org/10.1007/BF02535386

John Craven, R., & Lencki, R. W. (2011). Crystallization,

polymorphism, and binary phase behavior of model enantiopure and racemic 1,3-Diacylglycerols. *Crystal Growth and Design*, *11*(5), 1566–1572. https://doi.org/10.1021/cg101536q

Kallio, H., Nylund, M., Boström, P., & Yang, B. (2017). Triacylglycerol regioisomers in human milk resolved with an algorithmic novel electrospray ionization tandem mass spectrometry method. *Food Chemistry*, *233*, 351–360. https://doi.org/10.1016/j.foodchem.2017.04.122

Kalo, P., Kemppinen, A., Ollilainen, V., & Kuksis, A. (2003). Analysis of regioisomers of short-chain triacylglycerols by normal phase liquid chromatography-electrospray tandem mass spectrometry. *International Journal of Mass Spectrometry*, *229*(3), 167–180. https://doi.org/10.1016/S1387-3806(03)00302-6

Kalpio, M., Linderborg, K. M., Fabritius, M., Kallio, H., & Yang, B. (2021). Strategy for stereospecific characterization of natural triacylglycerols using multidimensional chromatography and mass spectrometry. *Journal of Chromatography A*, *1641*, 461992. https://doi.org/10.1016/j.chroma.2021.461992

Kalpio, M., Magnússon, J. D., Gudmundsson, H. G., Linderborg, K. M., Kallio, H., Haraldsson, G. G., & Yang, B. (2020). Synthesis and enantiospecific analysis of enantiostructured triacylglycerols containing n-3 polyunsaturated fatty acids. *Chemistry and Physics of Lipids*, *231*, 104937. https://doi.org/10.1016/j.chemphyslip.2020.104937

Kalpio, M., Nylund, M., Linderborg, K. M., Yang, B., Kristinsson, B., Haraldsson, G. G., & Kallio, H. (2015). Enantioselective chromatography in analysis of triacylglycerols common in edible fats and oils. *Food Chemistry*, *172*, 718–724. https://doi.org/10.1016/j.foodchem.2014.09.135

Kawakita, E., Hashimoto, M., & Shido, O. (2006). Docosahexaenoic acid promotes neurogenesis in vitro and in vivo. *Neuroscience*, *139*(3), 991–997. https://doi.org/10.1016/j.neuroscience.2006.01.021

Kawamura, A., Nemoto, K., & Sugita, M. (2023). Effect of 8-week intake of the n-3 fatty acid-rich perilla oil on the gut function and as a fuel source for female athletes: A randomised trial. *British Journal of Nutrition*, *129*(6), 981–991. https://doi.org/10.1017/S0007114522001805

Khan, I., Hussain, M., Jiang, B., Zheng, L., Pan, Y., Hu, J., Khan, A., Ashraf, A., & Zou, X. (2023). Omega-3 long-chain polyunsaturated fatty acids: Metabolism and health implications. *Progress in Lipid Research*, *92*(October), 101255. https://doi.org/10.1016/j.plipres.2023.101255

Khan, M. J., Chung, N. A., Hansen, S., Dumitrescu, L., Hohman, T.

J., Kamboh, M. I., Lopez, O. L., & Robinson, R. A. S. (2022). Targeted Lipidomics to Measure Phospholipids and Sphingomyelins in Plasma: A Pilot Study to Understand the Impact of Race/Ethnicity in Alzheimer's Disease. *Analytical Chemistry*, *94*(10), 4165–4174. https://doi.org/10.1021/acs.analchem.1c03821

Klein, D. R., Feider, C. L., Garza, K. Y., Lin, J. Q., Eberlin, L. S., & Brodbelt, J. S. (2018). Desorption Electrospray Ionization Coupled with Ultraviolet Photodissociation for Characterization of Phospholipid Isomers in Tissue Sections. *Analytical Chemistry*, *90*(17), 10100–10104. https://doi.org/10.1021/acs.analchem.8b03026

Kong, M., Hong, D. H., Paudel, S., Yoon, N. E., Jung, B. H., Kim, M., Kim, T. H., Jeong, J., Choi, D., & Lee, H. (2024). Metabolomics and miRNA profiling reveals feature of gallbladder cancer-derived biliary extracellular vesicles. *Biochemical and Biophysical Research Communications*, *705*(November 2023), 149724. https://doi.org/10.1016/j.bbrc.2024.149724

Kristinsson, B., & Haraldsson, G. (2008). Chemoenzymatic Synthesis of Enantiopure Structured Triacylglycerols. *Synlett*, *2008*(14), 2178–2182. https://doi.org/10.1055/s-2008-1077981

Kulkarni, A., Zhao, A., Yang, B., Zhang, Y., & Linderborg, K. M. (2022). Tissue-Specific Content of Polyunsaturated Fatty Acids in (n-3) Deficiency State of Rats. *Foods*, *11*(2), 208. https://doi.org/10.3390/foods11020208

Lagace, T. A., & Ridgway, N. D. (2013). The role of phospholipids in the biological activity and structure of the endoplasmic reticulum. *Biochimica et Biophysica Acta - Molecular Cell Research*, *1833*(11), 2499–2510. https://doi.org/10.1016/j.bbamcr.2013.05.018

Laguzzi, F., Åkesson, A., Marklund, M., Qian, F., Gigante, B., Bartz, T. M., Bassett, J. K., Birukov, A., Campos, H., Hirakawa, Y., Imamura, F., Jäger, S., Lankinen, M., Murphy, R. A., Senn, M., Tanaka, T., Tintle, N., Virtanen, J. K., Yamagishi, K., … Leander, K. (2024). Role of Polyunsaturated Fat in Modifying Cardiovascular Risk Associated With Family History of Cardiovascular Disease: Pooled De Novo Results From 15 Observational Studies. *Circulation*, *149*(4), 305–316. https://doi.org/10.1161/CIRCULATIONAHA.123.065530

Lan, Q. Y., Huang, S. Y., Jiang, C. Y., Yang, M. T., Wu, T., Chen, X. Y., Liu, Z. Y., Wei, W., Wang, X. G., & Zhu, H. L. (2022). Profiling of triacylglycerol composition in the breast milk of Chinese mothers at different lactation stages. *Food and Function*, *13*(18), 9674–9686. https://doi.org/10.1039/d2fo01877b

Lasekan, J. B., Hustead, D. S., Masor,

M., & Murray, R. (2017). Impact of palm olein in infant formulas on stool consistency and frequency: A meta-analysis of randomized clinical trials. *Food and Nutrition Research*, *61*(1). https://doi.org/10.1080/16546628.2017.1330104

Lee, A. G. (2011). Biological membranes: The importance of molecular detail. *Trends in Biochemical Sciences*, *36*(9), 493–500. https://doi.org/10.1016/j.tibs.2011.06.007

Léger, T., Brun, A., Lanchais, K., Rigaudière, J.-P., Briat, A., Guitton, Y., Marchand, F., Tournadre, A., & Capel, F. (2023). Docosahexaenoic acid and etanercept could reduce functional and metabolic alterations during collagen-induced arthritis in rats without any synergistic effect. *Life Sciences*, *327*(December 2022), 121826. https://doi.org/10.1016/j.lfs.2023.121826

Leveque, N. L., Acheampong, A., Heron, S., & Tchapla, A. (2012). Determination of triacylglycerol regioisomers using electrospray ionization-quadrupole ion trap mass spectrometry with a kinetic method. *Analytica Chimica Acta*, *722*, 80–86. https://doi.org/10.1016/j.aca.2012.02.016

Lévêque, N. L., Héron, S., & Tchapla, A. (2010). Regioisomer characterization of triacylglycerols by non-aqueous reversed-phase liquid chromatography/electrospray ionization mass spectrometry using silver nitrate as a post column reagent. *Journal of Mass Spectrometry*, *45*(3), 284–296. https://doi.org/10.1002/jms.1713

Li, J. J., Huang, C. J., & Xie, D. (2008). Anti-obesity effects of conjugated linoleic acid, docosahexaenoic acid, and eicosapentaenoic acid. *Molecular Nutrition and Food Research*, *52*(6), 631–645. https://doi.org/10.1002/mnfr.200700399

Li, Z., Agellon, L. B., Allen, T. M., Umeda, M., Jewell, L., Mason, A., & Vance, D. E. (2006). The ratio of phosphatidylcholine to phosphatidylethanolamine influences membrane integrity and steatohepatitis. *Cell Metabolism*, *3*(5), 321–331. https://doi.org/10.1016/j.cmet.2006.03.007

Liebisch, G., Fahy, E., Aoki, J., Dennis, E. A., Durand, T., Ejsing, C. S., Fedorova, M., Feussner, I., Griffiths, W. J., Köfeler, H., Merrill, A. H., Murphy, R. C., O'Donnell, V. B., Oskolkova, O., Subramaniam, S., Wakelam, M. J. O., & Spener, F. (2020). Update on LIPID MAPS classification, nomenclature, and shorthand notation for MS-derived lipid structures. *Journal of Lipid Research*, *61*(12), 1539–1555. https://doi.org/10.1194/jlr.S120001025

Lillja, J., & Lanekoff, I. (2022). Quantitative determination of sn-positional phospholipid isomers in MSn using silver

cationization. *Analytical and Bioanalytical Chemistry*, *414*(25), 7473–7482. https://doi.org/10.1007/s00216-022-04173-6

Lin, J. T., & Chen, G. Q. (2014). Quantification of the molecular species of TAG and DAG in lesquerella (Physaria fendleri) oil by HPLC and MS. *JAOCS, Journal of the American Oil Chemists' Society*, *91*(8), 1417–1424. https://doi.org/10.1007/s11746-014-2486-2

Linderborg, K. M., Kalpio, M., Mäkelä, J., Niinikoski, H., Kallio, H. P., & Lagström, H. (2014). Tandem mass spectrometric analysis of human milk triacylglycerols from normal weight and overweight mothers on different diets. *Food Chemistry*, *146*, 583–590. https://doi.org/10.1016/j.foodchem.2013.09.092

Linderborg, K. M., Kulkarni, A., Zhao, A., Zhang, J., Kallio, H., Magnusson, J. D., Haraldsson, G. G., Zhang, Y., & Yang, B. (2019). Bioavailability of docosahexaenoic acid 22:6(n-3) from enantiopure triacylglycerols and their regioisomeric counterpart in rats. *Food Chemistry*, *283*, 381–389. https://doi.org/10.1016/j.foodchem.2018.12.130

Lísa, M., Denev, R., & Holčapek, M. (2013). Retention behavior of isomeric triacylglycerols in silver-ion HPLC: Effects of mobile phase composition and temperature. *Journal of Separation Science*, *36*(17), 2888–2900. https://doi.org/10.1002/jssc.201300550

Lísa, M., & Holčapek, M. (2013). Characterization of triacylglycerol enantiomers using chiral HPLC/APCI-MS and synthesis of enantiomeric triacylglycerols. *Analytical Chemistry*, *85*(3), 1852–1859. https://doi.org/10.1021/ac303237a

Liu, Z., & Rochfort, S. (2022). Regio-distribution and double bond locations of unsaturated fatty acids in phospholipids of bovine milk. *Food Chemistry*, *373*(PB), 131515. https://doi.org/10.1016/j.foodchem.2021.131515

Mackie, A., Mulet-Cabero, A. I., & Torcello-Gomez, A. (2020). Simulating human digestion: Developing our knowledge to create healthier and more sustainable foods. *Food and Function*, *11*(11), 9397–9431. https://doi.org/10.1039/d0fo01981j

Masuda, K., Abe, K., & Murano, Y. (2021). A Practical Method for Analysis of Triacylglycerol Isomers Using Supercritical Fluid Chromatography. *JAOCS, Journal of the American Oil Chemists' Society*, *98*(1), 21–29. https://doi.org/10.1002/aocs.12432

Mattson, F. H., & Lutton, E. S. (1958). The specific distribution of fatty acids in the glycerides of animal and vegetable fats. *The Journal of Biological Chemistry*, *233*(4), 868–871. https://doi.org/10.1016/s0021-9258(18)64670-8

Mensink, R. P., Sanders, T. A., Baer, D. J., Hayes, K. C., Howles, P.

N., & Marangoni, A. (2016). The increasing use of interesterified lipids in the food supply and their effects on health parameters. *Advances in Nutrition*, *7*(4), 719–729. https://doi.org/10.3945/an.115.009662

Miao, Z., Chen, G. dong, Huo, S., Fu, Y., Wu, M. Y., Xu, F., Jiang, Z., Tang, J., Gou, W., Xiao, C., Liu, Y. ping, Wu, Y. Y., Sun, T. yu, Sun, L., Shen, L. R., Lin, X., Chen, Y. ming, & Zheng, J. S. (2022). Interaction of n-3 polyunsaturated fatty acids with host CD36 genetic variant for gut microbiome and blood lipids in human cohorts. *Clinical Nutrition*, *41*(8), 1724–1734. https://doi.org/10.1016/j.clnu.2022.05.021

Micha, R., Khatibzadeh, S., Shi, P., Fahimi, S., Lim, S., Andrews, K. G., Engell, R. E., Powles, J., Ezzati, M., & Mozaffarian, D. (2014). Global, regional, and national consumption levels of dietary fats and oils in 1990 and 2010: a systematic analysis including 266 country-specific nutrition surveys. *BMJ*, *348*, g2272–g2272. https://doi.org/10.1136/bmj.g2272

Michaeloudes, C., Christodoulides, S., Christodoulou, P., Kyriakou, T.-C., Patrikios, I., & Stephanou, A. (2023). Variability in the Clinical Effects of the Omega-3 Polyunsaturated Fatty Acids DHA and EPA in Cardiovascular Disease—Possible Causes and Future Considerations. *Nutrients*, *15*(22), 4830. https://doi.org/10.3390/nu15224830

Morley, N., & Kuksis, A. (1972). Positional Specificity of Lipoprotein Lipase. *Journal of Biological Chemistry*, *247*(20), 6389–6393. https://doi.org/10.1016/S0021-9258(19)44705-4

Murphy, R. A., Mourtzakis, M., & Mazurak, V. C. (2012). N-3 polyunsaturated fatty acids: The potential role for supplementation in cancer. *Current Opinion in Clinical Nutrition and Metabolic Care*, *15*(3), 246–251. https://doi.org/10.1097/MCO.0b013e328351c32f

Murthya, M., Hamiltonb, J., Greinera, R. S., Moriguchia, T., Salem, N., Jra, & Kimb, H. Y. (2002). Differential effects of n-3 fatty acid deficiency on phospholipid molecular species composition in the rat hippocampus. *Journal of Lipid Research*, *43*(4), 611–617. https://doi.org/10.1016/s0022-2275(20)31491-7

Nagai, T., Ishikawa, K., Yoshinaga, K., Yoshida, A., Beppu, F., & Gotoh, N. (2017). Homochiral asymmetric triacylglycerol isomers in egg yolk. *Journal of Oleo Science*, *66*(12), 1293–1299. https://doi.org/10.5650/jos.ess17128

Nagai, T., Kinoshita, T., Kasamatsu, E., Yoshinaga, K., Mizobe, H., Yoshida, A., Itabashi, Y., & Gotoh, N. (2019). Simultaneous separation of triacylglycerol enantiomers and positional isomers by chiral high performance liquid

chromatography coupled with mass spectrometry. *Journal of Oleo Science*, *68*(10), 1019–1026. https://doi.org/10.5650/jos.ess19122

Nagai, T., Kinoshita, T., Kasamatsu, E., Yoshinaga, K., Mizobe, H., Yoshida, A., Itabashi, Y., & Gotoh, N. (2020). Simultaneous quantification of mixed-acid triacylglycerol positional isomers and enantiomers in palm oil and lard by chiral high-performance liquid chromatography coupled with mass spectrometry. *Symmetry*, *12*(9), 1–7. https://doi.org/10.3390/SYM12091385

Nagai, T., Matsumoto, Y., Jiang, Y., Ishikawa, K., Wakatabe, T., Mizobe, H., Yoshinaga, K., Kojima, K., Kuroda, I., Saito, T., Beppu, F., & Gotoh, N. (2013). Actual ratios of triacylglycerol positional isomers and enantiomers comprising saturated fatty acids and highly unsaturated fatty acids in fishes and marine mammals. *Journal of Oleo Science*, *62*(12), 1009–1015. https://doi.org/10.5650/jos.62.1009

Nagai, T., Mizobe, H., Otake, I., Ichioka, K., Kojima, K., Matsumoto, Y., Gotoh, N., Kuroda, I., & Wada, S. (2011). Enantiomeric separation of asymmetric triacylglycerol by recycle high-performance liquid chromatography with chiral column. *Journal of Chromatography A*, *1218*(20), 2880–2886. https://doi.org/10.1016/j.chroma.2011.02.067

Nagai, T., Watanabe, N., Yoshinaga, K., Mizobe, H., Kojima, K., Kuroda, I., Odanaka, Y., Saito, T., Beppu, F., & Gotoh, N. (2015). Abundances of triacylglycerol positional isomers and enantiomers comprised of a dipalmitoylglycerol backbone and short- or medium-chain fatty acids in bovine milk fat. *Journal of Oleo Science*, *64*(9), 943–952. https://doi.org/10.5650/jos.ess15040

Oye Mintsa Mi-Mba, M. F., Lebbadi, M., Alata, W., Julien, C., Emond, V., Tremblay, C., Fortin, S., Barrow, C. J., Bilodeau, J. F., & Calon, F. (2024). Differential impact of eicosapentaenoic acid and docosahexaenoic acid in an animal model of Alzheimer's disease. *Journal of Lipid Research*, *65*(12), 100682. https://doi.org/10.1016/j.jlr.2024.100682

Paine, M. R. L., Poad, B. L. J., Eijkel, G. B., Marshall, D. L., Blanksby, S. J., Heeren, R. M. A., & Ellis, S. R. (2018). Mass Spectrometry Imaging with Isomeric Resolution Enabled by Ozone-Induced Dissociation. *Angewandte Chemie - International Edition*, *57*(33), 10530–10534. https://doi.org/10.1002/anie.201802937

Paltauf, F., Esfandi, F., & Holasek, A. (1974). Stereospecificity of lipases. Enzymic hydrolysis of enantiomeric alkyl diacylglycerols by lipoprotein lipase, lingual lipase and

pancreatic lipase. *FEBS Letters*. https://doi.org/10.1016/0014-5793(74)80907-5

Panzoldo, N. B., Urban, A., Parra, E. S., Oliveira, R., Zago, V. S., da Silva, L. R., & de Faria, E. C. (2011). Differences and similarities of postprandial lipemia in rodents and humans. *Lipids in Health and Disease*, *10*(1), 86. https://doi.org/10.1186/1476-511X-10-86

Park, J.-Y., & Park, K.-M. (2022). Lipase and Its Unique Selectivity: A Mini-Review. *Journal of Chemistry*, *2022*(1), 1–11. https://doi.org/10.1155/2022/7609019

Peña-de-la-Sancha, P., Muñoz-García, A., Espínola-Zavaleta, N., Bautista-Pérez, R., Mejía, A. M., Luna-Luna, M., López-Olmos, V., Rodríguez-Pérez, J. M., Fragoso, J. M., Carreón-Torres, E., & Pérez-Méndez, Ó. (2023). Eicosapentaenoic and Docosahexaenoic Acid Supplementation Increases HDL Content in n-3 Fatty Acids and Improves Endothelial Function in Hypertriglyceridemic Patients. *International Journal of Molecular Sciences*, *24*(6), 1–12. https://doi.org/10.3390/ijms24065390

Petrova, D., Bernabeu Litrán, M. A., García-Mármol, E., Rodríguez-Rodríguez, M., Cueto-Martín, B., López-Huertas, E., Catena, A., & Fonollá, J. (2019). Effects of fortified milk on cognitive abilities in school-aged children: results from a randomized-controlled trial. *European Journal of Nutrition*, *58*(5), 1863–1872. https://doi.org/10.1007/s00394-018-1734-x

Pham, H. T., Maccarone, A. T., Thomas, M. C., Campbell, J. L., Mitchell, T. W., & Blanksby, S. J. (2014). Structural characterization of glycerophospholipids by combinations of ozone- and collision-induced dissociation mass spectrometry: The next step towards "top-down" lipidomics. *Analyst*, *139*(1), 204–214. https://doi.org/10.1039/c3an01712e

Phillips, G. R., Hancock, S. E., Jenner, A. M., McLean, C., Newell, K. A., & Mitchell, T. W. (2022). Phospholipid Profiles Are Selectively Altered in the Putamen and White Frontal Cortex of Huntington's Disease. *Nutrients*, *14*(10), 2086. https://doi.org/10.3390/nu14102086

Pomponi, M., & Pomponi, M. (2008). DHA deficiency and Alzheimer's disease. *Clinical Nutrition*, *27*(1), 170. https://doi.org/10.1016/j.clnu.2007.10.009

Ponnampalam, E. N., Lewandowski, P., Nesaratnam, K., Dunshea, F. R., & Gill, H. (2011). Differential effects of natural palm oil, chemically- and enzymatically-modified palm oil on weight gain, blood lipid metabolites and fat deposition in a pediatric pig model. *Nutrition Journal*, *10*(1), 1–7. https://doi.org/10.1186/1475-2891-10-53

Proitsi, P., Kim, M., Whiley, L., Simmons, A., Sattlecker, M., Velayudhan, L., Lupton, M. K., Soininen, H., Kloszewska, I., Mecocci, P., Tsolaki, M., Vellas, B., Lovestone, S., Powell, J. F., Dobson, R. J. B., & Legido-Quigley, C. (2017). Association of blood lipids with Alzheimer's disease: A comprehensive lipidomics analysis. *Alzheimer's and Dementia*, *13*(2), 140–151. https://doi.org/10.1016/j.jalz.2016.08.003

Ramos-Martín, F., & D'Amelio, N. (2022). Biomembrane lipids: When physics and chemistry join to shape biological activity. *Biochimie*, *203*, 118–138. https://doi.org/10.1016/j.biochi.2022.07.011

Rapoport, S. I., Rao, J. S., & Igarashi, M. (2007). Brain metabolism of nutritionally essential polyunsaturated fatty acids depends on both the diet and the liver. *Prostaglandins, Leukotrienes, and Essential Fatty Acids*, *77*, 251–261. https://doi.org/10.1016/j.plefa.2007.10.023

Řezanka, T., Kolouchová, I., Čejková, A., Cajthaml, T., & Sigler, K. (2013). Identification of regioisomers and enantiomers of triacylglycerols in different yeasts using reversed- and chiral-phase LC-MS. *Journal of Separation Science*, *36*(20), 3310–3320. https://doi.org/10.1002/jssc.201300657

Řezanka, T., Kolouchová, I., Nedbalová, L., & Sigler, K. (2018). Enantiomeric separation of triacylglycerols containing very long chain fatty acids. *Journal of Chromatography A*, *1557*, 9–19. https://doi.org/10.1016/j.chroma.2018.04.064

Řezanka, T., Lukavský, J., Nedbalová, L., Kolouchová, I., & Sigler, K. (2012). Effect of starvation on the distribution of positional isomers and enantiomers of triacylglycerol in the diatom Phaeodactylum tricornutum. *Phytochemistry*, *80*, 17–27. https://doi.org/10.1016/j.phytochem.2012.05.021

Řezanka, T., Lukavský, J., Sigler, K., Nedbalová, L., & Vítová, M. (2015). Temperature dependence of production of structured triacylglycerols in the alga Trachydiscus minutus. *Phytochemistry*, *110*, 37–45. https://doi.org/10.1016/j.phytochem.2014.12.013

Řezanka, T., Nedbalová, L., & Sigler, K. (2015). Comparative analysis of triacylglycerols from different Stichococcus strains by RP-HPLC/APCI-MS and chiral HPLC. *Journal of Applied Phycology*, *27*(2), 685–696. https://doi.org/10.1007/s10811-014-0354-y

Řezanka, T., Vítová, M., Nováková, A., & Sigler, K. (2015). Separation and Identification of Odd Chain Triacylglycerols of the Protozoan Khawkinea quartana and the Mold Mortierella alpina Using LC-MS. *Lipids*, *50*(8), 811–820. https://doi.org/10.1007/s11745-015-4042-8

Rogalska, E., Cudrey, C., Ferrato, F., & Verger, R. (1993).

Stereoselective hydrolysis of triglycerides by animal and microbial lipases. *Chirality*, *5*(1), 24–30. https://doi.org/10.1002/chir.530050106

Rong, X., Albert, C. J., Hong, C., Duerr, M. A., Chamberlain, B. T., Tarling, E. J., Ito, A., Gao, J., Wang, B., Edwards, P. A., Jung, M. E., Ford, D. A., & Tontonoz, P. (2013). LXRs regulate ER stress and inflammation through dynamic modulation of membrane phospholipid composition. *Cell Metabolism*, *18*(5), 685–697. https://doi.org/10.1016/j.cmet.2013.10.002

Rossmeisl, M., Macek Jilkova, Z., Kuda, O., Jelenik, T., Medrikova, D., Stankova, B., Kristinsson, B., Haraldsson, G. G., Svensen, H., Stoknes, I., Sjövall, P., Magnusson, Y., Balvers, M. G. J., Verhoeckx, K. C. M., Tvrzicka, E., Bryhn, M., & Kopecky, J. (2012). Metabolic Effects of n-3 PUFA as Phospholipids Are Superior to Triglycerides in Mice Fed a High-Fat Diet: Possible Role of Endocannabinoids. *PLoS ONE*, *7*(6), e38834. https://doi.org/10.1371/journal.pone.0038834

Ruiz-Lopez, N., Stubhaug, I., Ipharraguerre, I., Rimbach, G., & Menoyo, D. (2015). Positional Distribution of Fatty Acids in Triacylglycerols and Phospholipids from Fillets of Atlantic Salmon (Salmo Salar) Fed Vegetable and Fish Oil Blends. *Marine Drugs*, *13*(7), 4255–4269. https://doi.org/10.3390/md13074255

Saini, R. K., & Keum, Y. S. (2018). Omega-3 and omega-6 polyunsaturated fatty acids: Dietary sources, metabolism, and significance — A review. *Life Sciences*, *203*(April), 255–267. https://doi.org/10.1016/j.lfs.2018.04.049

Saini, R. K., Prasad, P., Sreedhar, R. V., Naidu, K. A., Shang, X., & Keum, Y. S. (2021). Omega−3 polyunsaturated fatty acids (PUFAs): Emerging plant and microbial sources, oxidative stability, bioavailability, and health benefits—A review. *Antioxidants*, *10*(10), 1–23.

Sala-Vila, A., Castellote, A. I., & López-Sabater, M. C. (2008). The intramolecular position of docosahexaenoic acid in the triacylglycerol sources used for pediatric nutrition has a minimal effect on its metabolic use. *Nutrition Research*, *28*(3), 131–136. https://doi.org/10.1016/j.nutres.2007.11.007

Sazzad, M. A. Al, Fabritius, M., Boström, P., Tarvainen, M., Kalpio, M., Linderborg, K. M., Kallio, H., & Yang, B. (2022). A novel UHPLC-ESI-MS/MS method and automatic calculation software for regiospecific analysis of triacylglycerols in natural fats and oils. *Analytica Chimica Acta*, *1210*(April), 339887. https://doi.org/10.1016/j.aca.2022.339887

Schoeler, M., Ellero-Simatos, S., Birkner, T., Mayneris-Perxachs, J., Olsson, L., Brolin, H., Loeber, U., Kraft, J. D., Polizzi,

A., Martí-Navas, M., Puig, J., Moschetta, A., Montagner, A., Gourdy, P., Heymes, C., Guillou, H., Tremaroli, V., Fernández-Real, J. M., Forslund, S. K., … Caesar, R. (2023). The interplay between dietary fatty acids and gut microbiota influences host metabolism and hepatic steatosis. *Nature Communications*, *14*(1), 5329. https://doi.org/10.1038/s41467-023-41074-3

Schverer, M., O'Mahony, S. M., O'Riordan, K. J., Donoso, F., Roy, B. L., Stanton, C., Dinan, T. G., Schellekens, H., & Cryan, J. F. (2020). Dietary phospholipids: Role in cognitive processes across the lifespan. *Neuroscience and Biobehavioral Reviews*, *111*(January), 183–193. https://doi.org/10.1016/j.neubiorev.2020.01.012

Segura, J., Cambero, M. I., Cámara, L., Loriente, C., Mateos, G. G., & López-Bote, C. J. (2015). Effect of sex, dietary glycerol or dietary fat during late fattening, on fatty acid composition and positional distribution of fatty acids within the triglyceride in pigs. *Animal*, *9*(11), 1904–1911. https://doi.org/10.1017/S1751731115001639

Segura, J., Ruiz-López, N., Menoyo, D., Cambero, M. I., & López-Bote, C. J. (2015). Comparison of analytical techniques for the determination of the positional distribution of fatty acids in triacylglycerols. Relationship with pig fat melting point and hardness. *Grasas y Aceites*, *66*(2). https://doi.org/10.3989/gya.1073142

Shirouchi, B., Nagao, K., Inoue, N., Ohkubo, T., Hibino, H., & Yanagita, T. (2007). Effect of dietary omega 3 phosphatidylcholine on obesity-related disorders in obese Otsuka Long-Evans Tokushima fatty rats. *Journal of Agricultural and Food Chemistry*, *55*(17), 7170–7176. https://doi.org/10.1021/jf071225x

Sivakanthan, S., & Madhujith, T. (2020). Current trends in applications of enzymatic interesterification of fats and oils: A review. *Lwt*, *132*(December 2019), 109880. https://doi.org/10.1016/j.lwt.2020.109880

Smith, S. B., Yang, A., Larsen, T. W., & Tume, R. K. (1998). Positional analysis of triacylglycerols from bovine adipose tissue lipids varying in degree of unsaturation. *Lipids*, *33*(2), 197–207. https://doi.org/10.1007/s11745-998-0196-8

Smorenburg, J. N., Hodun, K., McTavish, P. V., Wang, C., Pinheiro, M. A., Wells, K. R. D., Brunt, K. R., Nakamura, M. T., Chabowski, A., & Mutch, D. M. (2025). EPA/DHA but Not ALA Reduces Visceral Adiposity and Adipocyte Size in High Fat Diet-Induced Obese Delta-6 Desaturase Knockout Mice. *Molecular Nutrition & Food Research*, *69*(2), 1–11. https://doi.org/10.1002/mnfr.202400721

Song, R., Li, W., Deng, S., Zhao, Y., & Tao, N. (2023). Assessment of lipid composition and

eicosapentaenoic acid/docosahexaenoic acid bioavailability in fish oil obtained through different enrichment methods. *Frontiers in Nutrition*, *10*(March), 1–10. https://doi.org/10.3389/fnut.2023.1136490

Song, X., Huang, Y., Neuhouser, M. L., Tinker, L. F., Vitolins, M. Z., Prentice, R. L., & Lampe, J. W. (2017). Dietary long-chain fatty acids and carbohydrate biomarker evaluation in a controlled feeding study in participants from the Women's Health Initiative cohort. *The American Journal of Clinical Nutrition*, *105*(6), 1272–1282. https://doi.org/10.3945/ajcn.117.153072

Sun, S. tao, Jiang, Y. jie, Guo, X., Zhang, M. qi, Ren, Q. dong, Simal-Gandara, J., Wang, M. xuan, Xue, X. jia, Li, N. yang, & Liu, C. (2025). An overview of the chirality of diet-related fatty acids, glycerolipids, and glycerophospholipids. *Trends in Food Science and Technology*, *156*(November 2024), 104856. https://doi.org/10.1016/j.tifs.2024.104856

Swinkels, D., & Baes, M. (2023). The essential role of docosahexaenoic acid and its derivatives for retinal integrity. *Pharmacology & Therapeutics*, *247*, 108440. https://doi.org/10.1016/j.pharmthera.2023.108440

Tang, S., Chen, X., Ke, Y., Wang, F., & Yan, X. (2022). Voltage-Controlled Divergent Cascade of Electrochemical Reactions for Characterization of Lipids at Multiple Isomer Levels Using Mass Spectrometry. *Analytical Chemistry*, *94*(37), 12750–12756. https://doi.org/10.1021/acs.analchem.2c02375

Tarvainen, M., Kallio, H., & Yang, B. (2019). Regiospecific Analysis of Triacylglycerols by Ultrahigh-Performance-Liquid Chromatography-Electrospray Ionization-Tandem Mass Spectrometry [Research-article]. *Analytical Chemistry*, *91*(21), 13695–13702. https://doi.org/10.1021/acs.analchem.9b02968

Teixeira-Santos, L., Martins, S., Sousa, T., Teixeira, A. A., & Pinho, D. (2023). The pro-resolving lipid mediator Maresin 1 ameliorates pain responses and neuroinflammation in the spared nerve injury-induced neuropathic pain: A study in male and female mice. *PLoS ONE*, *18*(6 June), 1–24. https://doi.org/10.1371/journal.pone.0287392

Tian, H., Wu, Y., Lin, Y., Chen, X., Yu, M., Lu, T., & Xie, L. (2019). Dietary patterns affect maternal macronutrient intake levels and the fatty acid profile of breast milk in lactating Chinese mothers. *Nutrition (Burbank, Los Angeles County, Calif.)*, *58*, 83–88. https://doi.org/10.1016/j.nut.2018.06.009

Uauy, R. D., Birch, D. G., Birch, E. E., Tyson, J. E., & Hoffman, D. R. (1990). Effect of dietary omega-3 fatty acids on retinal function of very-low-birth-weight neonates. *Pediatric*

*Research*, *28*(5), 485–492. https://doi.org/10.1203/00006450-199011000-00014

Valentini, K. J., Pickens, C. A., Wiesinger, J. A., & Fenton, J. I. (2018). The effect of fish oil supplementation on brain DHA and EPA content and fatty acid profile in mice. *International Journal of Food Sciences and Nutrition*, *69*(6), 705–717. https://doi.org/10.1080/09637486.2017.1413640

Vosskötter, F., Burhop, M., Hahn, A., & Schuchardt, J. P. (2023). Equal bioavailability of omega-3 PUFA from Calanus oil, fish oil and krill oil: A 12-week randomized parallel study. *Lipids*, *58*(3), 129–138. https://doi.org/10.1002/lipd.12369

Wang, Y., Gajewski, B. J., Valentine, C. J., Crawford, S. A., Brown, A. R., Mudaranthakam, D. P., Camargo, J. T., & Carlson, S. E. (2023). DHA, nutrient intake, and maternal characteristics as predictors of pregnancy outcomes in a randomised clinical trial of DHA supplementation. *Clinical Nutrition*, *42*(11), 2229–2240. https://doi.org/10.1016/j.clnu.2023.09.005

Wang, Z., Yang, T., Brenna, J. T., & Wang, D. H. (2023). Fatty acid isomerism: analysis and selected biological functions. *Food and Function*, *15*(3), 1071–1088. https://doi.org/10.1039/d3fo03716a

Wei, W., Hu, M., Huang, J., Yu, S., Li, X., Li, Y., & Mao, L. (2021). Anti-obesity effects of DHA and EPA in high fat-induced insulin resistant mice. *Food and Function*, *12*(4), 1614–1625. https://doi.org/10.1039/d0fo02448a

Weisinger, H. S., Vingrys, A. J., Abedin, L., & Sinclair, A. J. (1998). Effect of diet on the rate of depletion of n-3 fatty acids in the retina of the guinea pig. *Journal of Lipid Research*, *39*(6), 1274–1279. https://doi.org/10.1016/s0022-2275(20)32552-9

Weisinger, H. S., Vingrys, A. J., Bui, B. V., & Sinclair, A. J. (1999). Effects of dietary n-3 fatty acid deficiency and repletion in the guinea pig retina. *Investigative Ophthalmology and Visual Science*, *40*(2), 327–338.

Weisinger, H. S., Vingrys, A. J., & Sinclair, A. J. (1996). The effect of docosahexaenoic acid on the electroretinogram of the guinea pig. *Lipids*, *31*(1), 65–70. https://doi.org/10.1007/BF02522413

Williams, P. E., Klein, D. R., Greer, S. M., & Brodbelt, J. S. (2017). Pinpointing Double Bond and sn-Positions in Glycerophospholipids via Hybrid 193 nm Ultraviolet Photodissociation (UVPD) Mass Spectrometry. *Journal of the American Chemical Society*, *139*(44), 15681–15690. https://doi.org/10.1021/jacs.7b06416

Xu, S., Zhu, Z., Delafield, D. G., Rigby, M. J., Lu, G., Braun, M., Puglielli, L., & Li, L. (2024). Spatially and temporally probing distinctive glycerophospholipid alterations in Alzheimer's disease mouse brain via high-resolution ion

mobility-enabled sn-position resolved lipidomics. *Nature Communications*, *15*(1), 1–18. https://doi.org/10.1038/s41467-024-50299-9

Yamagata, K. (2017). Docosahexaenoic acid regulates vascular endothelial cell function and prevents cardiovascular disease. *Lipids in Health and Disease*, *16*(1), 118. https://doi.org/10.1186/s12944-017-0514-6

Yan, T., Naeem, Z., Liang, Z., Azari, H., Reynolds, B. A., & Prentice, B. M. (2025). Spatial mapping of phosphatidylcholine sn-positional isomers using CID of divalent metal complexes in imaging mass spectrometry. *International Journal of Mass Spectrometry*, *508*(November 2024), 117370. https://doi.org/10.1016/j.ijms.2024.117370

Yeo, J. D., & Parrish, C. C. (2020). Evaluation of triacylglycerol (TAG) profiles and their contents in salmon muscle tissue using ESI-MS/MS spectrometry with multiple neutral loss scans. *Food Chemistry*, *324*(April), 126816. https://doi.org/10.1016/j.foodchem.2020.126816

Yoshinaga, K., Sasaki, K., Watanabe, H., Nagao, K., Inoue, N., Shirouchi, B., Yanagita, T., Nagai, T., Mizobe, H., Kojima, K., Beppu, F., & Gotoh, N. (2015). Differential effects of triacylglycerol positional isomers containing n-3 series highly unsaturated fatty acids on lipid metabolism in C57BL/6J mice. *The Journal of Nutritional Biochemistry*, *26*(1), 57–63. https://doi.org/10.1016/j.jnutbio.2014.09.004

Young, R. S. E., Bowman, A. P., Tousignant, K. D., Poad, B. L. J., Gunter, J. H., Philp, L. K., Nelson, C. C., Ellis, S. R., Heeren, R. M. A., Sadowski, M. C., & Blanksby, S. J. (2022). Isomeric lipid signatures reveal compartmentalized fatty acid metabolism in cancer. *Journal of Lipid Research*, *63*(6), 1–16. https://doi.org/10.1016/j.jlr.2022.100223

Youzbachi, N., Trabelsi, H., Elfalleh, W., Khaldi, A., Nasri, N., & Tlili, N. (2019). Fatty acids and triacylglycerols composition from Tunisian Acacia species seed oil. *Arabian Journal of Chemistry*, *12*(8), 3302–3308. https://doi.org/10.1016/j.arabjc.2015.08.020

Zhang, Xin, Yuan, T., Chen, X., Liu, X., Hu, J., & Liu, Z. (2024). Effects of DHA on cognitive dysfunction in aging and Alzheimer's disease: The mediating roles of ApoE. *Progress in Lipid Research*, *93*(October 2023), 101256. https://doi.org/10.1016/j.plipres.2023.101256

Zhang, Xinghe, Qi, C., Zhang, Y., Wei, W., Jin, Q., Xu, Z., Tao, G., & Wang, X. (2019). Identification and quantification of triacylglycerols in human milk fat using ultra-performance convergence chromatography and quadrupole time-of-flight mass spectrometery with supercritical carbon dioxide as a mobile phase. *Food Chemistry*,

*275*(March 2018), 712–720. https://doi.org/10.1016/j.foodchem.2018.09.150

Zhang, Xinghe, Wei, W., Tao, G., Jin, Q., & Wang, X. (2022). Triacylglycerol regioisomers containing palmitic acid analyzed by ultra-performance supercritical fluid chromatography and quadrupole time-of-flight mass spectrometry: Comparison of standard curve calibration and calculation equation. *Food Chemistry*, *391*(May), 133280. https://doi.org/10.1016/j.foodchem.2022.133280

Zhang, Y., Kalpio, M., Haraldsdóttir, H., Gudmundsson, H. G., Haraldsson, G. G., Sigurjónsson, S., Kristinsson, B., Linderborg, K. M., & Yang, B. (2024). Enantiomeric Separation of Triacylglycerols Consisting of Three Different Fatty Acyls and Their Chiral Chromatographic Elution Behavior. *Analytical Chemistry*, *96*, 13936–13943. https://doi.org/10.1021/acs.analchem.4c02513

Zhang, Y., Kalpio, M., Tao, L., Haraldsson, G. G., Guðmundsson, H. G., Fang, X., Linderborg, K. M., Zhang, Y., & Yang., B. (2023). Metabolic fate of DHA from regio- and stereospecific positions of triacylglycerols in a long-term feeding trial in rats. *Food Research International*, *174*, 113626. https://doi.org/10.1016/j.foodres.2023.113626

Zhao, X., Zhang, W., Zhang, D., Liu, X., Cao, W., Chen, Q., Ouyang, Z., & Xia, Y. (2019). A lipidomic workflow capable of resolving: Sn - And CC location isomers of phosphatidylcholines. *Chemical Science*, *10*(46), 10740–10748. https://doi.org/10.1039/c9sc03521d

Zou, H., Zhang, H., Zhao, Y., Li, X., Wang, Y., Zhang, T., & Xue, C. (2023). N-3 PUFA Deficiency Aggravates Streptozotocin-Induced Pancreatic Injury in Mice but Dietary Supplementation with DHA/EPA Protects the Pancreas via Suppressing Inflammation, Oxidative Stress and Apoptosis. *Marine Drugs*, *21*(1), 39. https://doi.org/10.3390/md21010039

## DOCTORAL THESES IN FOOD SCIENCES AT THE UNIVERSITY OF TURKU

1. **REINO R. LINKO (1967)** Fatty acids and other components of Baltic herring flesh lipids. (Organic chemistry).
2. **HEIKKI KALLIO (1975)** Identification of volatile aroma compounds in arctic bramble, *Rubus arcticus* L. and their development during ripening of the berry, with special reference to *Rubus stellatus* SM.
3. **JUKKA KAITARANTA (1981)** Fish roe lipids and lipid hydrolysis in processed roe of certain *Salmonidae* fish as studied by novel chromatographic techniques.
4. **TIMO HIRVI (1983)** Aromas of some strawberry and blueberry species and varieties studied by gas liquid chromatographic and selected ion monitoring techniques.
5. **RAINER HUOPALAHTI (1985)** Composition and content of aroma compounds in the dill herb, *Anethum graveolens* L., affected by different factors.
6. **MARKKU HONKAVAARA (1989)** Effect of porcine stress on the development of PSE meat, its characteristics and influence on the economics of meat products manufacture.
7. **PÄIVI LAAKSO (1992)** Triacylglycerols – approaching the molecular composition of natural mixtures.
8. **MERJA LEINO (1993)** Application of the headspace gas chromatography complemented with sensory evaluation to analysis of various foods.
9. **KAISLI KERROLA (1994)** Essential oils from herbs and spices: isolation by carbon dioxide extraction and characterization by gas chromatography and sensory evaluation.
10. **ANJA LAPVETELÄINEN (1994)** Barley and oat protein products from wet processes: food use potential.
11. **RAIJA TAHVONEN (1995)** Contents of lead and cadmium in foods in Finland.
12. **MAIJA SAXELIN (1995)** Development of dietary probiotics: estimation of optimal *Lactobacillus* GG concentrations.
13. **PIRJO-LIISA PENTTILÄ (1995)** Estimation of food additive and pesticide intakes by means of a stepwise method.
14. **SIRKKA PLAAMI (1996)** Contents of dietary fiber and inositol phosphates in some foods consumed in Finland.
15. **SUSANNA EEROLA (1997)** Biologically active amines: analytics, occurrence and formation in dry sausages.
16. **PEKKA MANNINEN (1997)** Utilization of supercritical carbon dioxide in the analysis of triacylglycerols and isolation of berry oils.
17. **TUULA VESA (1997)** Symptoms of lactose intolerance: influence of milk composition, gastric emptying, and irritable bowel syndrome.
18. **EILA JÄRVENPÄÄ (1998)** Strategies for supercritical fluid extraction of analytes in trace amounts from food matrices.
19. **ELINA TUOMOLA (1999)** *In vitro* adhesion of probiotic lactic acid bacteria.
20. **ANU JOHANSSON (1999)** Availability of seed oils from Finnish berries with special reference to compositional, geographical and nutritional aspects.
21. **ANNE PIHLANTO-LEPPÄLÄ (1999)** Isolation and characteristics of milk-derived bioactive peptides.
22. **MIKA TUOMOLA (2000)** New methods for the measurement of androstenone and skatole – compounds associated with boar taint problem. (Biotechnology).
23. **LEEA PELTO (2000)** Milk hypersensitivity in adults: studies on diagnosis, prevalence and nutritional management.
24. **ANNE NYKÄNEN (2001)** Use of nisin and lactic acid/lactate to improve the microbial and sensory quality of rainbow trout products.
25. **BAORU YANG (2001)** Lipophilic components of sea buckthorn (*Hippophaë rhamnoides*) seeds and berries and physiological effects of sea buckthorn oils.
26. **MINNA KAHALA (2001)** Lactobacillar S-layers: Use of *Lactobacillus brevis* S-layer signals for heterologous protein production.
27. **OLLI SJÖVALL (2002)** Chromatographic and mass spectrometric analysis of non-volatile oxidation products of triacylglycerols with emphasis on core aldehydes.
28. **JUHA-PEKKA KURVINEN (2002)** Automatic data processing as an aid to mass spectrometry of dietary triacylglycerols and tissue glycerophospholipids.
29. **MARI HAKALA (2002)** Factors affecting the internal quality of strawberry (*Fragaria x ananassa* Duch.) fruit.
30. **PIRKKA KIRJAVAINEN (2003)** The intestinal microbiota – a target for treatment in infant atopic eczema?
31. **TARJA ARO (2003)** Chemical composition of Baltic herring: effects of processing and storage on fatty acids, mineral elements and volatile compounds.
32. **SAMI NIKOSKELAINEN (2003)** Innate immunity of rainbow trout: effects of opsonins, temperature and probiotics on phagocytic and complement activity as well as on disease resistance.
33. **KAISA YLI-JOKIPII (2004)** Effect of triacylglycerol fatty acid positional distribution on postprandial lipid metabolism.
34. **MARIKA JESTOI (2005)** Emerging *Fusarium*-mycotoxins in Finland.
35. **KATJA TIITINEN (2006)** Factors contributing to sea buckthorn (*Hippophaë rhamnoides* L.) flavour.
36. **SATU VESTERLUND (2006)** Methods to determine the safety and influence of probiotics on the adherence and viability of pathogens.
37. **FANDI FAWAZ ALI IBRAHIM (2006)** Lactic acid bacteria: an approach for heavy metal detoxification.
38. **JUKKA-PEKKA SUOMELA (2006)** Effects of dietary fat oxidation products and flavonols on lipoprotein oxidation.
39. **SAMPO LAHTINEN (2007)** New insights into the viability of probiotic bacteria.

40. **SASKA TUOMASJUKKA (2007)** Strategies for reducing postprandial triacylglycerolemia.
41. **HARRI MÄKIVUOKKO (2007)** Simulating the human colon microbiota: studies on polydextrose, lactose and cocoa mass.
42. **RENATA ADAMI (2007)** Micronization of pharmaceuticals and food ingredients using supercritical fluid techniques.
43. **TEEMU HALTTUNEN (2008)** Removal of cadmium, lead and arsenic from water by lactic acid bacteria.
44. **SUSANNA ROKKA (2008)** Bovine colostral antibodies and selected lactobacilli as means to control gastrointestinal infections.
45. **ANU LÄHTEENMÄKI-UUTELA (2009)** Foodstuffs and medicines as legal categories in the EU and China. Functional foods as a borderline case. (Law).
46. **TARJA SUOMALAINEN (2009)** Characterizing *Propionibacterium freudenreichii* ssp. *shermanii* JS and *Lactobacillus rhamnosus* LC705 as a new probiotic combination: basic properties of JS and pilot *in vivo* assessment of the combination.
47. **HEIDI LESKINEN (2010)** Positional distribution of fatty acids in plant triacylglycerols: contributing factors and chromatographic/mass spectrometric analysis.
48. **TERHI POHJANHEIMO (2010)** Sensory and non-sensory factors behind the liking and choice of healthy food products.
49. **RIIKKA JÄRVINEN (2010)** Cuticular and suberin polymers of edible plants – analysis by gas chromatographic-mass spectrometric and solid state spectroscopic methods.
50. **HENNA-MARIA LEHTONEN (2010)** Berry polyphenol absorption and the effect of northern berries on metabolism, ectopic fat accumulation, and associated diseases.
51. **PASI KANKAANPÄÄ (2010)** Interactions between polyunsaturated fatty acids and probiotics.
52. **PETRA LARMO (2011)** The health effects of sea buckthorn berries and oil.
53. **HENNA RÖYTIÖ (2011)** Identifying and characterizing new ingredients *in vitro* for prebiotic and synbiotic use.
54. **RITVA REPO-CARRASCO-VALENCIA (2011)** Andean indigenous food crops: nutritional value and bioactive compounds.
55. **OSKAR LAAKSONEN (2011)** Astringent food compounds and their interactions with taste properties.
56. **ŁUKASZ MARCIN GRZEŚKOWIAK (2012)** Gut microbiota in early infancy: effect of environment, diet and probiotics.
57. **PENGZHAN LIU (2012)** Composition of hawthorn (*Crataegus* spp.) fruits and leaves and emblic leafflower (*Phyllanthus emblica*) fruits.
58. **HEIKKI ARO (2012)** Fractionation of hen egg and oat lipids with supercritical fluids. Chemical and functional properties of fractions.
59. **SOILI ALANNE (2012)** An infant with food allergy and eczema in the family – the mental and economic burden of caring.
60. **MARKO TARVAINEN (2013)** Analysis of lipid oxidation during digestion by liquid chromatography-mass spectrometric and nuclear magnetic resonance spectroscopic techniques.
61. **JIE ZHENG (2013)** Sugars, acids and phenolic compounds in currants and sea buckthorn in relation to the effects of environmental factors.
62. **SARI MÄKINEN (2014)** Production, isolation and characterization of bioactive peptides with antihypertensive properties from potato and rapeseed proteins.
63. **MIKA KAIMAINEN (2014)** Stability of natural colorants of plant origin.
64. **LOTTA NYLUND (2015)** Early life intestinal microbiota in health and in atopic eczema.
65. **JAAKKO HIIDENHOVI (2015)** Isolation and characterization of ovomucin – a bioactive agent of egg white.
66. **HANNA-LEENA HIETARANTA-LUOMA (2016)** Promoting healthy lifestyles with personalized, *APOE* genotype based health information: The effects on psychological-, health behavioral and clinical factors.
67. **VELI HIETANIEMI (2016)** The *Fusarium* mycotoxins in Finnish cereal grains: How to control and manage the risk.
68. **MAARIA KORTESNIEMI (2016)** NMR metabolomics of foods – Investigating the influence of origin on sea buckthorn berries, *Brassica* oilseeds and honey.
69. **JUHANI AAKKO (2016)** New insights into human gut microbiota development in early infancy: influence of diet, environment and mother's microbiota.
70. **WEI YANG (2017)** Effects of genetic and environmental factors on proanthocyanidins in sea buckthorn (*Hippophaë rhamnoides*) and flavonol glycosides in leaves of currants (*Ribes* spp.).
71. **LEENAMAIJA MÄKILÄ (2017)** Effect of processing technologies on phenolic compounds in berry products.
72. **JUHA-MATTI PIHLAVA (2017)** Selected bioactive compounds in cereals and cereal products – their role and analysis by chromatographic methods.
73. **TOMMI KUMPULAINEN (2018)** The complexity of freshness and locality in a food consumption context
74. **XUEYING MA (2018)** Non-volatile bioactive and sensory compounds in berries and leaves of sea buckthorn (*Hippophaë rhamnoides*)
75. **ANU NUORA (2018)** Postprandial lipid metabolism resulting from heated beef, homogenized milk and interesterified palm oil.
76. **HEIKKI AISALA (2019)** Sensory properties and underlying chemistry of Finnish edible wild mushrooms.
77. **YE TIAN (2019)** Phenolic compounds from Finnish berry species to enhance food safety.
78. **MAIJA PAAKKI (2020)** The importance of natural colors in food for the visual attractiveness of everyday lunch.

79. **SHUXUN LIU (2020**) Fermentation with non-*Saccharomyces* yeasts as a novel biotechnology for berry wine production.
80. **MARIKA KALPIO (2020)** Strategies for analyzing the regio- and stereospecific structures of individual triacylglycerols in natural fats and oils.
81. **JOHANNA JOKIOJA (2020)** Postprandial effects and metabolism of acylated anthocyanins originating from purple potatoes.
82. **NIINA KELANNE (2021)** Novel bioprocessing for increasing consumption of Nordic berries.
83. **NIKO MARKKINEN (2021)** Bioprocessing of berry materials with malolactic fermentation.
84. **GABRIELE BELTRAME (2021)** Polysaccharides from Finnish fungal resources.
85. **SALLA LAITO (2022)** Bioactive compounds in oats and gut health.
86. **KANG CHEN (2022)** Multi-omics study on the effects of anthocyanin extracts from bilberries and purple potatoes on type 2 diabetes in Zucker diabetic fatty rats.
87. **WENJIA HE (2022)** Bioprocessing of alcoholic beverages from apples and pears: Effects of raw materials and processes on quality.
88. **TANJA KAKKO (2023)** Alternative approaches to improve the processing and quality of under-utilized fish.
89. **MIKAEL FABRITIUS (2023)** Mass spectrometric methodologies for analysis of triacylglycerol and phospholipid regioisomers in natural fats and oils.
90. **ELLA AITTA (2023)** Green technologies for the extraction of oil and protein from Baltic herring (*Clupea harengus membras*).
91. **AMRUTA KULKARNI (2023)** Effect of omega-3 deficiency and positional distribution of docosahexaenoic acid in triacylglycerols on tissue lipids in rats.
92. **LIZ A. GUTIÉRREZ QUEQUEZANA (2023)** Effect of cultivar, growth environment and developmental stage on phenolic compounds and ascorbic acid in potato tubers grown in Finland.
93. **MINNA ROTOLA-PUKKILA (2024)** The umami compounds in Nordic food raw materials and the effect of cooking.
94. **EIJA AHONEN (2024)** Impact of lipid structure and selected antioxidants on the oxidation of docosahexaenoic acid.
95. **MARINA FIDELIS (2024)** Valorization of underutilized biomass for biorefinery and food applications: Exploring the processing, plant material composition, bioactivity and fortified bread models
96. **YUQING ZHANG (2025)** Structural Analysis of Triacylglycerols and Bioavailability of Docosahexaenoic Acid from Regio- and Enantiopure Triacylglycerols

TURUN
YLIOPISTO
UNIVERSITY
OF TURKU